

**Diagnostic Analyses
of the GATE A/B Scale Area
at Individual Time Periods**

By

William M. Frank

P.I. William M. Gray

Department of Atmospheric Science
Colorado State University
Fort Collins, Colorado

NSF ATM 75-01424-A02



**Department of
Atmospheric Science**

Paper No. 297

DIAGNOSTIC ANALYSES OF THE GATE A/B
SCALE AREA AT INDIVIDUAL TIME PERIODS

By

William M. Frank

This paper has been financially supported by
the National Science Foundation
Grant No. ATM-75-01424 A02

Department of Atmospheric Science
Colorado State University
Fort Collins, Colorado
November, 1978

Atmospheric Science Paper No. 297

ABSTRACT

Diagnostic moisture and static energy budgets for the GATE A/B scale area are performed at individual time periods using rawinsonde, radar and satellite data. The data are sufficiently accurate to permit quantitative analysis of that area with 3-6 hour time resolution.

According to the budget analyses, radar rainfall estimates for the GATE master array are generally too low and lag the budget rainfalls by 4-6 hours. This most likely results from underestimates of rainfall from small clouds/weak echoes and overestimates of strong echo precipitation. There is no apparent lag between the A/B-scale vertical motion at 800 mb and the net condensation rate within the time resolution of the present data.

Temperature changes for the GATE A/B-area are dominated by the diurnal cycle of radiational heating. Evidence that convection warms the upper troposphere and cools the lower levels is presented, but cloud warming is smaller than the normal diurnal temperature variations. The net moisture content of the atmosphere varied little during GATE.

Frictionally forced convergence in the planetary boundary layer is shown to be a relatively unimportant component of total A/B-area convergence and may be considered negligible for many purposes.

TABLE OF CONTENTS

	Page
ABSTRACT.	i
1. INTRODUCTION	1
2. METHOD	2
2.1 Data Set	2
2.2 Data Analysis	3
2.3 Budget Computations.	5
3. BUDGET RESULTS	9
3.1 Phase Mean Budgets	9
3.2 Individual Time Period Budgets	16
3.3 Lag Between Budget Condensation and Radar Rainfall .	24
3.4 Summary	36
3.5 Budget Condensation and Large Scale Vertical Motion.	38
4. TROPOSPHERIC WARMING BY CLOUDS AND RADIATION.	56
5. CONVERGENCE VS. VORTICITY IN THE BOUNDARY LAYER	80
6. CONCLUSIONS	95
ACKNOWLEDGEMENTS	97
BIBLIOGRAPHY.	98
APPENDIX	102

1. INTRODUCTION

The GARP Atlantic Tropical Experiment (GATE) of the Global Atmospheric Research Program (GARP) has provided the first data set suitable for high time resolution analysis of tropical meso-synoptic scale weather phenomena. This study utilizes rawinsonde, radar and satellite data from all three phases of GATE to analyze the heat and moisture budgets of the A/B scale ship array at individual time periods. The results of the diagnostic budget analyses are used to investigate temporal variations of the tropical troposphere and certain interactions between moist convection, radiation, and the state of the atmosphere on the GATE A/B scale, namely:

- 1) the atmospheric temperature response to moist convection and to radiative heating,
- 2) changes in the total atmospheric moisture content during periods of enhanced/suppressed convection,
- 3) phase lag between observed A/B scale mean moisture convergence and master array radar precipitation,
- 4) diurnal variations of precipitation and temperature, and
- 5) the importance of low level friction as a forcing mechanism for boundary layer convergence.

As will be shown, the results indicate that:

- 1) changes in the temperature of the tropical troposphere are more strongly dependent upon radiational heating than on latent heat release,
- 2) atmospheric moisture is quite steady throughout GATE,
- 3) precipitation responds rapidly to low level convergence, but the radar-observed precipitation tends to lag calculated net condensation by 3-6 hours. Problems with the radar rainfall estimates are suspected, and
- 4) boundary layer friction does not have a significant effect upon low level convergence.

2. METHOD

2.1 Data Set

Rawinsonde data from 8 ships of the GATE A/B and B-scale arrays were used (Fig. 1). The rawinsondes were scheduled for launch at 3-hour intervals although this goal was consistently met only in Phase III. In general, the data allow time resolution of 3-6 hours. Data were taken from the GATE processed and validated data tapes from the National Weather Records Center at Asheville, NC. Data flagged as suspicious by CEDDA¹ were deleted. Only time periods containing at least 3 reports (surface through 100 mb) from the outer 6 Russian Ship positions were selected.

Divergence values were computed using data from the 6 A/B array Russian ships and from the Vize and Vanguard. These 8 ships used compatible systems. The remaining B-scale ships using the Very Low Frequency (VLF) wind measurement system did not provide wind data of sufficient accuracy to compute meaningful divergence values. Thompson et al. (1978) have also found that the B-array winds yielded poor budget results during Phase III. The above wind problems necessitated the computation of budgets for the broader A/B scale array. This is unfortunate since radar coverage extended only slightly beyond the B-scale area.

Temperature and moisture data and the u and v components of the wind from all 12 B and A/B array ships (Fig. 1) were used for each selected time period. Satellite cloud cover and height estimates were used with a radiation model to obtain estimates of the A/B scale radiational heating profiles (Cox and Griffith, 1978)

¹Center for Experiment Design and Data Analysis.

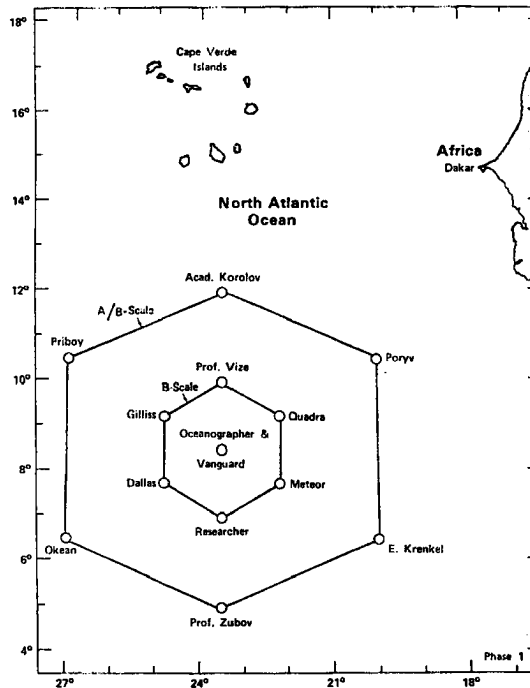


Fig. 1. GATE A/B and B scale arrays for Phase I. The six A/B ships plus ships at the center and at the northern most position of the B array (8 total) were used in divergence computations.

2.2 Data Analysis

Winds. Divergence at each level was obtained by fitting wind data from the 8 ships (noted above) to a plane by the least squares method (Panofsky and Brier, 1968; Appendix). Equations 1 and 2 were obtained:

$$\bar{u} = a_1x + a_2y + a_3 \quad (1)$$

$$\bar{v} = b_1x + b_2y + b_3 \quad (2)$$

Divergence was then computed by Eq. 3:

$$\vec{\nabla} \cdot \vec{v} = \frac{\partial \bar{u}}{\partial x} + \frac{\partial \bar{v}}{\partial y} = a_1 + b_2 \quad (3)$$

Each divergence profile was adjusted by a constant correction factor at

every level to give $\bar{\omega} = 0$ at 100 mb when Eq. 4 was integrated upward from the surface. The size of this mass balance correction gave some indication of the quality of the divergence values, and time periods with corrections greater than $\pm 4 \times 10^{-6}$ were omitted. The average correction was much smaller.

$$\bar{\omega}(p) = - \int_{p_0}^{p_{100}} \frac{\nabla \cdot \mathbf{v}}{\rho} dp \quad (4)$$

Temperature and Moisture. Analysis of the rawinsonde temperature data indicated large persistent differences even between different ships using the same measurement systems (Ooyama and Esbensen, 1977). The problem was most pronounced in the Russian ships. Therefore, it was extremely difficult to compare directly measurements from more than one point in the A/B array. These bias errors overwhelmed the typically weak tropical temperature gradients. The best way to overcome this difficulty seems to be the use of deviation fields (Frank, 1978). To obtain vertical profiles of temperature (T) and specific humidity (q), mean profiles were constructed for each phase using data from the 5 U.S. ships of the B array (assumed to be the most accurate). Phase mean profiles were then constructed for each of the 12 individual ships in the B and A/B arrays. At each level and time period, the phase mean temperature and specific humidity for a ship were subtracted from the observed values yielding deviations from the ship phase mean as in Eqs. 5 and 6.

$$\Delta T = T - \bar{T} \quad (5)$$

$$\Delta q = q - \bar{q} \quad (6)$$

where ΔT , Δq are deviations from phase means; T , q are observed values at a single time period, and \bar{T} , \bar{q} are phase mean values for that ship. The deviations were averaged for all ships reporting in each array to obtain mean deviations for the B-array and for the A/B-array. The B and A/B deviations were averaged linearly yielding a mean deviation value for the A/B-scale. Throughout the remainder of this paper ΔT and Δq will refer to the mean deviation values at one level and one time period averaged over the 2 arrays. By adding the deviation values to the U.S. phase mean vertical profile, the A/B-scale temperature and moisture values at each level were obtained at individual time periods.

It was not possible to obtain estimates of mean temperature and moisture gradients across the A/B-scale using deviation values. Therefore, the long term mean advections of these quantities do not appear explicitly in the budgets. It was possible, however, to compute deviation advections. This was done by fitting individual ship deviation T and q values to a plane to obtain gradients of these quantities ($\partial \Delta T / \partial x$, $\partial \Delta T / \partial y$, etc.) as in the divergence computation. The mean wind components (\bar{u} , \bar{v}) were combined with these gradients to give the advection in excess/deficit of the mean advection at each time period.

2.3 Budget Computations

Diagnostic budget analyses of moisture and dry static energy (s) were performed. Budgets on the momentum/vorticity fields are planned for the near future. Dry static energy is defined by Eq. 7:

$$s = C_p T + gz \quad (7)$$

where C_p = specific heat at constant pressure,
 g = gravitational constant, and
 z = height.

The individual time period budget equations are (8, 9):

$$\frac{L}{C_p} \left[\frac{\partial \bar{q}}{\partial t} + \nabla \cdot \bar{v}q + \frac{\partial \bar{q}\omega}{\partial p} \right] = \frac{-L}{C_p} (c-e) \quad (8)$$

$$\frac{\partial \bar{s}}{\partial t} + \nabla \cdot \bar{v}s + \frac{\partial \bar{s}\omega}{\partial p} = Q_R + \frac{L}{C_p} (c-e) \quad (9)$$

where the overbar represents a spacial average of the observations over the A/B-array, L = latent heat of condensation, c = total condensation, e = total evaporation and Q_R = radiative heating rate.

Time Rates of Change. The first terms on the left side of Eqs. 8 and 9 are the time rates of change of q, s . These were determined from the mean array vertical profiles at the previous and subsequent time periods. Changes in s were assumed to result only from changes in $\frac{C_p T}{p}$ due to poor resolution of $\bar{g}z$ at individual time periods. During convective conditions, however, there may have been a sampling problem. Active convective cloud elements covered only a small fraction of the array. Since a maximum of 12 soundings were available at any time period, a representative sampling of the clouds was impossible. This was further complicated by the instrument problems encountered when rawinsondes entered intense clouds. Water and freezing problems often resulted in premature termination of such soundings. In most cases the soundings probably undersampled clouds. This causes no great problems in the s budget since the small differences between \bar{s} (mean outside clouds) and s_c (s in clouds) coupled with the small area coverage of

active buoyant updrafts permit the accurate approximation:

$$\bar{s} \approx \tilde{s} \quad (10)$$

In the q budget undersampling or missampling are more important. Differences between environmental (\bar{q}) and cloud (q_c) moisture values are high even in the numerous weak and small clouds and could lead to inaccuracies in observed values of $\partial\bar{q}/\partial t$. The possibility that the storage of water vapor in clouds is not measured properly is discussed later.

Horizontal Fluxes. The second terms on the left side of Eqs. 8 and 9 are the horizontal flux convergence of q and s . No attempt was made to resolve spacial eddy fluxes (deviations from the areal mean fluxes). These terms were broken down into advective and convergent terms, e.g.:

$$\overline{\nabla \cdot vq} \approx \underbrace{\bar{q} \overline{\nabla \cdot v}}_{(1)} + \underbrace{\bar{v} \cdot \overline{\nabla q}}_{(2)} \quad (11)$$

Term (1) is simply the mean divergence multiplied by the mean values of q at each level. Term (2) is obtained from applying the mean \bar{u} and \bar{v} wind components to the A/B-scale eddy gradients of moisture as discussed in the previous section. Since deviation q values (Δq) were used, there is a missing component - the time and space averaged advection for the A/B-array; i.e.:

$$\bar{v} \cdot \overline{\nabla q} = \underbrace{\bar{v} \cdot \overline{\nabla [q]}}_{(a)} + \underbrace{\bar{v} \cdot \overline{\nabla (\Delta q)}}_{(b)} \quad (12)$$

where $[q]$ is the phase mean average moisture. Only term (b) is measured here.

Surface Fluxes. The third terms on the left side of Eqs. 8 and 9 are the vertical flux terms. Since the budget will be integrated from the surface to 100 mb (where $\bar{\omega} = 0$), these terms are merely the sea surface to air fluxes of q and s (E_o and S_o , respectively). These fluxes are taken from the bulk aerodynamic formulae:

$$E_o = \rho_o C_E \bar{V}_o (q_s - q_o) \quad (13)$$

$$S_o = \rho_o C_s \bar{V}_o (T_s - T_o) \quad (14)$$

where q_s , T_s are values for the ocean surface and q_o , T_o , \bar{V}_o are values at 10 m elevation. The coefficients used are $C_E = 1.6 \times 10^{-3}$ and $C_s = 1.4 \times 10^{-3}$ (Businger and Seguin, 1977).

Radiation. The radiation term in Eq. 9 (Q_R) was obtained from computations of Cox and Griffith (1978) for Phase III. Mean Phase III Q_R values for each time of day were computed for disturbed and undisturbed conditions and applied to Phases I and II according to the estimated rainfall at each time period. As will be shown, the net tropospheric radiational heating at a given time of day varied only weakly with the intensity of the convection.

Condensation. The remaining terms of Eqs. 8 and 9 are the net condensation warming $[\frac{L}{C_p} \cdot (c-e)]$ terms which are found as a residual. These are compared with radar precipitation estimates for the GATE master array made by Hudlow (1978). The master array is a circle of approximately 204 km radius in the center of the A/B-array. It is slightly larger than the B-scale area and covers about 25% of the A/B-scale area.

3. BUDGET RESULTS

3.1 Phase Mean Budgets

The averaged budgets for each phase are presented first to illustrate the mean conditions during GATE. Tables 1-3 show the mean q and s budgets for Phases I - III and the extreme variations of each term at individual time periods. Units are $^{\circ}\text{C d}^{-1}$ where 1°C d^{-1} averaged through a 1012 mb to 100 mb layer is equivalent to $0.374 \text{ g cm}^{-2}\text{d}^{-1}$ of water vapor. Averaged over an entire phase, the water budget is primarily a balance between large scale moisture convergence, surface evaporation, and condensation. There is some deviation dry advection in every phase ($-.22$ to $-.44^{\circ}\text{C d}^{-1}$), while the storage term $(\frac{L}{C} \frac{\partial \bar{q}}{\partial t})$ is very small. About 20-30% of the GATE A/B-scale precipitation results from surface evaporation within the array. The phase mean s budgets show a balance between mean convergence of s , radiation and condensation, with the storage, advection and surface flux terms being 1 or 2 orders of magnitude smaller.

The picture is quite different at individual time periods. While the convergence and condensation are usually the largest terms, the storage and advective terms vary rapidly and are often important at individual time periods. The magnitudes of their largest variations can be seen in Tables 1-3. In contrast, the surface flux terms (E_o, S_o) change rather slowly with modest amplitudes. The radiational heating term exhibits a marked diurnal variation which accounts for virtually all of the range shown in Tables 1-3. This will be discussed later.

Table 4 compares the diagnosed net condensation values from the q and s budgets ($C(q)$ and $C(s)$ respectively) to radar-determined

TABLE 1

Phase I Mean A/B-Scale Moisture and Dry Static Energy Budgets
 (Vertically integrated, surface - 100 mb ($^{\circ}\text{C d}^{-1}$))
 Each Term is Written Such That a Positive Number Corresponds to
 Positive Condensation From Eqs. 8 and 9.

	<u>q</u>			<u>s</u>	
	Mean	Individual Period Range		Mean	Individual Period Range
$-\frac{L}{C_p} \frac{\partial \bar{q}}{\partial t}$.03	-8.26 to 5.57	$\frac{\partial \bar{s}}{\partial t}$	0	+2.40 to -1.88
$-\frac{L}{C_p} \bar{q} \overline{\nabla \cdot \nabla}$	3.48	14.00 to -3.71	$\bar{s} \overline{\nabla \cdot \nabla}$	2.88	14.43 to -5.57
$-\frac{L}{C_p} \overline{\nabla \cdot \nabla (\Delta q)}$	-.24	+1.49 to -2.69	$\overline{\nabla \cdot \nabla (\Delta s)}$	-.03	-1.14 to 1.33
E_o	.94	+1.79 to +.48	$-S_o$	-.10	-.27 to -.02
			$-Q_R$	1.16	.16 to 1.81
$\frac{L}{C_p} (c-e)$	4.21		$\frac{L}{C_p} (c-e)$	3.91	
(vapor equivalent)	(1.57 g cm ⁻² d ⁻¹)		(vapor equivalent)	(1.46 g cm ⁻² d ⁻¹)	

TABLE 2

As in Table 1 for Phase II

	q		s	
	Mean	Individual Period Range	Mean	Individual Period Range
$-\frac{L}{C_p} \frac{\partial q}{\partial t}$.11	-4.88 to +3.78	.04	+3.28 to -2.44
$-\frac{L}{C_p} \bar{q} \bar{v} \bar{v}$	2.68	9.66 to -3.24	1.90	9.35 to -3.67
$-\frac{L}{C_p} \overline{\bar{v} \cdot \bar{v}} (\Delta q)$	-.32	1.47 to -2.39	-.10	-1.83 to .80
E_o	.99	+1.74 to +.48	-.09	-.20 to -.01
			- Q_R	.16 to 1.81
			$\frac{L}{C_p} (c-e)$	
	3.46		2.91	
	(1.29 g cm ⁻² d ⁻¹)		(vapor equivalent)	(1.09 g cm ⁻² d ⁻¹)

TABLE 3

As in Table 1 for Phase III

	\bar{q}		\bar{s}	
	Mean	Individual Period Range	Mean	Individual Period Range
$-\frac{L}{C_p} \frac{\partial \bar{q}}{\partial t}$.09	-3.88 to +4.80	$\frac{\partial \bar{s}}{\partial t}$ 0	+2.08 to -3.00
$-\frac{L}{C_p} \bar{q} \bar{V} \cdot \bar{V}$	2.87	10.70 to -3.15	$\bar{s} \cdot \bar{V} \cdot \bar{V}$ 2.24	11.00 to -3.81
$-\frac{L}{C_p} \bar{V} \cdot \bar{V} (\Delta \bar{q})$	-.44	+1.37 to -2.31	$\bar{V} \cdot \bar{V} (\Delta \bar{s})$ -.03	-.90 to +.61
E_o	1.10	+1.74 to +.53	$-S_o$ -.11	-.22 to -.01 .10 to +1.99
			$-Q_R$ 1.16	
$\frac{L}{C_p} (c-e)$ (vapor equivalent)	3.62 (1.35 g cm ⁻² d ⁻¹)		$\frac{L}{C_p} (c-e)$ 3.26 (vapor equivalent) (1.22 g cm ⁻² d ⁻¹)	

TABLE 4

Net Condensation for the GATE A/B-Scale Determined From q and S Budgets and From Radar Rainfall for Master Array. ($^{\circ}\text{C}/\text{d}$) ($1^{\circ}\text{C}/\text{d} \approx .37 \text{ g cm}^{-2} \text{ d}^{-1}$).

	q-budget $\frac{L}{C_p}$ (c-e)	s-budget $\frac{L}{C_p}$ (c-e)	Master Array P (R) Radar Rainfall Hudlow, 1978 ($\times \frac{L}{C_p}$)
Phase I	4.29	3.91	2.97
Phase II	3.01*	2.47*	2.23
Phase III	3.62	3.26	3.01
Mean	3.64 ($1.36 \text{ g cm}^{-2} \text{ d}^{-1}$)	3.21 ($1.20 \text{ g cm}^{-2} \text{ d}^{-1}$)	2.74 ($1.02 \text{ g cm}^{-2} \text{ d}^{-1}$)

*Three days of rainfall data from 21 GMT 30 Jul 74 through 18 GMT 2 Aug 74 were omitted since the radar was inoperative during that period.

rainfall ($P(R)$) for the GATE master array (Hudlow, 1978). In each phase the q budget rate exceeded the s budget, and both budgets exceeded the radar estimate. For phase averaged budgets the storage of water vapor, liquid water or warm air, in or out of clouds, cannot explain the discrepancy between the budget rainfall rates. It is also unlikely that the surface flux term is responsible. The surface flux computations are in good agreement with the results of small scale studies of the GATE boundary layer summarized by Businger and Seguin (1977). Surface fluxes of vapor would have had to be estimated about 40 percent too large to explain these s - q differences. The Q_R values for Phase III obtained by Cox and Griffith (1978) should likely be adequate for the other phases. Since the Cox and Griffith model-determined net tropospheric radiational heating for the whole A/B-area varied little with changes in convection or synoptic condition during Phase III, it is assumed that the Q_R values for Phases I and II also did not show large variation with convective state and can also be used during these phases.

The exact source of the q - s budget condensation differences cannot be determined with certainty. These differences would be resolved if the inward vapor fluxes could be reduced by 15 percent or if cooling were -1.56°C/d rather than the value of -1.16°C/d (from Cox and Griffith) which was used. But this discrepancy in calculated vs. estimated (Cox and Griffith) radiation appears too large. Can this radiational cooling estimate be 30% too low? These s - q budget differences may result from a 15 percent overestimate of the inward vapor transport of the q -budget. Although the same divergence profiles were used in both s and q budgets, systematic inaccuracies may exist in either the upper or lower tropospheric divergence profiles and one or both divergence calculations

could be slightly in error. However, there is no reason to expect systematic divergence errors. Small scale spatial eddy fluxes were neglected, but horizontal eddy transports of water vapor and static energy are usually small in the tropics, even in intense tropical cyclones at radii similar to the A/B-scale (Frank, 1977b). The most likely source of s-q budget error (assuming the Cox and Griffith radiation values are correct) is in the advection terms which omitted the time averaged mean advection. Horizontal temperature gradients are generally weak in the tropics, but moisture gradients in the vicinity of the Inter Tropical Convergence Zone (ITCZ) may be significant. The deviation advection values of Tables 1-3 show a degree of dry advection into the A/B-area while temperature advection was comparatively weak. This suggests that there may have been a small amount of long term advection of dry air into the GATE region as well.

Most of the deviation dry air advection occurs between 600-800 mb and is associated with the middle level jet coming off of Africa (Fig. 2). It should not be surprising if the prevailing easterly flow in that layer averaged for a phase also acted to dry the GATE A/B-area. Such a small mean advection drying requires that the USSR eastern and western ship data have some systematic error because this affect cannot be directly calculated.

The precipitation values derived from the s and q budgets agree rather well. Each approach has its advantages. The s budget has only a slight storage sampling problem, and variations in the sea surface to air flux are insignificant. The q budget is less sensitive to upper level wind measurements and requires no Q_R estimate.

The Hudlow (1978) A/B-array combined radar-satellite rain estimates

of 1.02 cm/d (1.08, .86 and 1.12 by phase) require (using the s budget) a tropospheric radiational cooling of only about $0.5^{\circ}\text{C}/\text{d}$ which is more than 50% lower than Cox and Griffith radiation estimates and only one-third as much as the combined s and q budget estimates. These combined radar-satellite estimates are considered to be much too low.

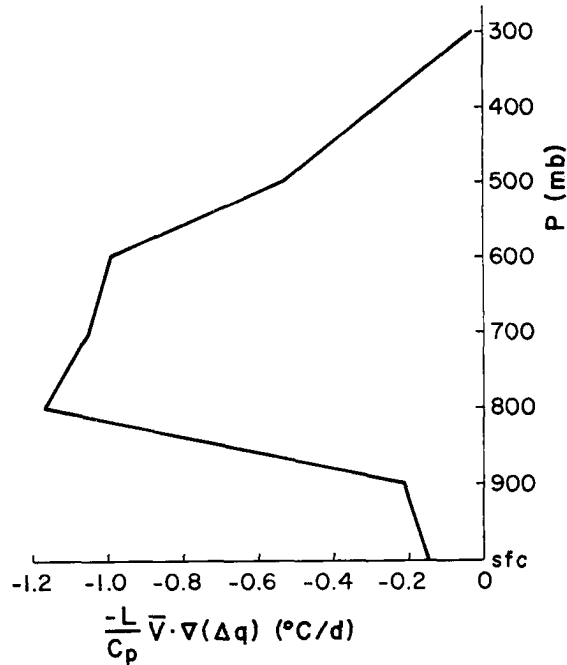


Fig. 2. Advection of moisture for the A/B-area computed using deviation moisture values (Δq).

3.2 Individual Time Period Budgets

s Budget and q Budget Condensation. Comparisons of individual time period condensation rates derived from the s and q budgets are shown in Figs. 3-5. Except for the small differences in the overall phase mean values, the two curves agree very well. The condensation estimates for individual convective disturbances are very nearly in phase indicating that undersampling of the cloud water vapor storage is not a significant problem in analyses on the A/B-scale. If $\frac{\partial q_c}{\partial t}$ were large, the s budget condensation would be expected to lag the q budget curve noticeably, but the observed lag is very small and can be detected only in averaged data.

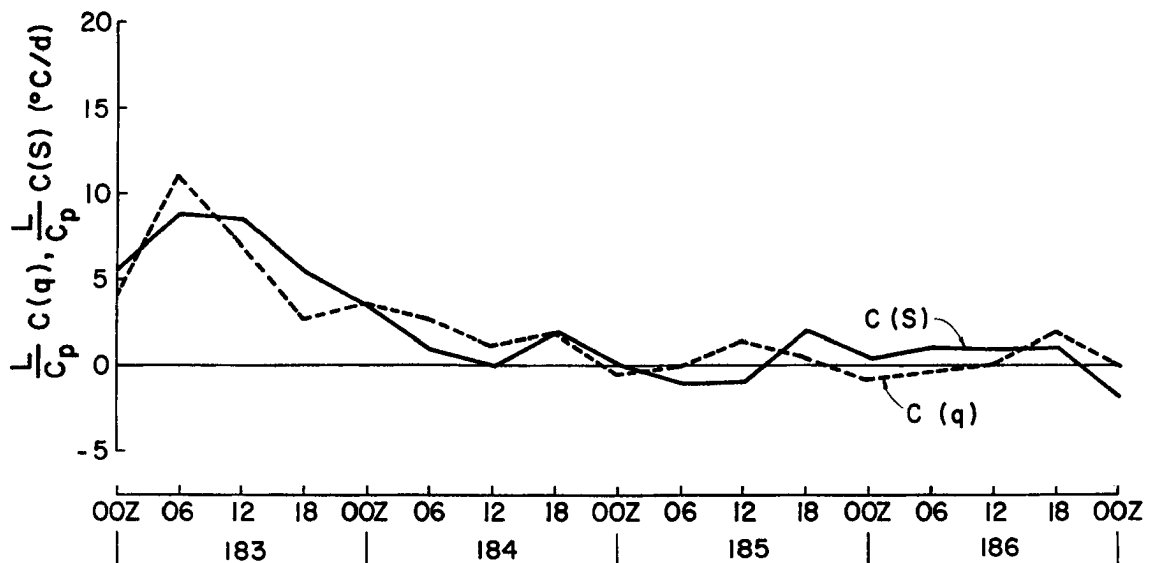
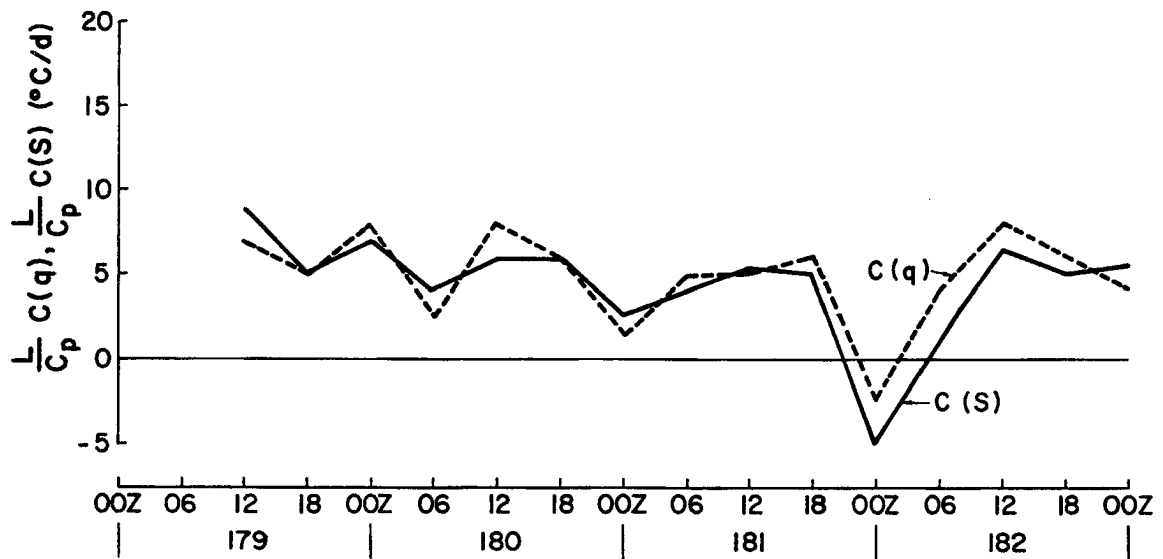


Fig. 3. Net condensation computed from s and q budgets ($C(s)$ and $C(q)$ respectively) at individual time periods. Phase I. ($^{\circ}\text{C d}^{-1}$). ($1^{\circ}\text{C d}^{-1} \sim .37 \text{ g cm}^{-2} \text{ d}^{-1}$).

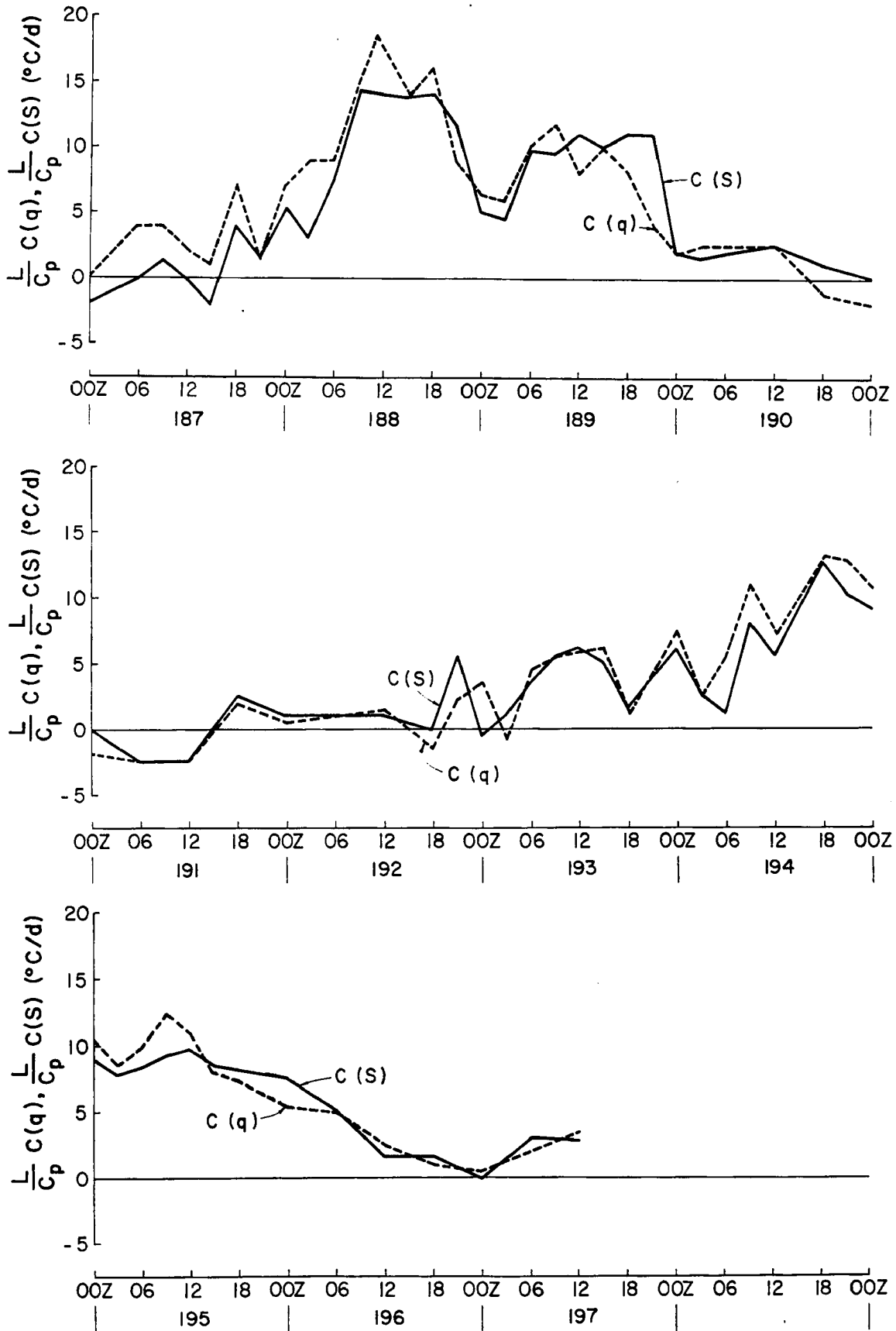


Fig. 3. Continued.

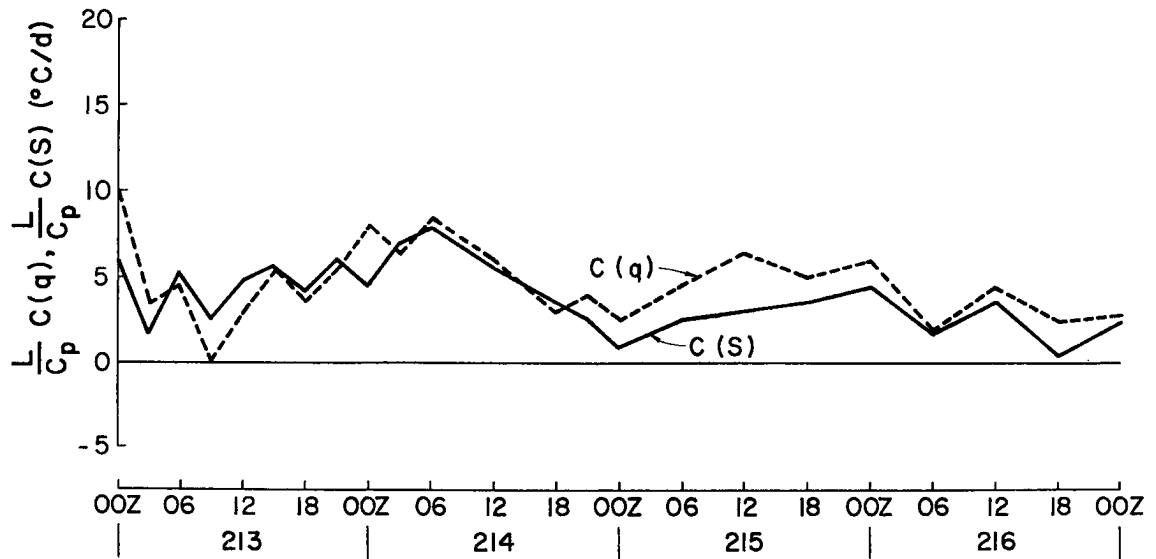
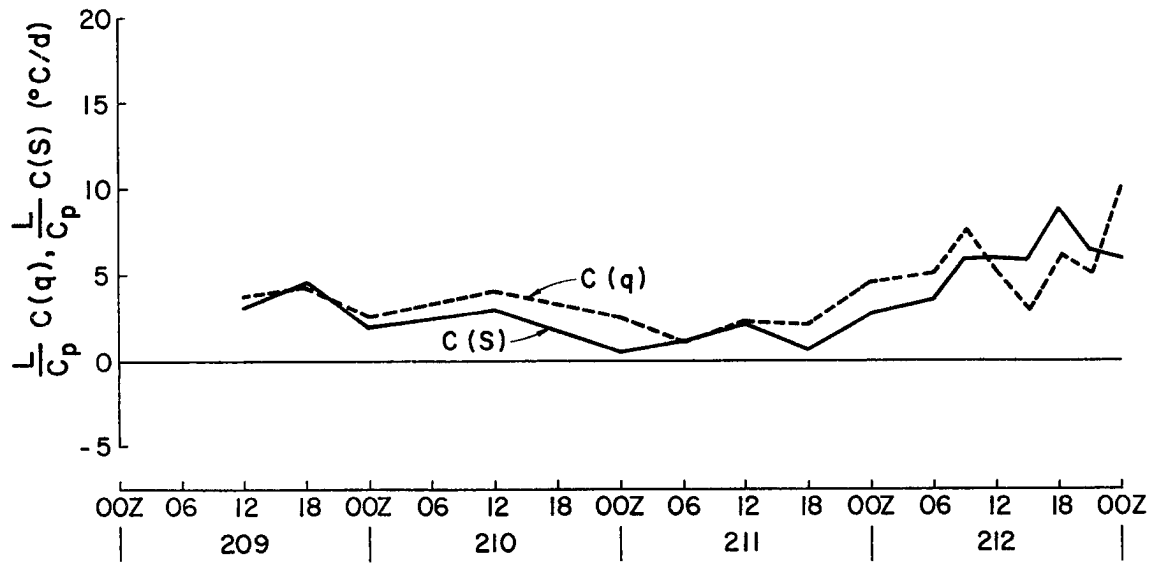


Fig. 4. Same as Fig. 3 except for Phase II.

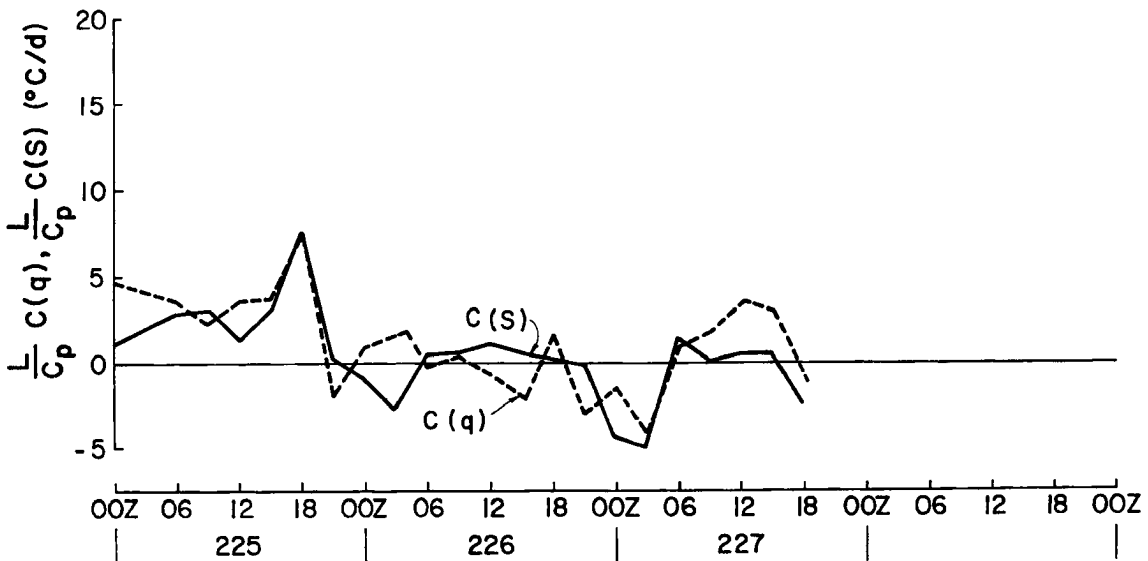
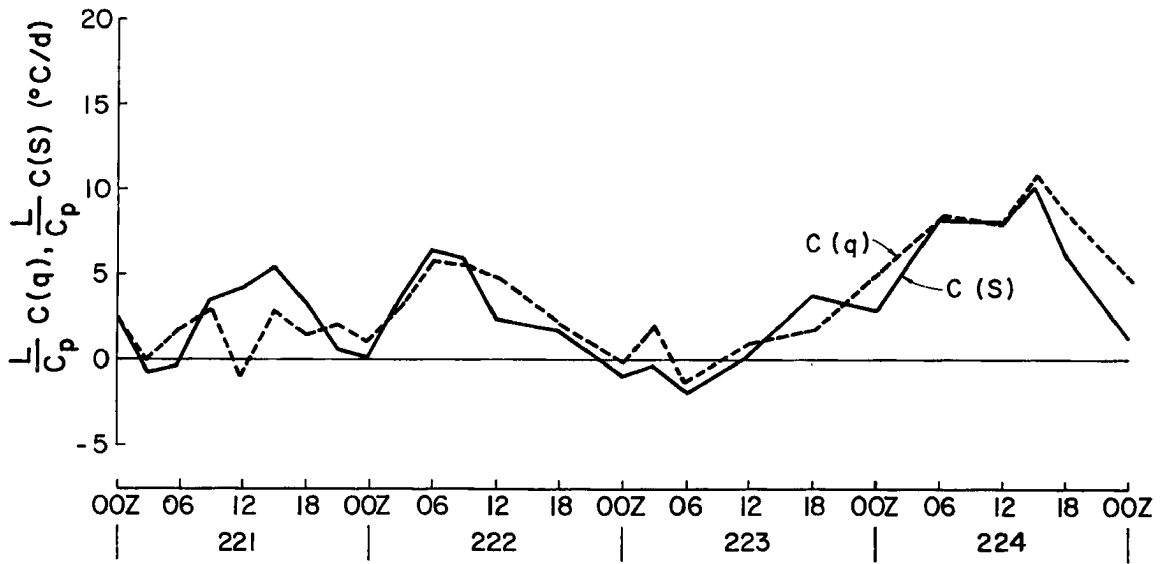
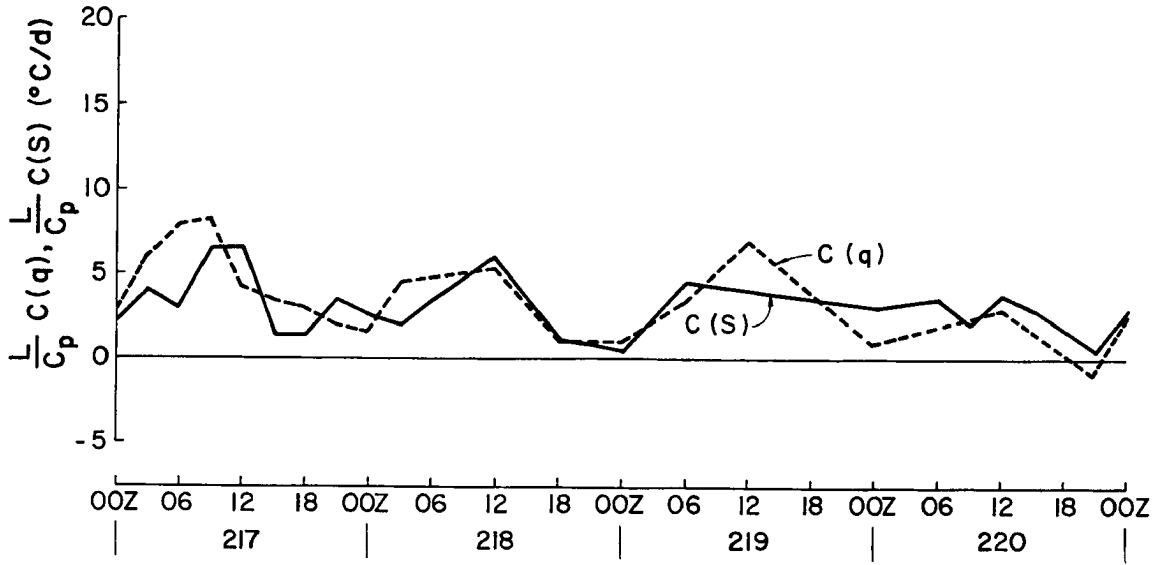


Fig. 4. Continued.

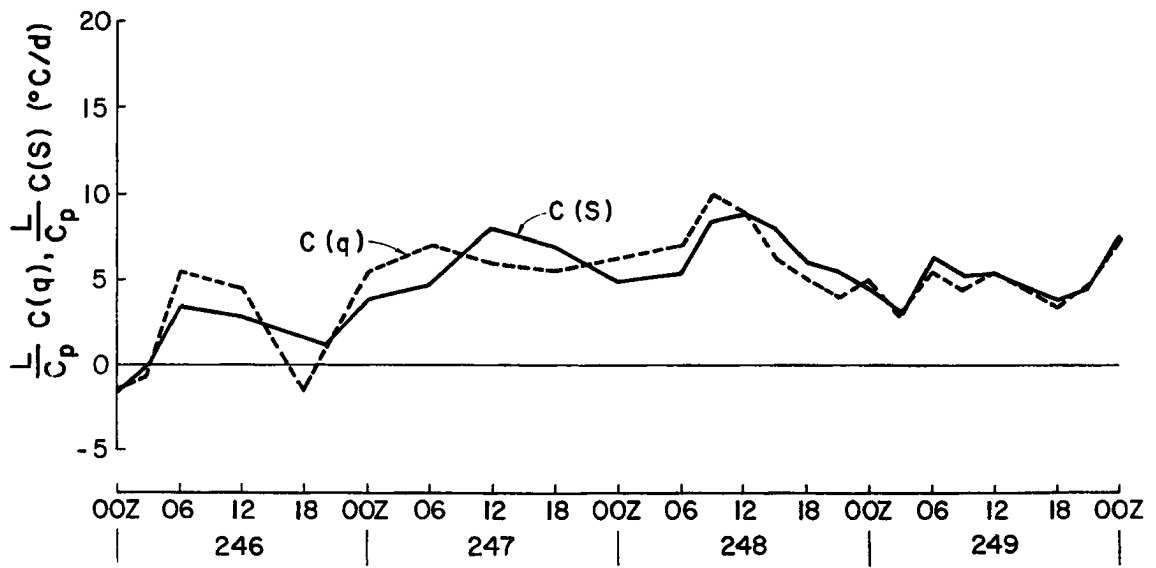
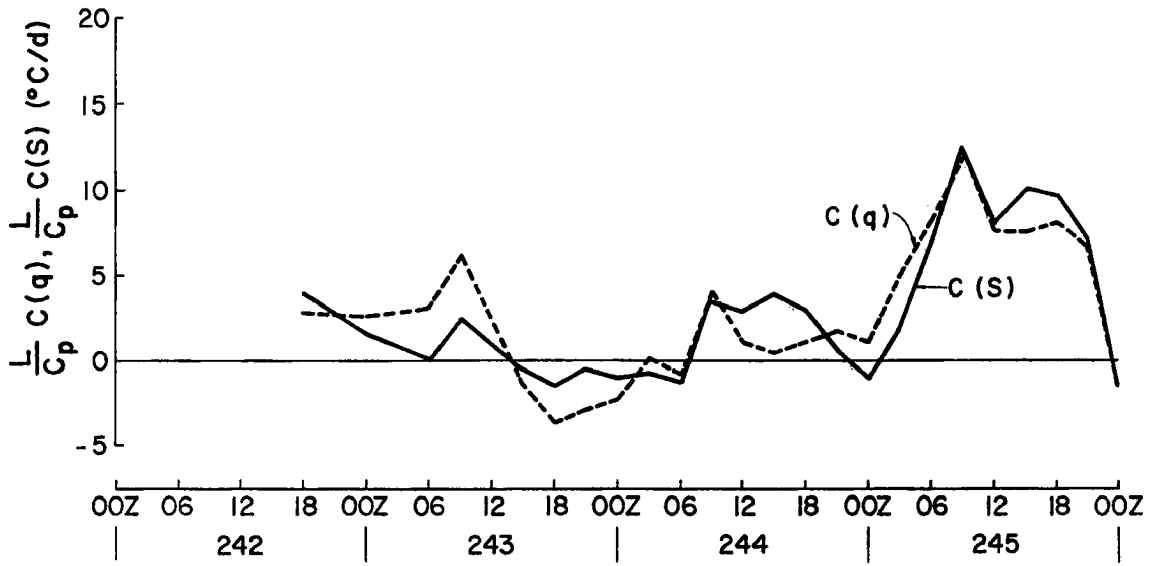


Fig. 5. Same as Fig. 3 except for Phase III.

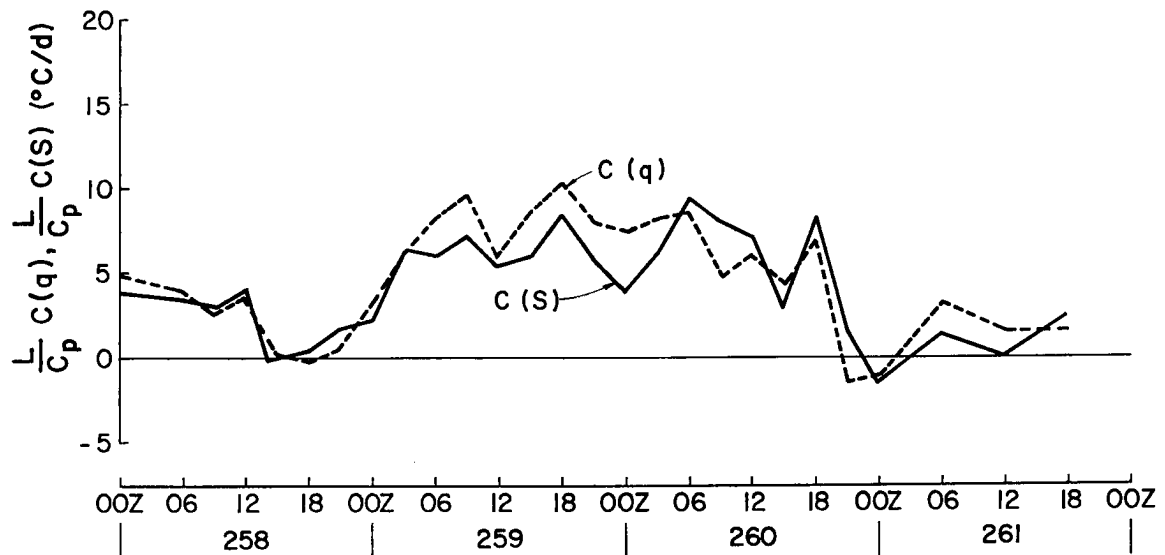
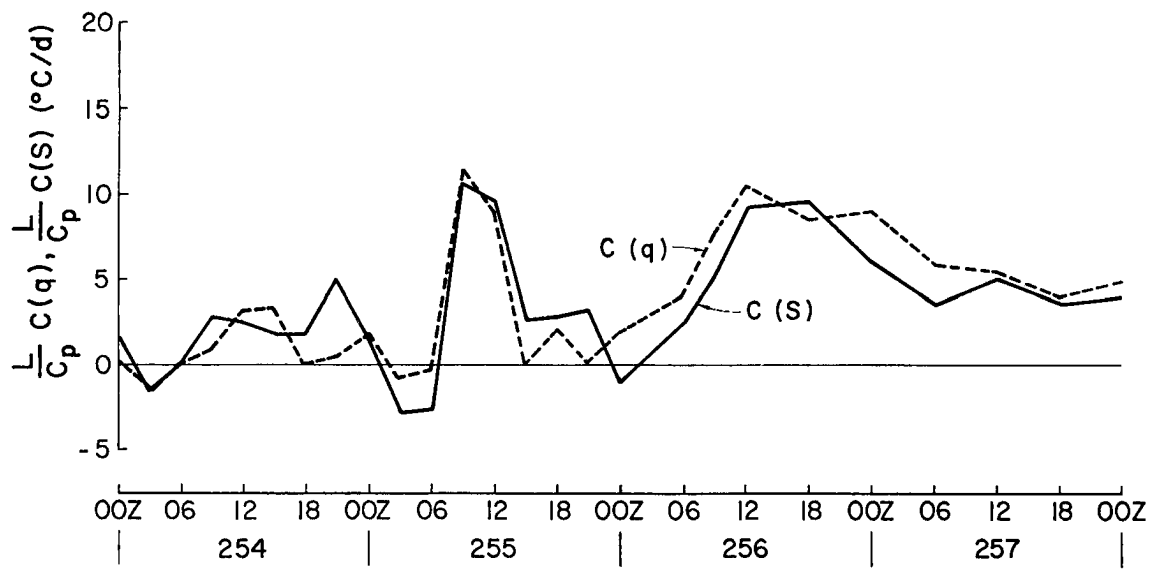
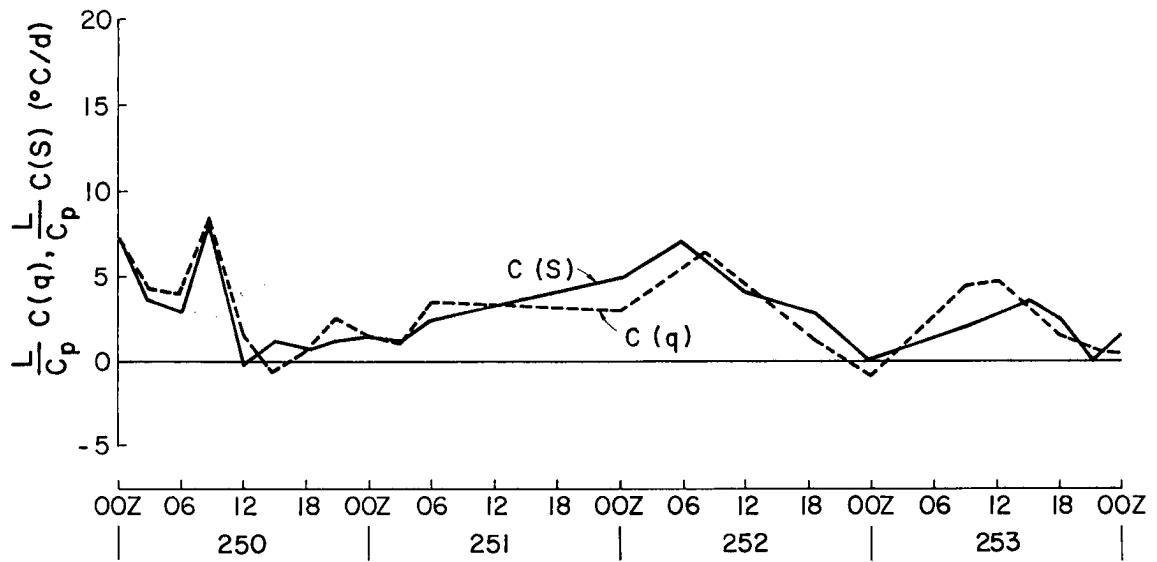


Fig. 5. Continued.

s Budget vs. Radar Rainfall. Table 4 showed that the s budget net condensation rate exceeded the radar rainfall rate in all three phases by an average of $.47^{\circ}\text{C d}^{-1}$ ($.18 \text{ g/cm}^2\text{d}$) or about 15%. Comparison of the two figures is hampered by the fact that the radar sampled only about the center 25% of the A/B-array. Nevertheless, combined satellite and radar rainfall estimates indicate that mean precipitation rates in the B-scale and master array areas were higher than rates for the entire A/B-area (Hudlow, 1978). There is clearly a discrepancy. Figures 6-8 compare s budget condensation with master array rainfall estimates. Two features are obvious:

- 1) During very disturbed or high rainfall periods the total episode rainfalls estimated by the s budget and by the radar are comparable, but a significant lag is observed.
- 2) During periods of light to moderate rainfall the s budget consistently predicts more rainfall than does the radar.

Based on the results of Tables 1-4 and Figs. 3-8, it is concluded that the radar rainfall estimates are too low during periods of light to moderate rainfall ($0-5^{\circ}\text{C d}^{-1}$). This may result from incorrect Z-R ratios applied to low radar reflectivity values. There are noticeable differences between Z-R ratios for GATE derived by different groups (Cunning and Sax, 1977). This does not mean to imply that the s budget analyses are free from error. There could be unknown problems with the s divergence term (the remaining terms are too small or well known when averaged over a phase to contain errors large enough to explain the mean s budget and radar differences). However, in the absence of any known biases in the A/B-array wind measurements, the budget rainfall values appear to offer the best estimate of the true GATE A/B-scale rainfall.

3.3 Lag Between Budget Condensation and Radar Rainfall

Figures 6-8 show that during most disturbed periods with deep convection the radar precipitation lagged the s budget condensation. Table 5 shows the lag between the peak budget condensation and the peak radar rainfall for the 10 distinct rainfall episodes with maximum rainfall/condensation rates $\geq 7^{\circ}\text{C d}^{-1}$ ($2.6 \text{ g cm}^{-2} \text{ d}^{-1}$). The peak is defined as the time at which the rainfall reached either its maximum value or the beginning of a "steady" plateau. Also shown is the lag between the times when the increasing rainfall/condensation rate first exceeded 5°C d^{-1} ($1.9 \text{ g cm}^{-2} \text{ d}^{-1}$). This value was selected to provide comparable points during the system intensifications. It must be noted that s budget computations were made at 3 or 6-hour intervals restricting the time resolution in individual cases. Radar rainfall data are hourly averages.

The data show considerable scatter but indicate a lag on the order of 4-6 hours. The only case without a peak lag of at least 3 hours is day 224 (12 Aug 74), and this may be due to an inability to resolve the time of maximum condensation accurately (Fig. 7).

There are several possible hypotheses to explain the budget/radar time lag:

- 1) The s budget computations are in error and diagnose the rainfall peak too early.
- 2) The radar rainfall underestimated rain in the growing stages and overestimated rain in the latter stages of convective system development.
- 3) There was significant storage of liquid water (q_l) so that the condensation rate of the s budget does not coincide with the true precipitation rate.
- 4) There was an area sampling problem, i.e. - rainfall within the radar coverage of the master array occurred later than the mean rain for the entire A/B-array.

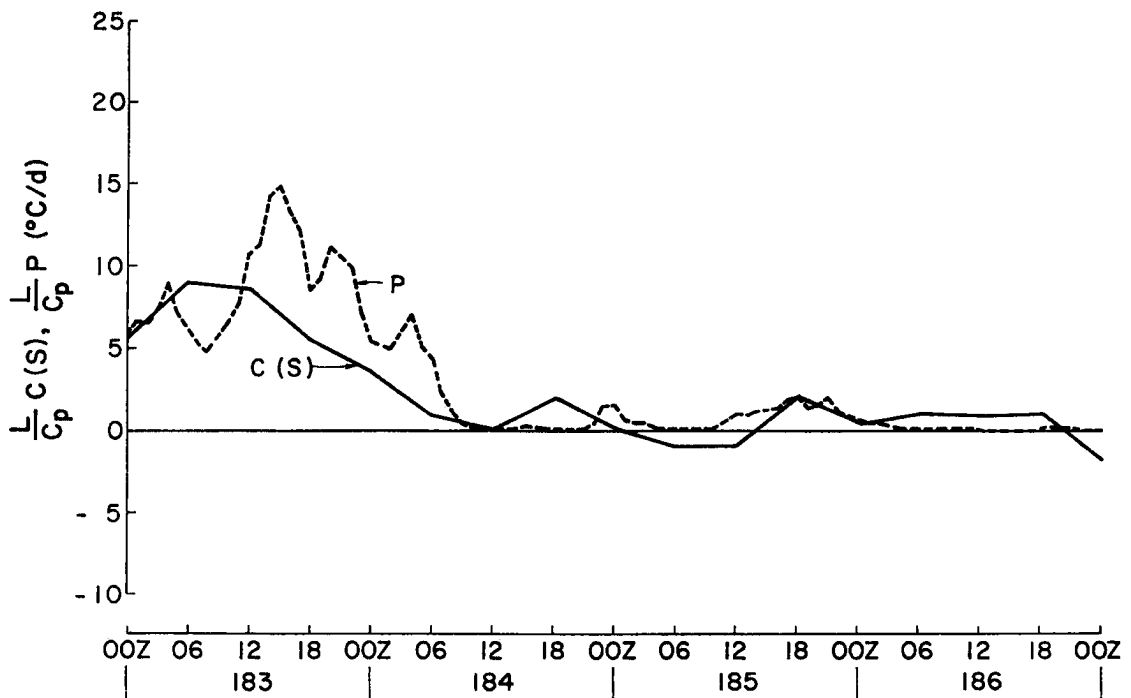
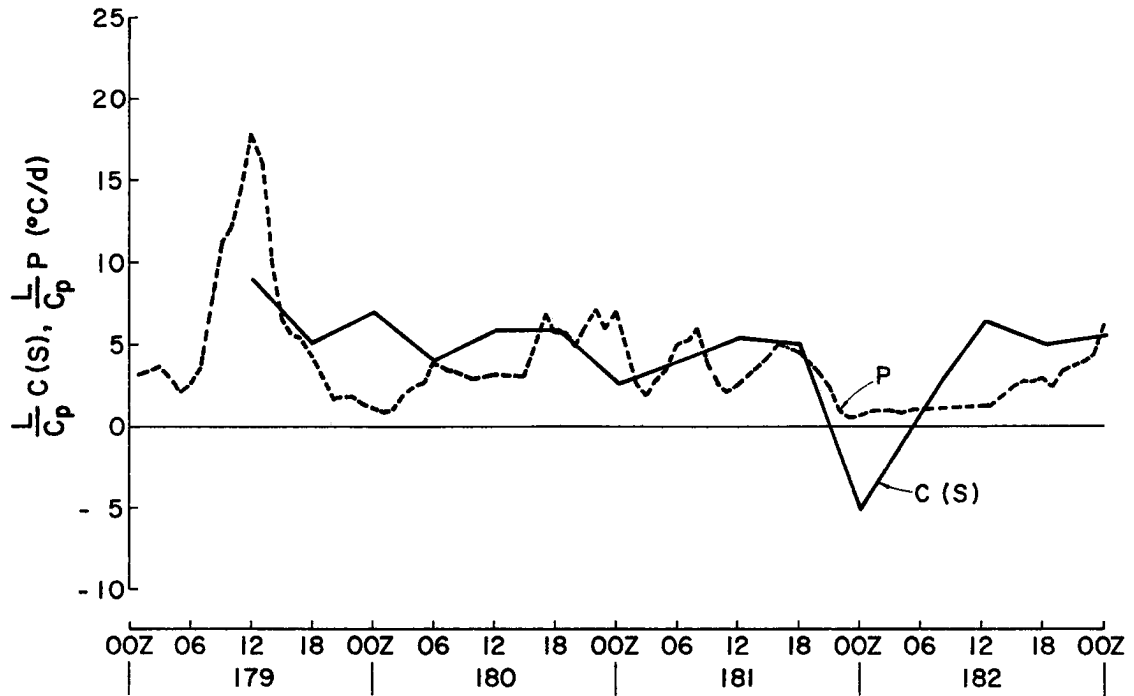


Fig. 6. s-budget condensation ($C(s)$) and master array radar rainfall (P) for Phase I. ($^\circ C d^{-1}$). ($1^\circ C d^{-1} \sim .37 g cm^{-2} d^{-1}$).

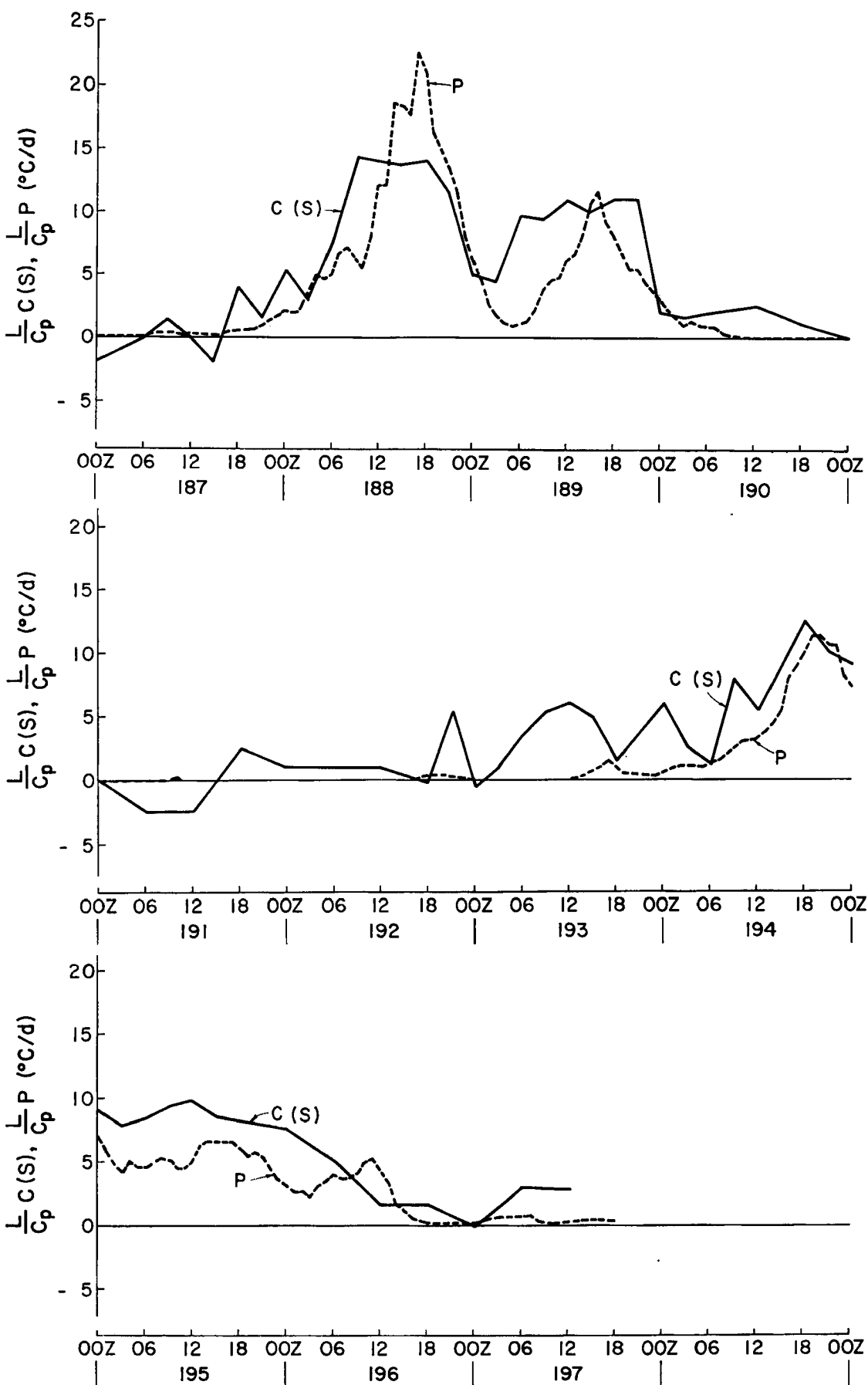


Fig. 6. Continued.

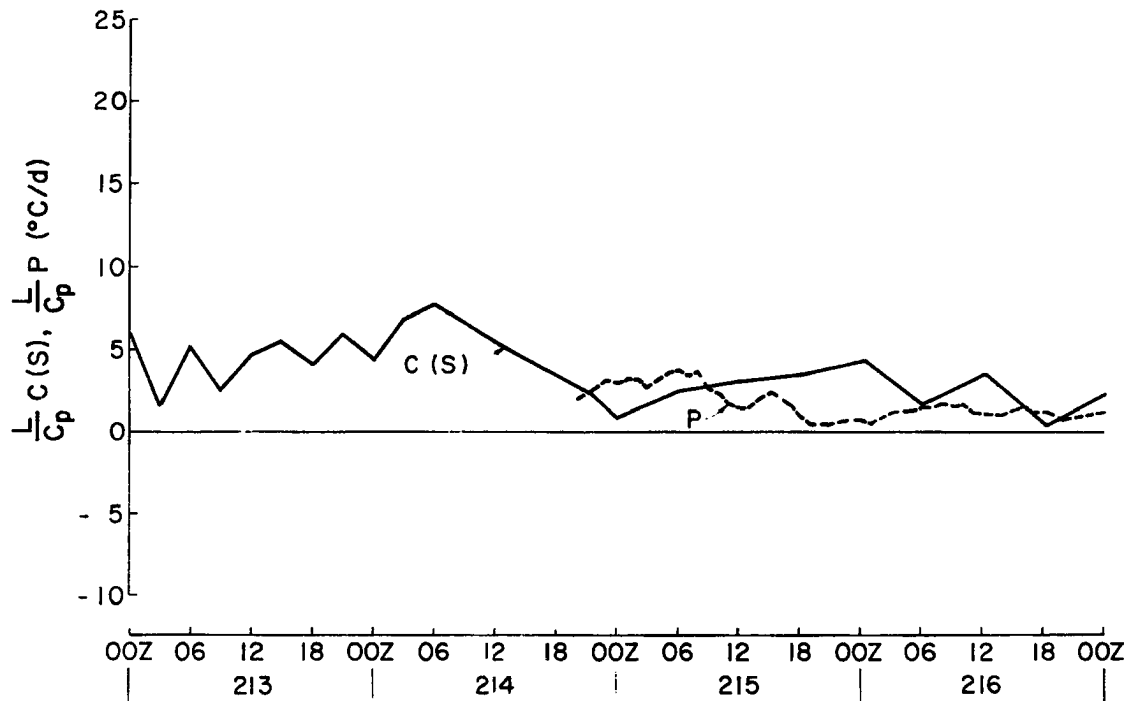
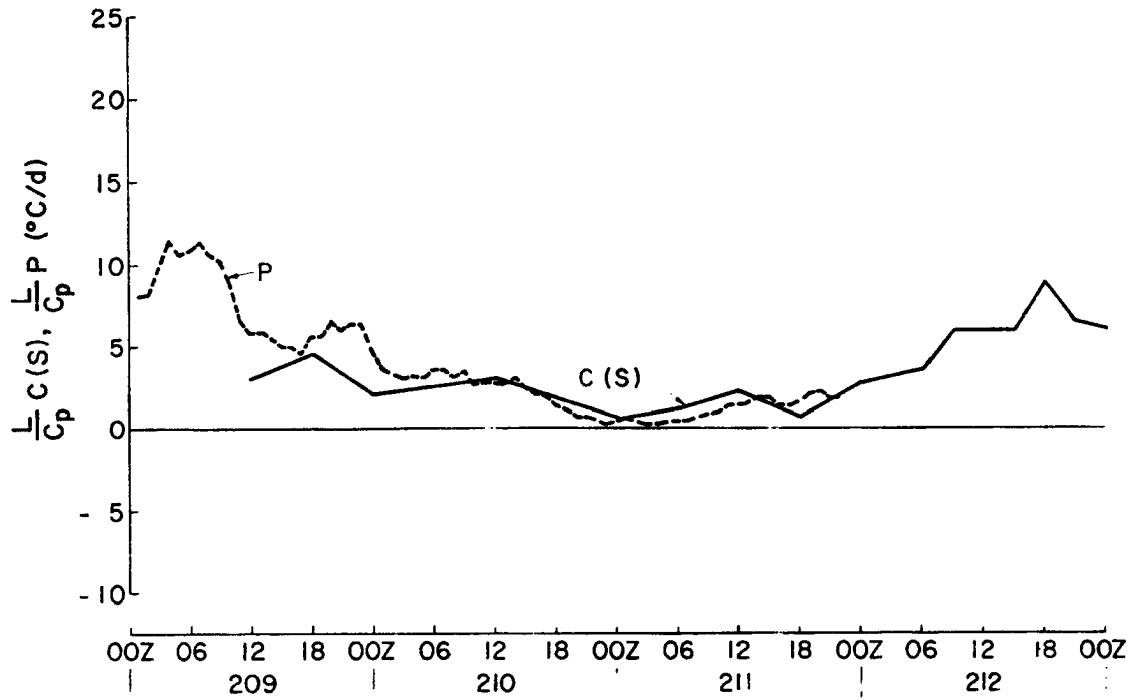


Fig. 7. Same as Fig. 6 except for Phase II.

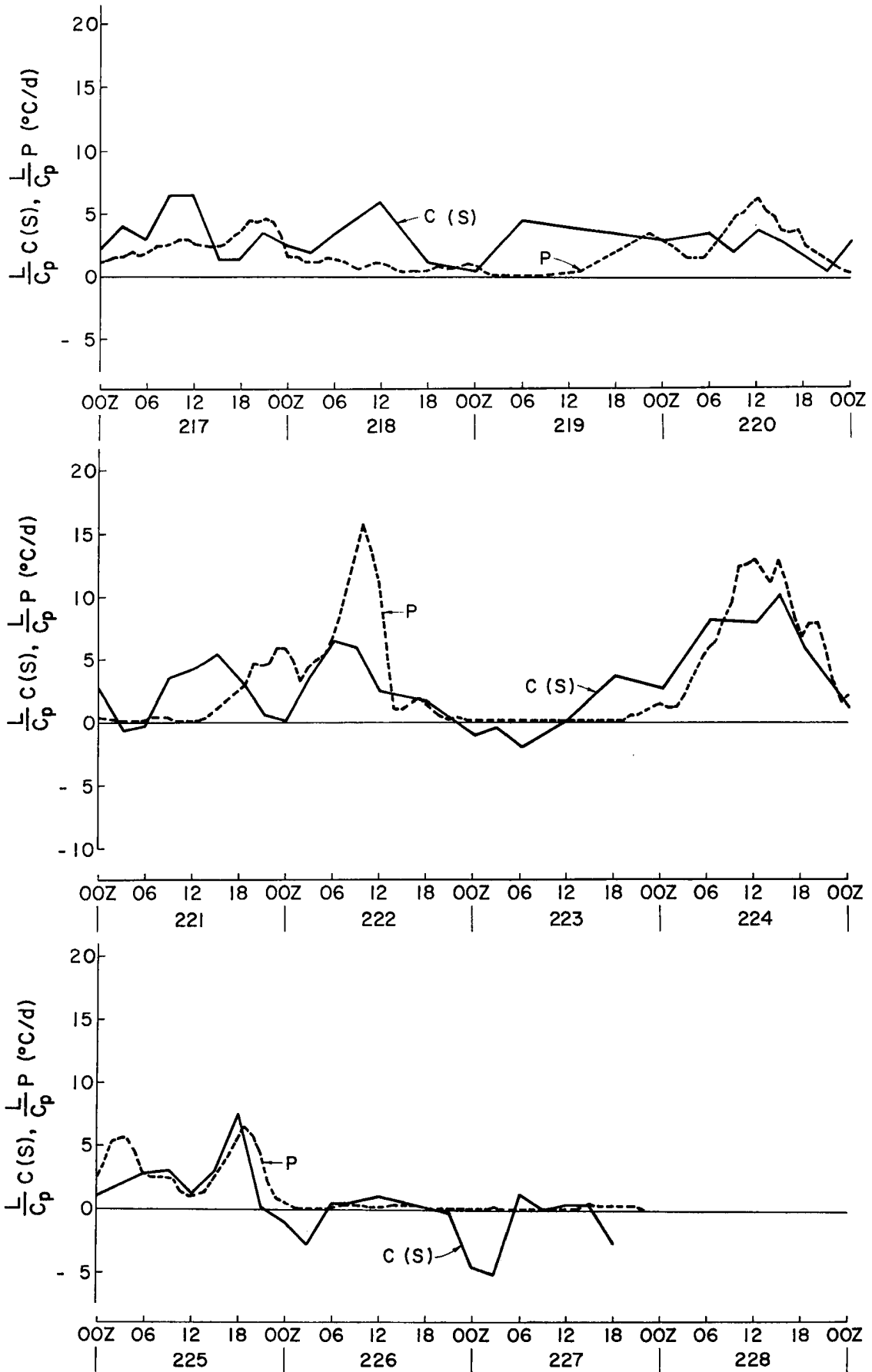


Fig. 7. Continued.

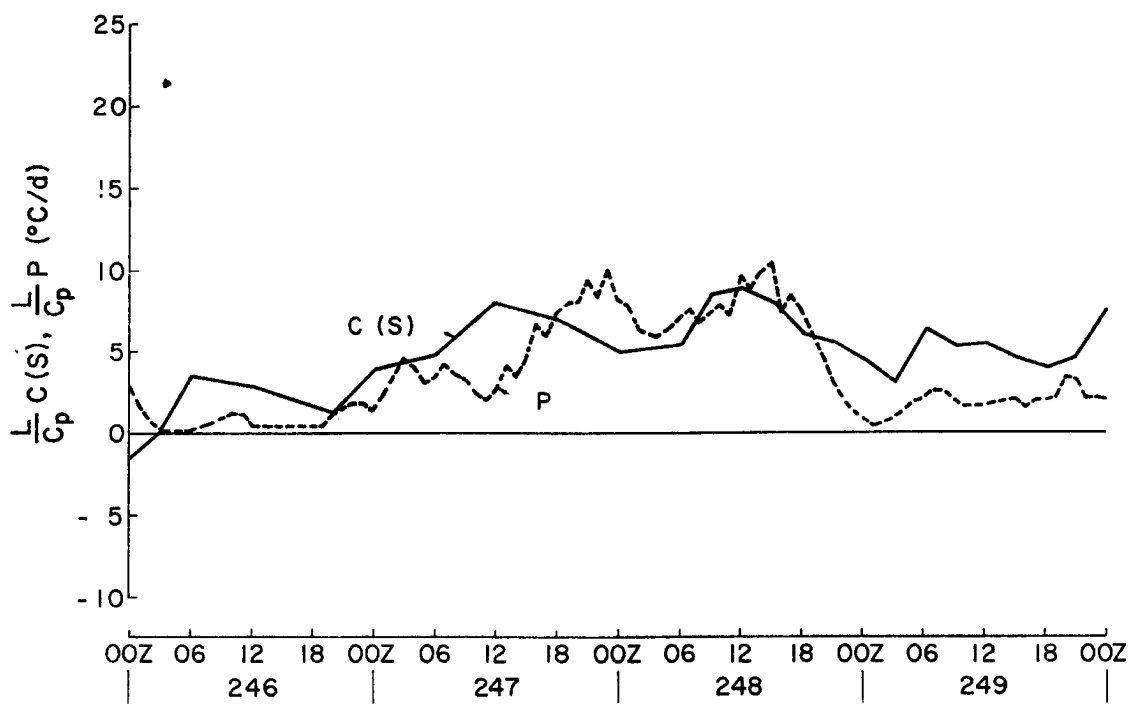
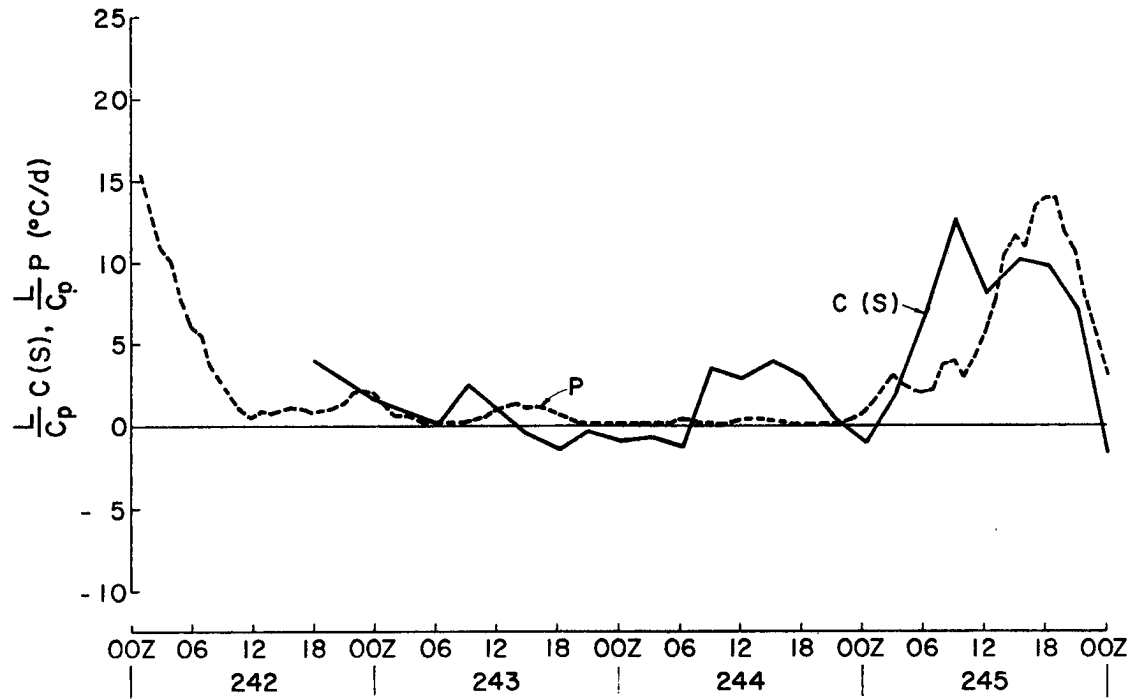


Fig. 8. Same as Fig. 6 except for Phase III.

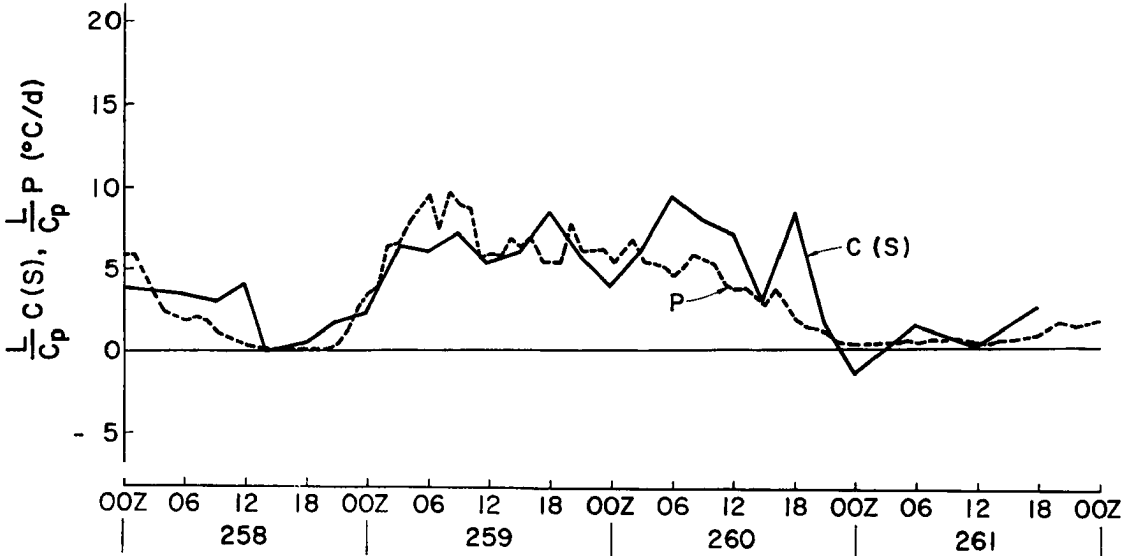
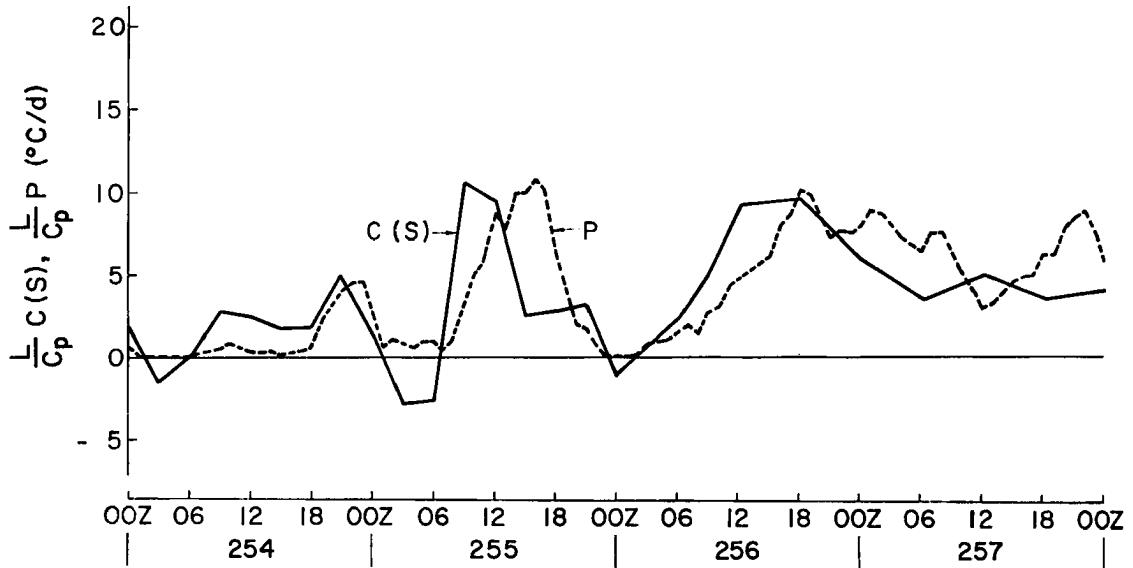
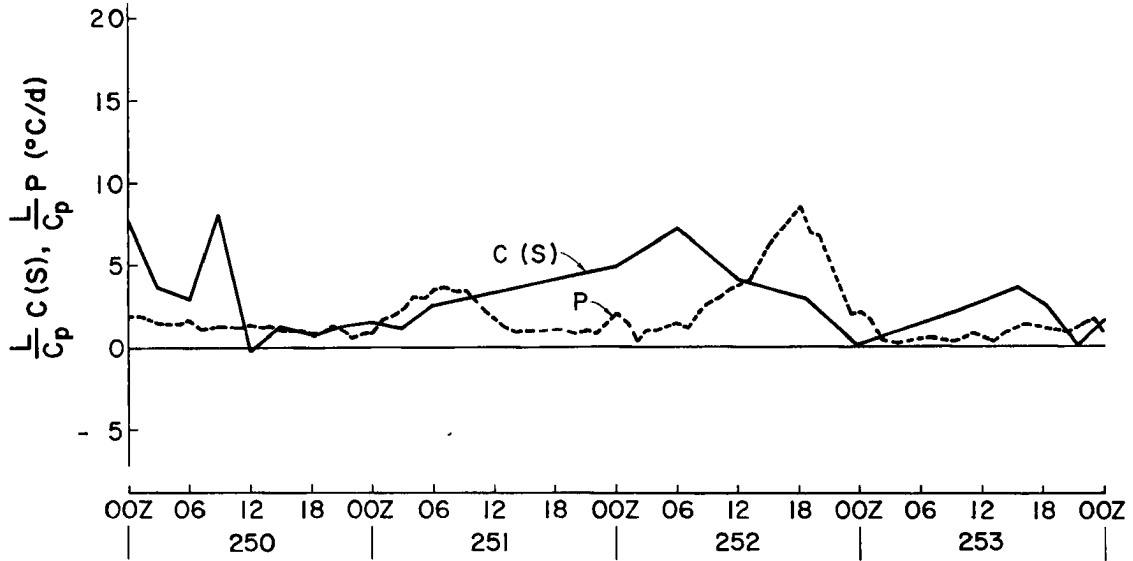


Fig. 8. Continued.

TABLE 5

Lag Time Between s-Budget A/B-Scale Condensation and Master Array
Radar-Observed Precipitation

Day	Time of Radar Rainfall Maximum (Hour Ending)	(1) Peak Lag (Hours)	(2) 5°C d^{-1} Threshold Lag (Hours)
183	15 GMT	9	3
188	17	8	8
194	20	3	7
222	10	4	0
224	12	-3*	4
245	18	9	7
247	23	12	9
255	16	7	2
256	17	5	3
259	6	3	-1
Mean		5.7	4.2

(1) Time at which s-budget condensation reached peak or plateau minus time of radar rainfall peak/plateau.

(2) Time at which the increasing s-budget condensation rate exceeded 5°C d^{-1} minus similar time for radar rainfall. (Comparison of similar points during the indicated growth phase of the system).

$$5^{\circ}\text{C d}^{-1} \sim 1.9 \text{ g/cm}^{-2} \text{ d}^{-1}$$

*s-budget peak is broad and poorly defined.

Explanation #1 must be rejected out of hand since there is no reason to expect systematic lag errors in the rawinsonde or radiation data. Cloud storage of s , even if unsampled, is at least 1-2 orders of magnitude too small to cause a significant lag in the first term of Eq. 9. The other terms are all based upon measurements at a single time period and hence do not have time resolution problems.

It has already been shown that radar rainfall estimates are probably too low during relatively light rainfall. Thus, it would be reasonable to assume that radar underestimates rain during the buildup of a strong convective cloud cluster or squall line. The GATE A/B-area was less unstable than most tropical oceanic regimes, and there was a considerable time between the first formation of precipitating convective lines and the time of maximum cumulonimbus height and activity. This might explain the right hand column of Table 5 showing the difference between the budget/radar estimates of the time when condensation/rainfall exceeded 5°C d^{-1} during the indicated convective system growth phase. It is harder, however, to explain the lag between the times of peak convection. This would require a significant overestimate of precipitation by radar during the latter stages of GATE convective system life cycles. If true, as the convective lines became concentrated into fewer but more intense Cb systems, the overall A/B-scale rainfall must have decreased while the strong echo rainfall continued to increase. Thus, for hypothesis #2 to be valid, the Z-R relationships used by Hudlow would have to be altered to increase precipitation for low reflectivities and decrease rainfall for higher reflectivities. Cunning and Sax (1977) suggested that the Z-R relationships for GATE used by Austin et al. (1976)

and Hudlow (1978) should be altered in the above sense, though their modifications do not seem large enough to bring the radar rainfall into line with the s-budget condensation.

The mean storage of liquid water in the GATE A/B-area (hypothesis #3) cannot be measured directly with conventional data. During the transition from undisturbed conditions to a deep convective situation there is a considerable increase in the amount of cloud water in the atmosphere, and there is a corresponding decrease during the decay of the system. The storage of liquid water is the difference between s budget condensation and s budget precipitation. The condensation from Eq. 9 may be written:

$$(c-e) = P(s) + \frac{\partial q_{\ell}}{\partial t} \quad (15)$$

where $P(s)$ is the precipitation estimated from the s budget. During the growth stage of a convective system $\frac{\partial q_{\ell}}{\partial t}$ is positive and $P(s) < (c-e)$ while the reverse is true during the latter portions of the life cycle. Hence, inclusion of $\frac{\partial q_{\ell}}{\partial t}$ in Eq. 9 should introduce a lag between the condensation and precipitation curves with the former preceding the latter. Total rainfall would not be affected since $\frac{\partial q_{\ell}}{\partial t}$ is nearly zero when averaged over a complete system life cycle.

There is no question that storage of q_{ℓ} acts in the right sense to explain the s-budget/radar rainfall lag. However, there is considerable doubt as to whether the storage could be large enough to explain phase differences of the observed magnitudes. Grody (1976) using microwave satellite data found maximum liquid water contents of only $0.1-0.2 \text{ g cm}^{-2}$ averaged over the central regions of a mature tropical cyclone - a much

stronger convective system than GATE cloud clusters. Tropical cyclones in the Western North Pacific and the West Indies average about 9 cm d^{-1} of rainfall over their inner 220 km radius (Frank, 1977a; Miller, 1958). The liquid water content of the GATE A/B-scale area (about 400 km radius) probably did not exceed 0.1 g cm^{-2} . Only about 5% of a tropical cloud cluster is covered by active deep convection (Ruprecht and Gray, 1976; Lopez, 1973). If an equal area were covered by non-precipitating clouds, the average cloud height was 500 mb, and mean cloud liquid water content was 2 g m^{-3} , then the mean liquid water content of the atmosphere would be 0.1 g cm^{-2} . This is a rather generous estimate of atmospheric water content.

It is difficult to estimate the liquid water storage over the GATE A/B-area due to the limited area coverage of the radar. Rainfall is highly concentrated in tropical weather systems, and the master array could be receiving substantially more or less mean rainfall than the larger A/B-array at any given time period. Nevertheless, for 9 of the 10 rainfall systems listed in Table 5 the s-budget condensation and radar rainfall rates had comparable peak values suggesting that the mean master array precipitation for the 9 cases should be representative of the A/B-array mean rainfall. These cases are listed in Table 6 with the total amounts of liquid water storage required (to explain the lag) from the time the s-budget condensation exceeded 5°C d^{-1} ($1.9 \text{ g cm}^{-2} \text{ d}^{-1}$) until that curve intersected the radar estimate. Storage prior to the 5°C d^{-1} level was omitted to eliminate the presumed underestimate by the radar at lower precipitation levels, and it has been assumed here that the radar rainfall is accurate above that level and representative of the A/B-area.

TABLE 6

Storage of liquid water during convective build-up required to bring s budget condensation and radar rainfall into phase.

<u>Days</u>	<u>Interval</u>	<u>Required Storage Of Liquid Water</u> ($\frac{g}{cm^2}$)
182-183	18GMT(182)-11GMT(183)	0.4
188	04-12GMT	0.5
194	08-19GMT	0.5
224	*	0 or slightly negative
245	05-13GMT	0.7
247	06-17GMT	0.4
255	08-12GMT	0.2
256	09-17GMT	0.4
259		~ 0
Mean		0.34

*s budget peak hard to specify

(Day 222 from Table 5 is omitted since the peak rainfall values were much different for the two estimates).

The mean liquid water storage for the 9 cases was 0.34 g cm^{-2} , and the mean for the 7 cases with distinct phase lags (days 224 and 259 omitted) was 0.44 g cm^{-2} . These values are too large to be realistic. It is concluded that while liquid water storage contributed to the lag between C(s) and P(R), it could not have been the primary cause. Introduction of accurate $\frac{\partial q_l}{\partial t}$ values in Eq. 9 would reduce the observed phase lag by no more than 20-30%.

The difference between the sampling areas of the radar and the budget analyses introduces the possibility that perhaps there was a real time lag between convection over the entire A/B-array and convection in the master array (hypothesis #4). Satellite data analyzed by

McGarry and Reed (1978) appeared to show a tendency for the time of maximum convection to become later as one proceeded west from the coast of Africa. Such a tendency, if coupled with a strong east-west gradient in amount of precipitation (maximum to the east) could result in the observed effect. During Phase I and II of GATE the radar did indicate stronger convection on the east side of the master array than on the west side (Hudlow and Marks, 1977). Phase III precipitation had a slight west side predominance. The strongest east side maximum occurred during Phase I. However, longitudinal analysis of master array radar rainfall for Phase I does not show a phase shift across the ~ 400 km area (Figs. 9-10). This indicates that a true lag in rainfall between the A/B-area and the master array located at its center is unlikely.

3.4 Summary

There was a definite lag of several hours between s (and q) budget condensation and radar-observed rainfall. Part of this resulted from the storage of liquid water in clouds, but another greater process must also be operating to explain the lag. A true rainfall lag between the master and A/B-arrays is not indicated by the data, but this cannot be ruled out completely since we do not know the radar rainfall outside the master array.

By process of elimination, suspicion is cast upon the radar rainfall estimates. It is likely that underestimates of true precipitation by the radar during small cloud precipitation occurrences resulted in at least part of the $C(s)/P(R)$ lag during early system growth. To explain the peak lag phenomenon, however, the radar would also have had to overestimate rain from larger clouds. A shift in the Z-R relationship

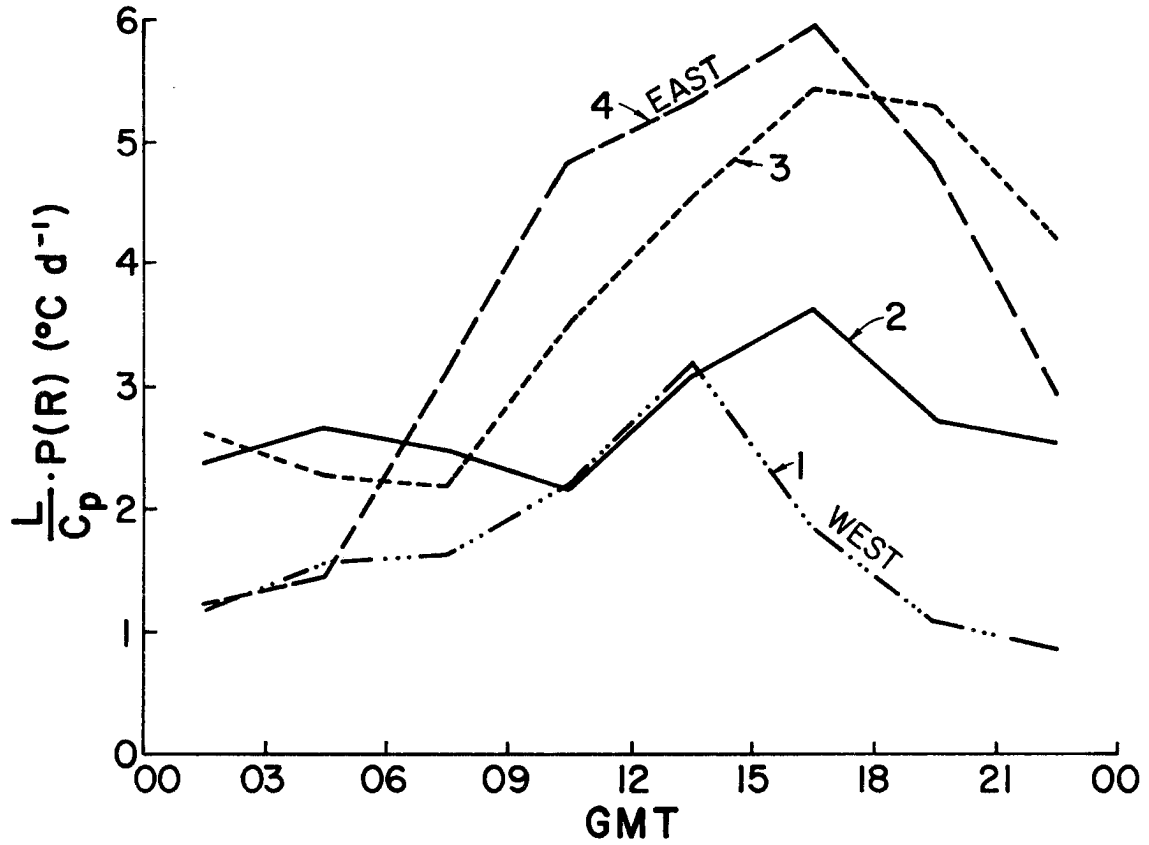


Fig. 9. Master array radar rainfall in each of 4 longitudinal bands. Each band is 100 km in width. Band #1 is the western most and #4 is on the east side. (Bands #2 and #3 contain more area than #1 and #4). Phase I.

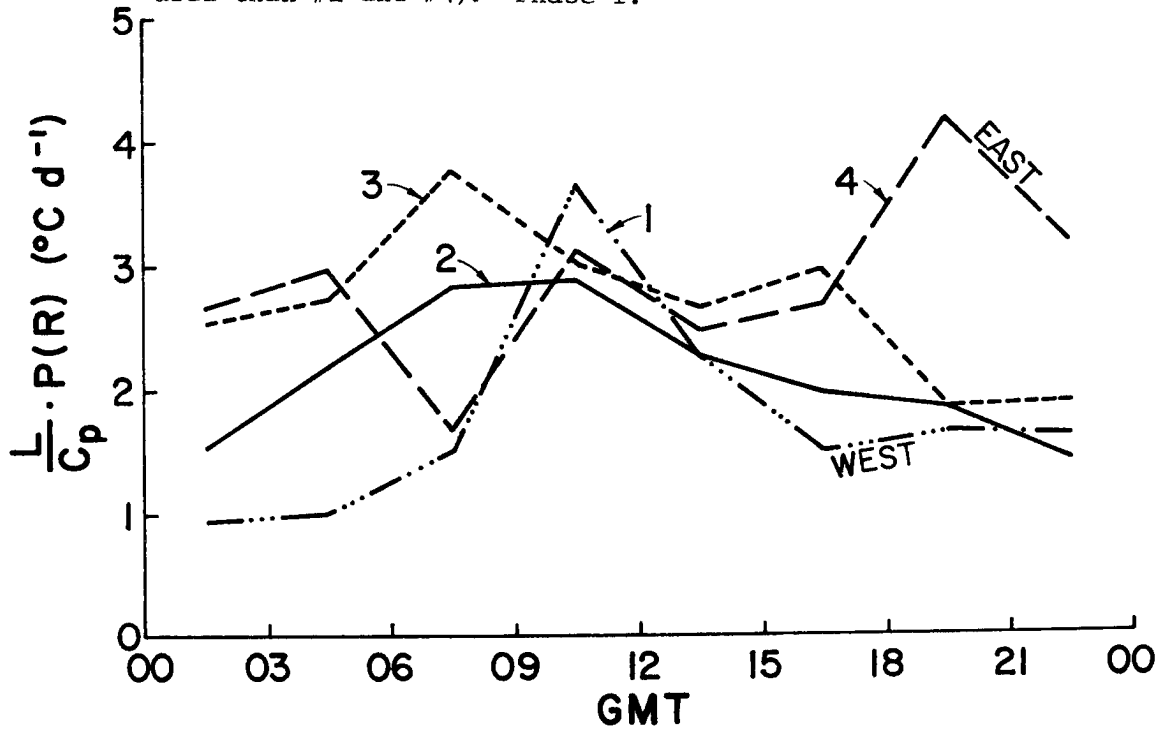


Fig. 10. Same as Fig. 9 except for Phase II.

would be required with increases in rainfall for low reflectivities and corresponding reductions in rainfall for high reflectivities. It is suggested that research into GATE Z-R relationships be continued utilizing diagnostic budget analyses for better ground truth estimates.

3.5 Budget Condensation and Large Scale Vertical Motion

Analysis of A/B-scale GATE convective systems has shown that low level convergence increased prior to noticeable increases in the B-scale radar echo population. This lag between large scale forcing and precipitating cloud response was typically on the order of 3-6 hours (Frank, 1978; Ogura et al., 1977) and has also been observed in middle latitude convective systems (Ogura, 1975).

It is unlikely that gradual moistening of the entire A/B-scale was responsible for the above lag (Frank, 1978). The GATE A/B-area remained very moist even during strongly suppressed conditions. The maximum variations in A/B-area precipitable water during each phase are shown in Table 7.

TABLE 7

Maximum, Minimum and Mean Observed A/B-area Precipitable Water During Each Phase (g cm^{-2})

	Phase I	Phase II	Phase III
Maximum	5.55	5.82	5.64
Minimum	4.48	4.34	4.63
Mean	5.16	5.16	5.13

Despite variations in the mean state from heavily precipitating to suppressed with mean subsidence, the A/B-area moisture varied only about $\pm 11\%$. It follows that GATE weather systems were quite efficient at converting converged moisture into precipitation. The near constancy of the A/B-scale moisture argues strongly against any theory calling for convective development as a consequence of increased moistening of the middle levels on that scale.

Figures 11-13 show the large scale vertical motion at 800 mb (approximate top of the A/B-area inflow layer), the s budget condensation and the radar rainfall. Condensation does not lag the low level upward motion within the time resolution of the data. When an increase in low level mass and moisture convergence occurs, clouds form rapidly. Some of the clouds are undoubtedly precipitating but are undetected or underestimated by the radar. Many observers have remarked that frequent rainfall occurred from clouds with tops of only 4-5,000 ft during GATE. The lag between the convergence and echo growth must result from the time required to organize the small clouds into larger precipitating ones with distinct echoes.

It is not accidental that the lag between low level convergence and deep echo growth is about the same as the lag between s budget condensation and radar rainfall. What is being observed is a characteristic growth time of deep mesoscale convective systems. Small clouds moisten the middle levels and enhance instability in local Cb scale areas thereby encouraging the growth of deeper clouds. The lag between the large scale forcing (and condensation) and the formation of concentrated strong echo regions is the time between the onset of unstable synoptic scale uplifting and the establishment of a "steady" ensemble of mesoscale systems. This is an area deserving future research effort.

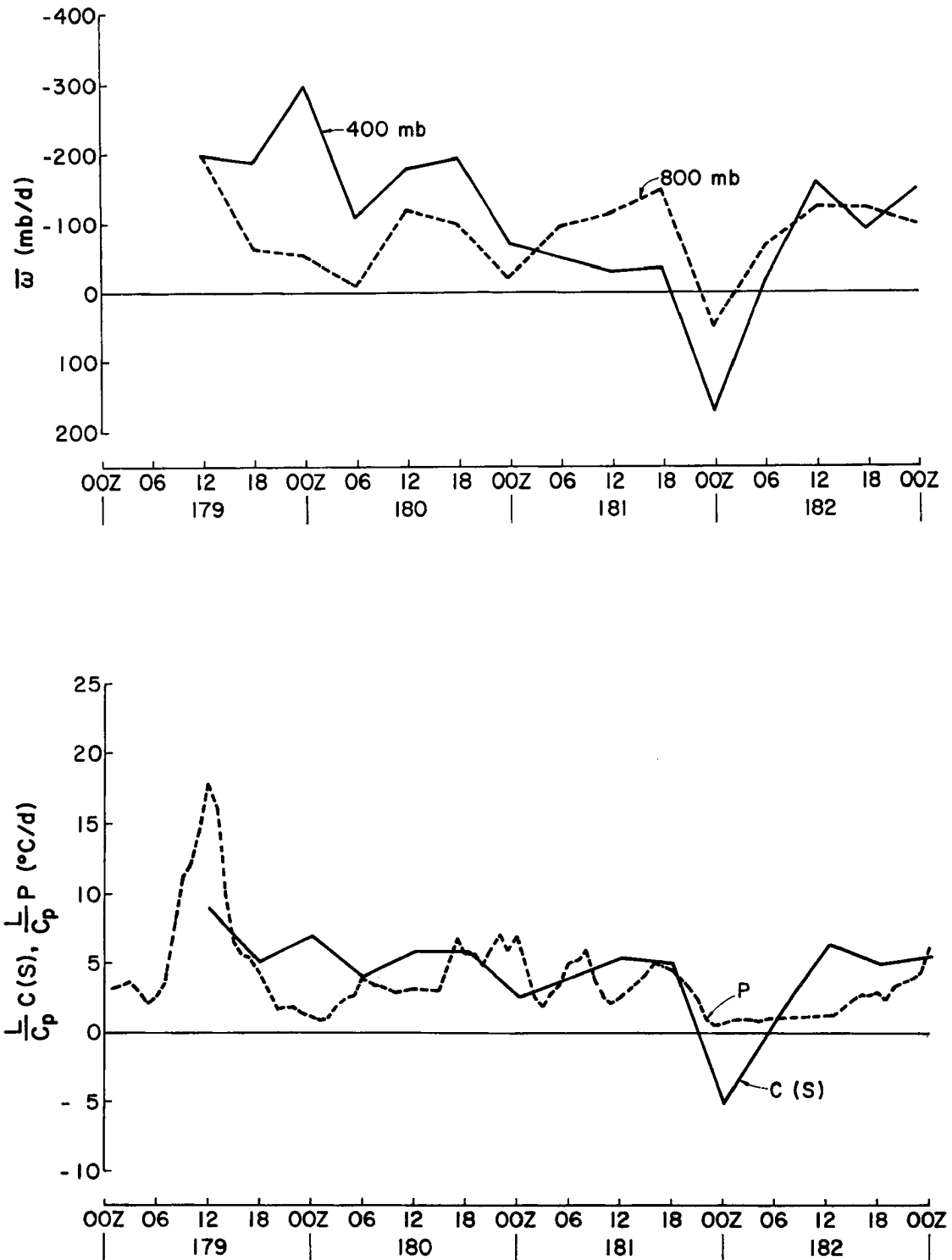


Fig. 11. Mean A/B-scale vertical motion ($\bar{\omega}$) at 400 mb and 800 mb. Also C(s) and P as in Fig. 6. Phase I.

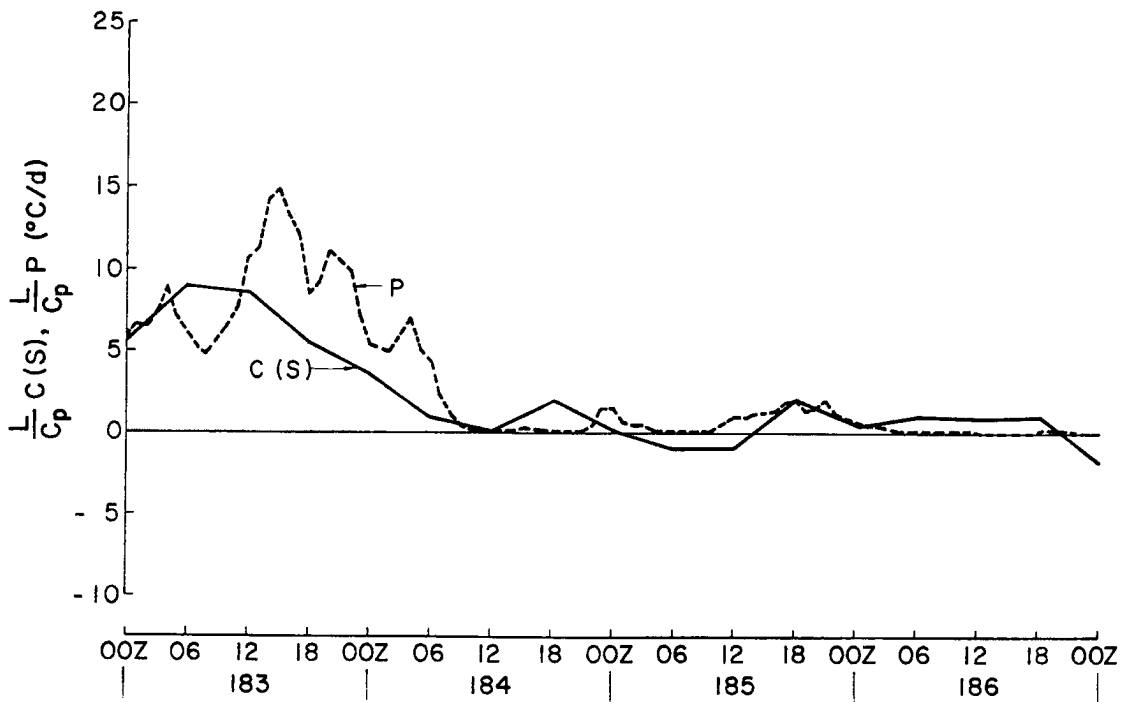
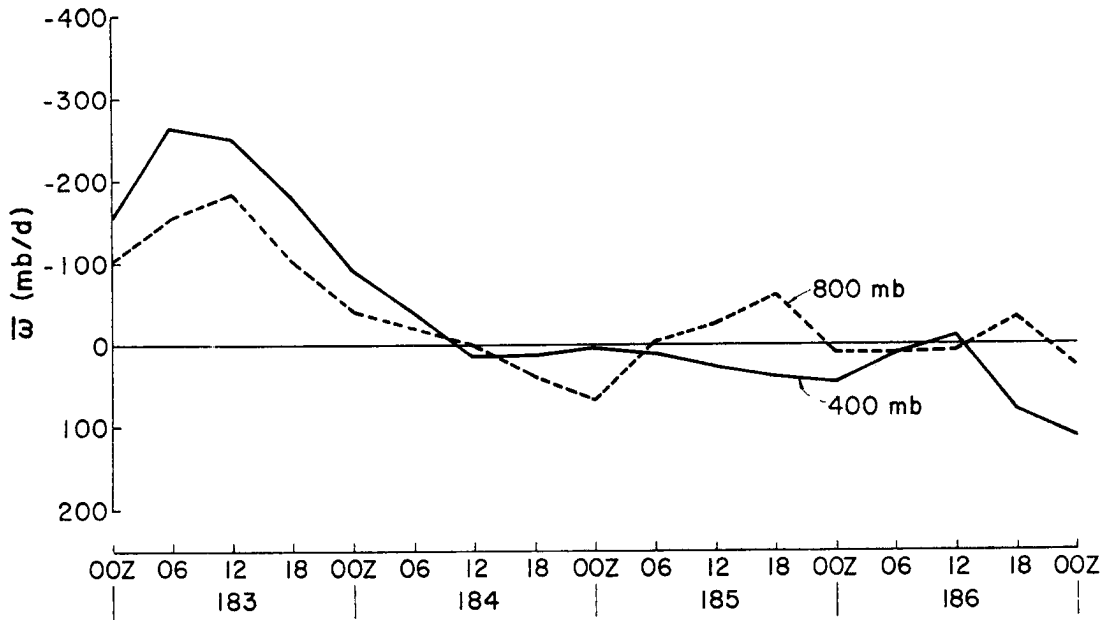


Fig. 11. Continued.

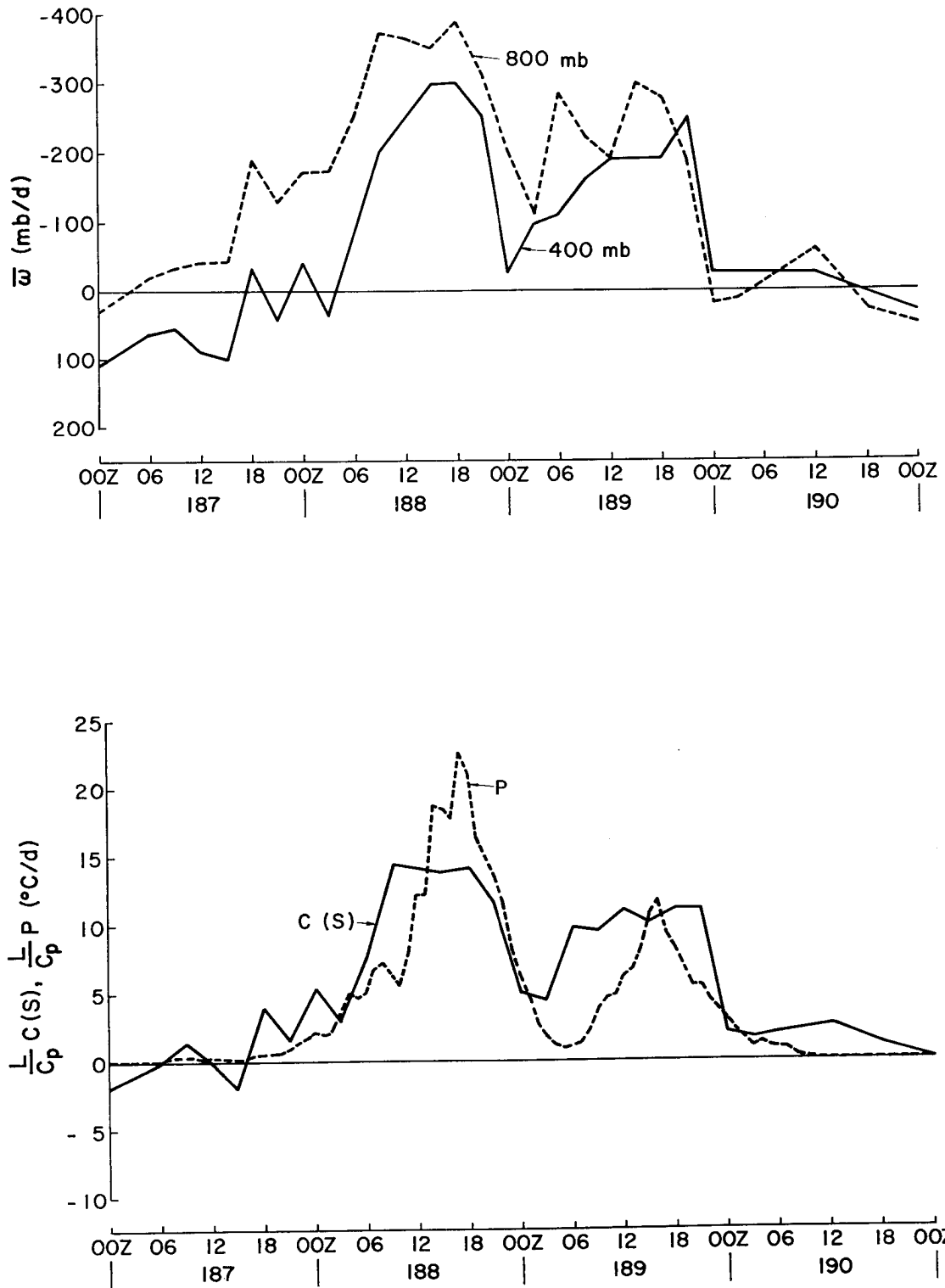


Fig. 11. Continued.

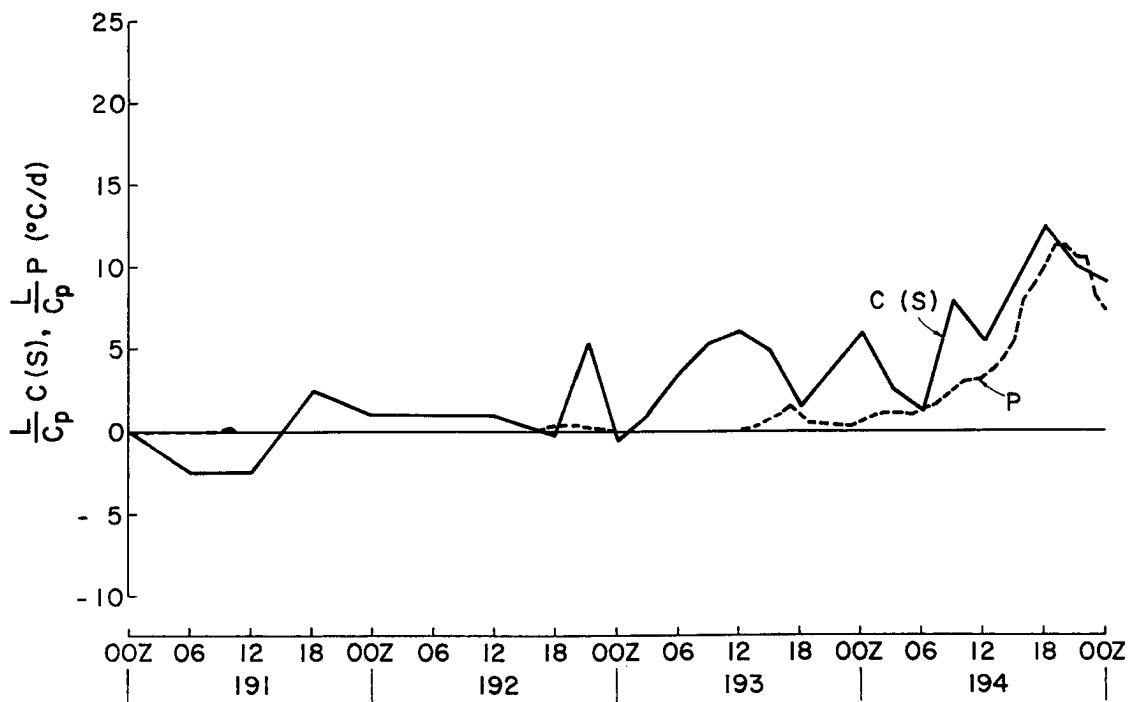
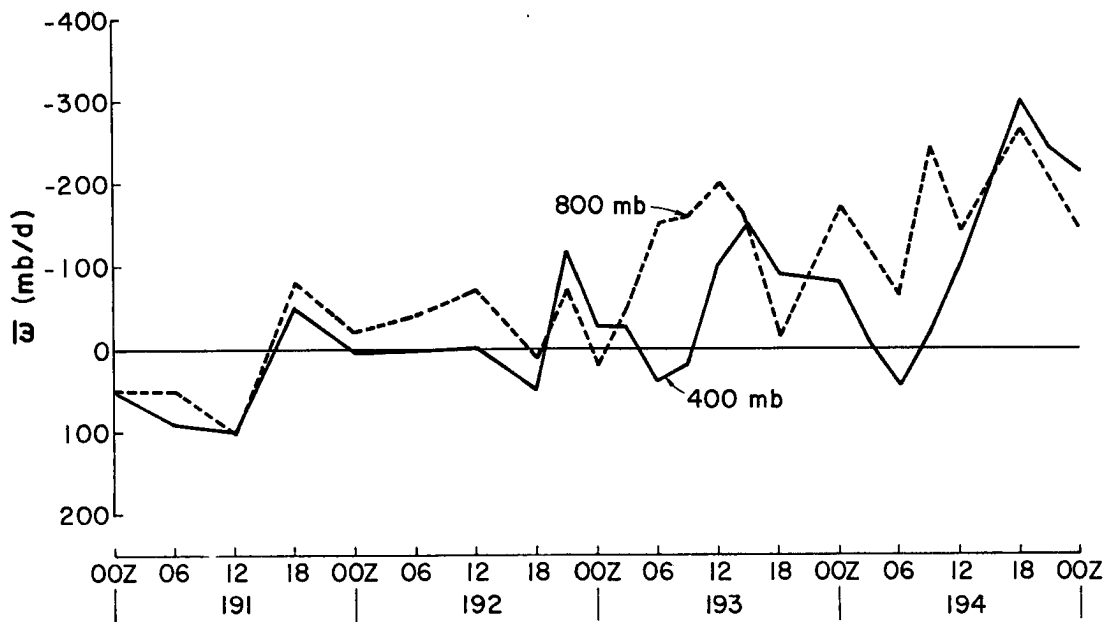


Fig. 11. Continued.

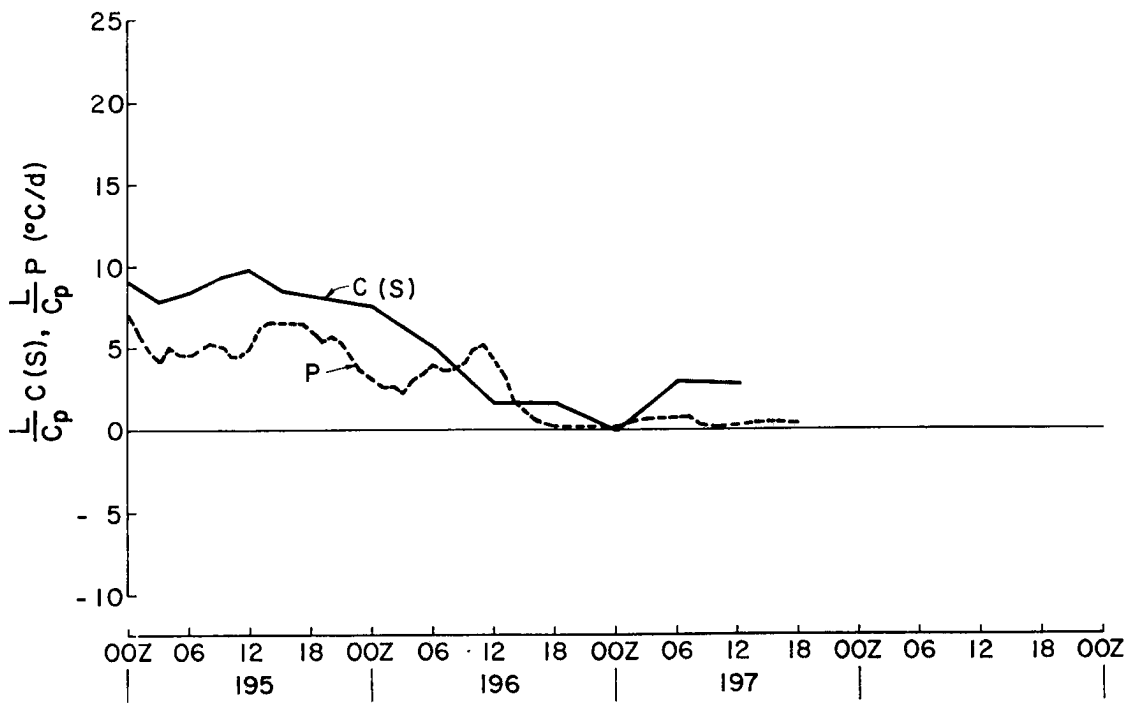
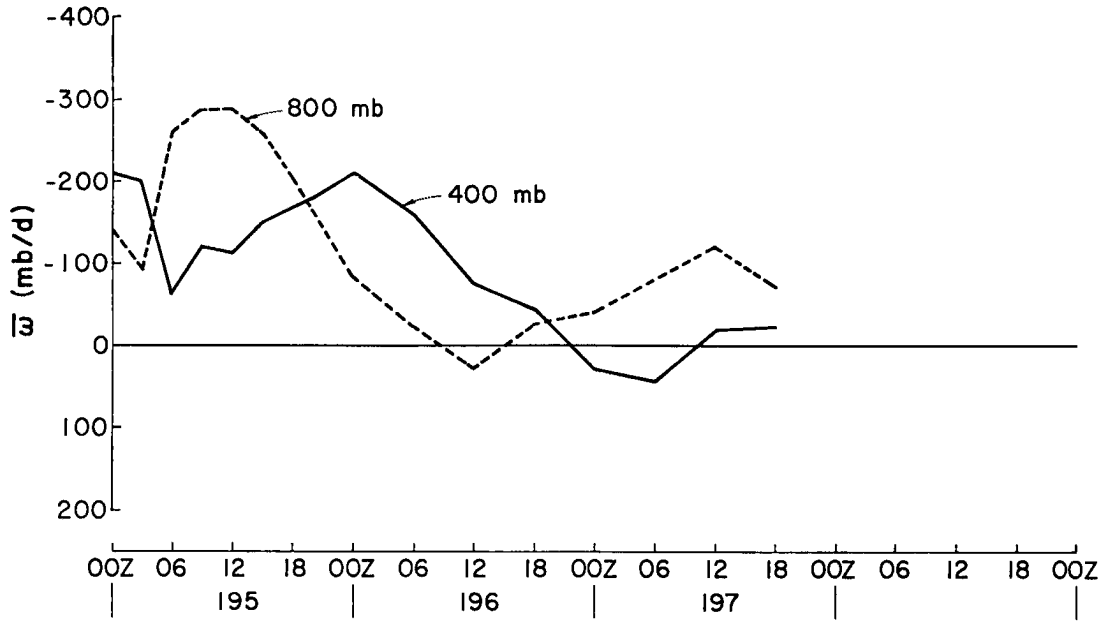


Fig. 11. Continued.

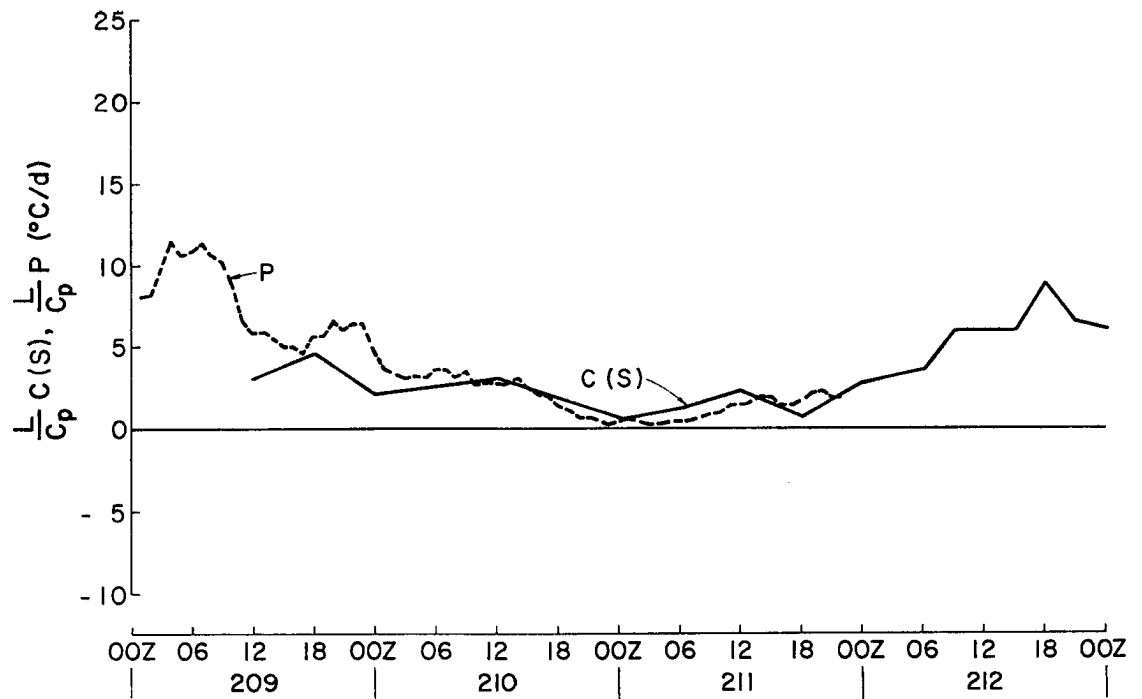
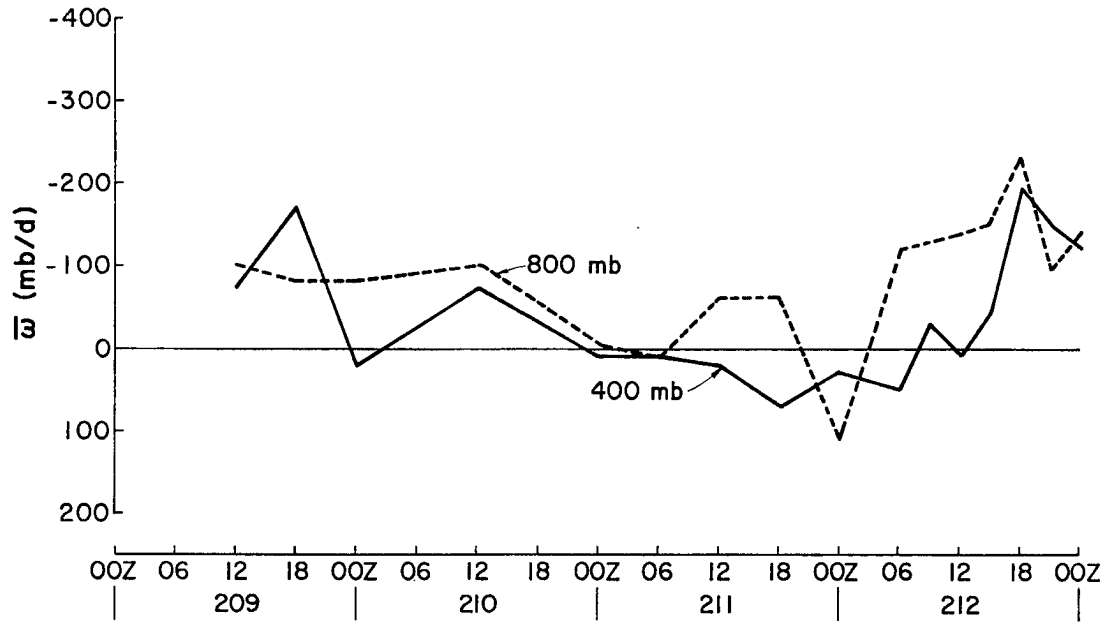


Fig. 12. Same as Fig. 11 except for Phase II.

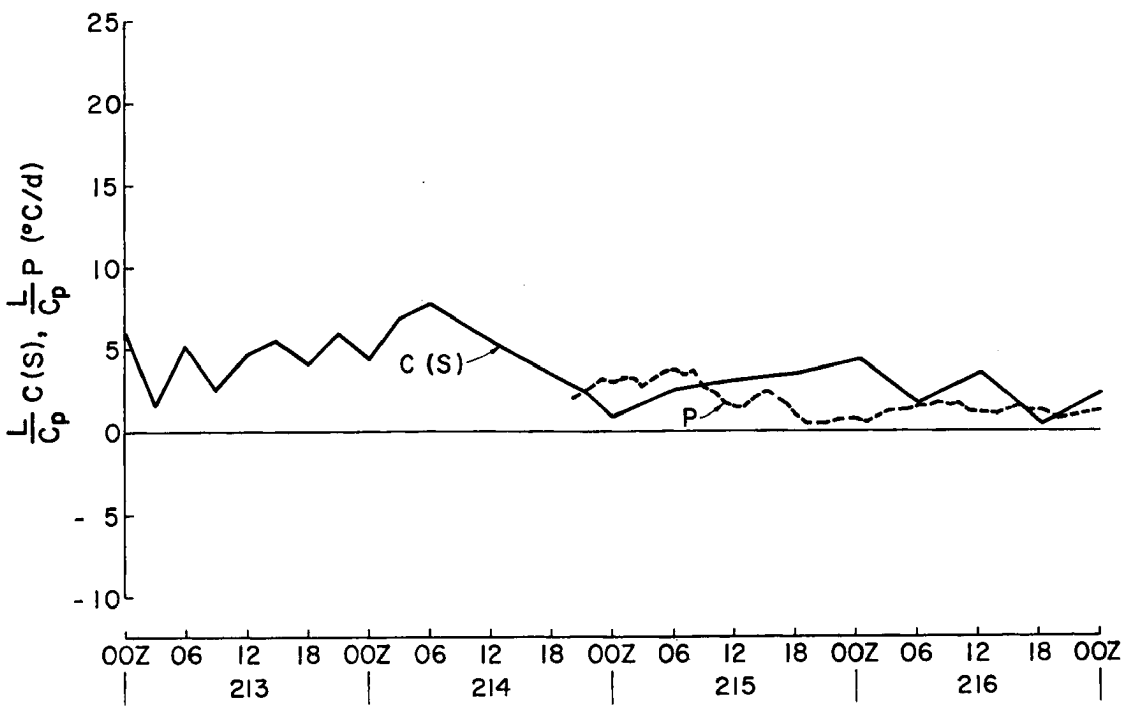
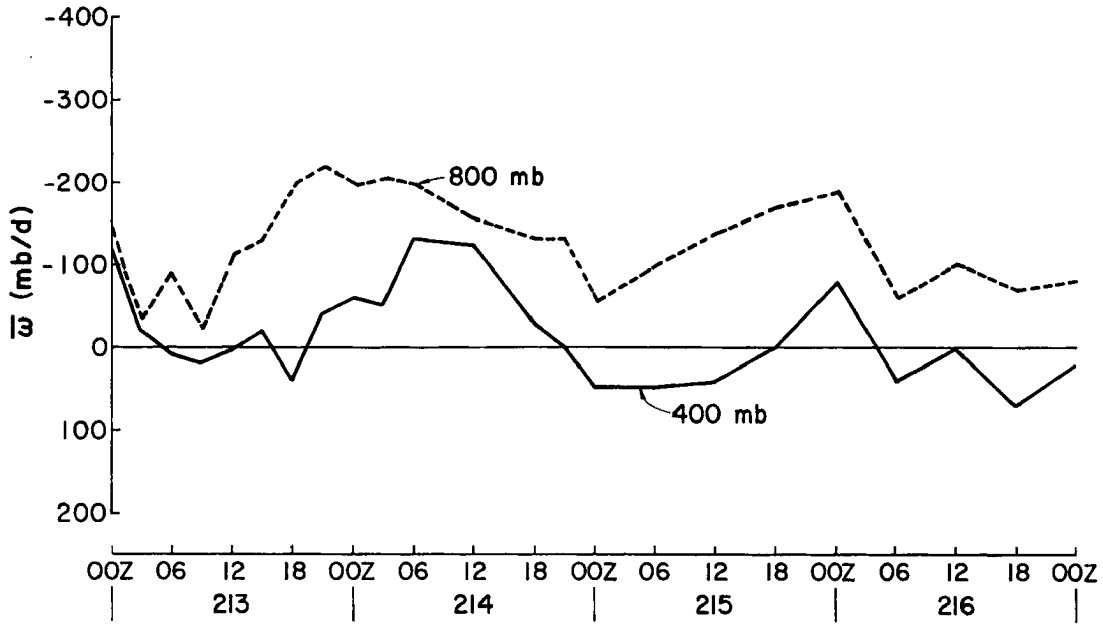


Fig. 12. Continued.

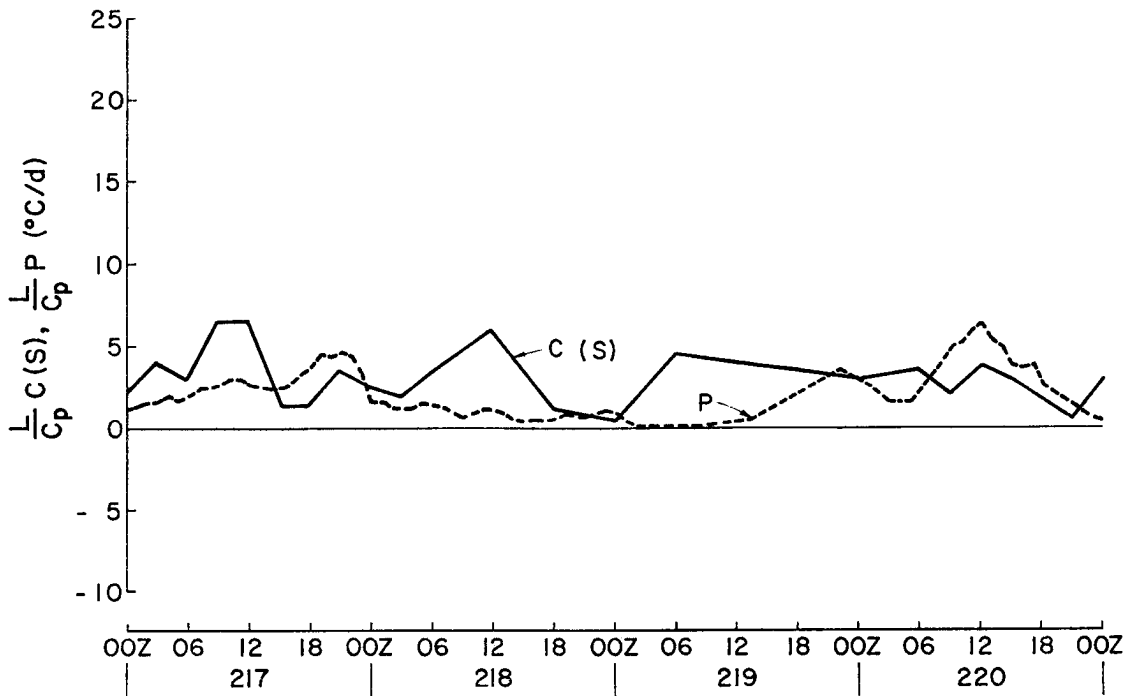
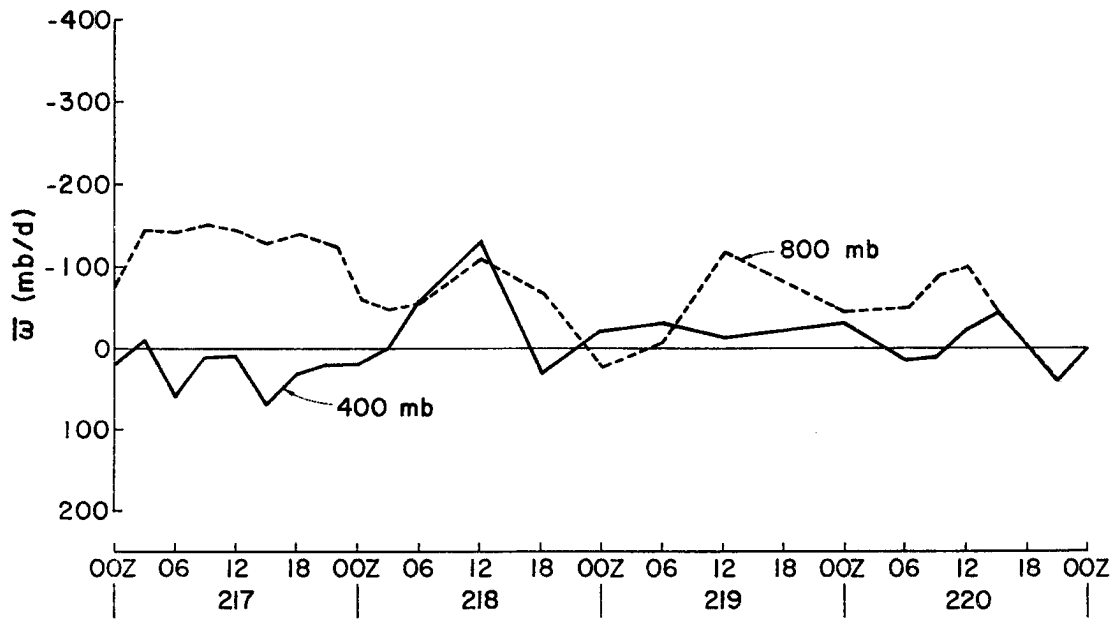


Fig. 12. Continued.

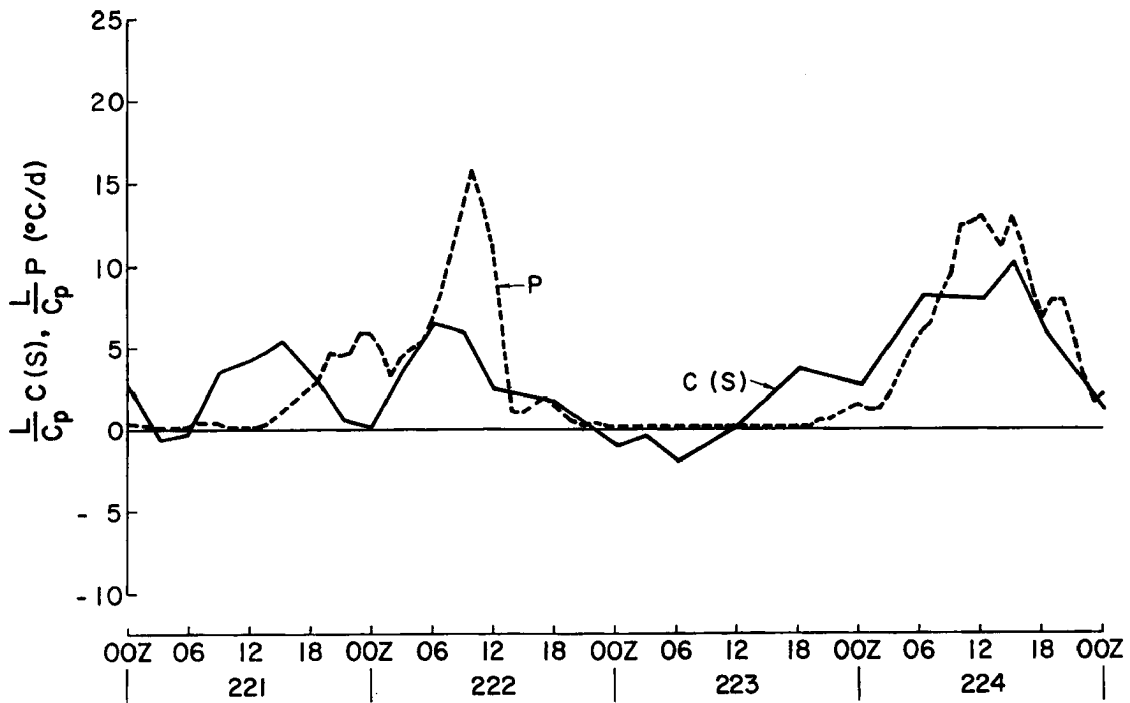
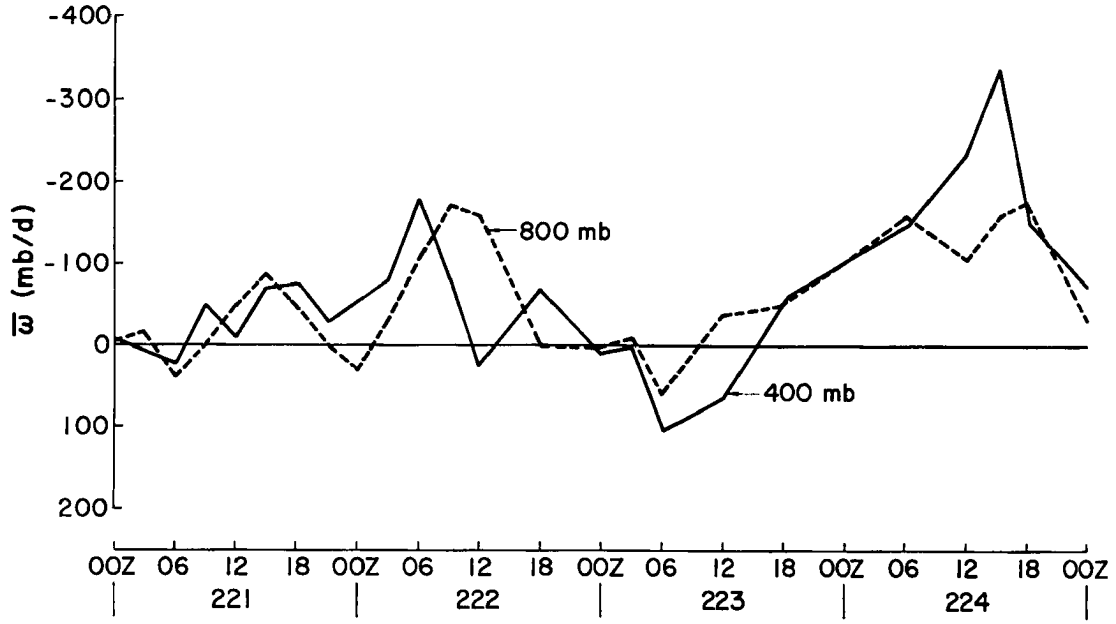


Fig. 12. Continued.

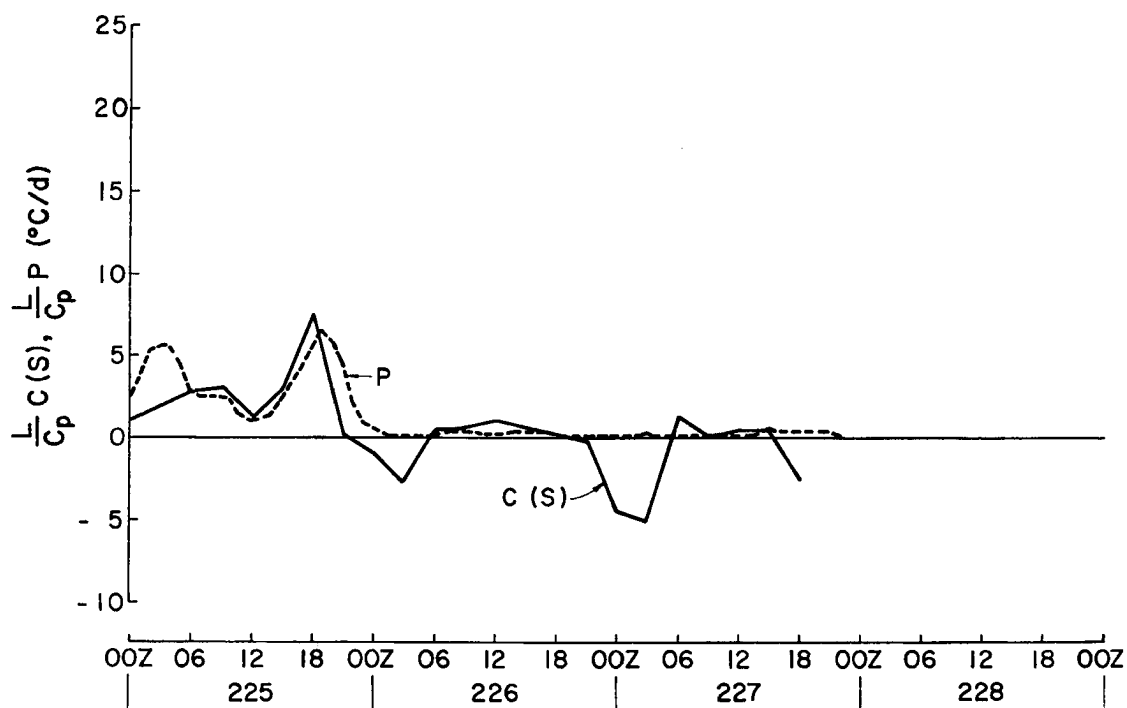
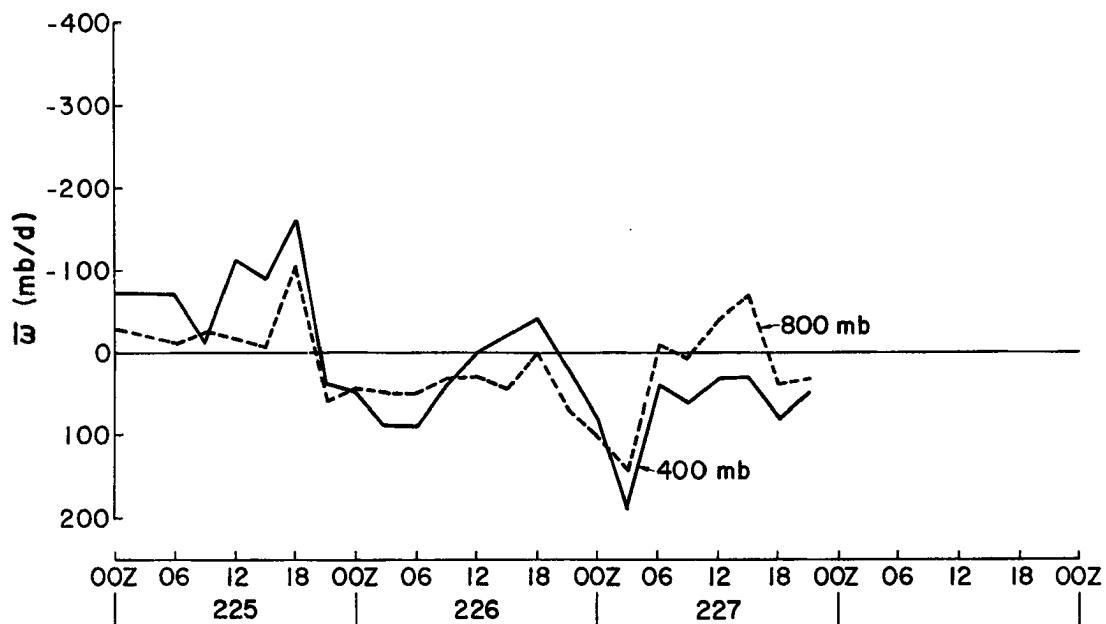


Fig. 12. Continued.

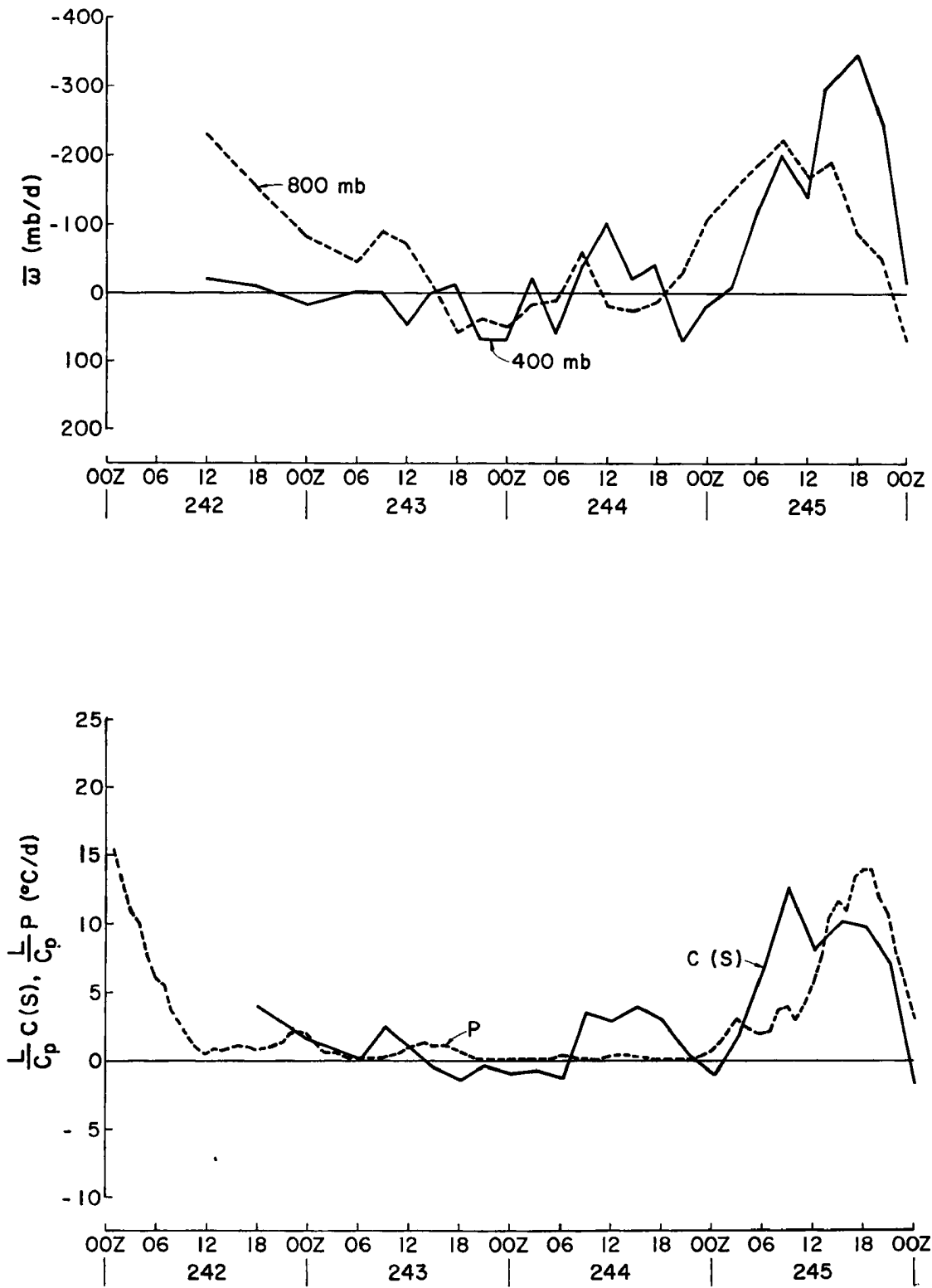


Fig. 13. Same as Fig. 11 except for Phase III.

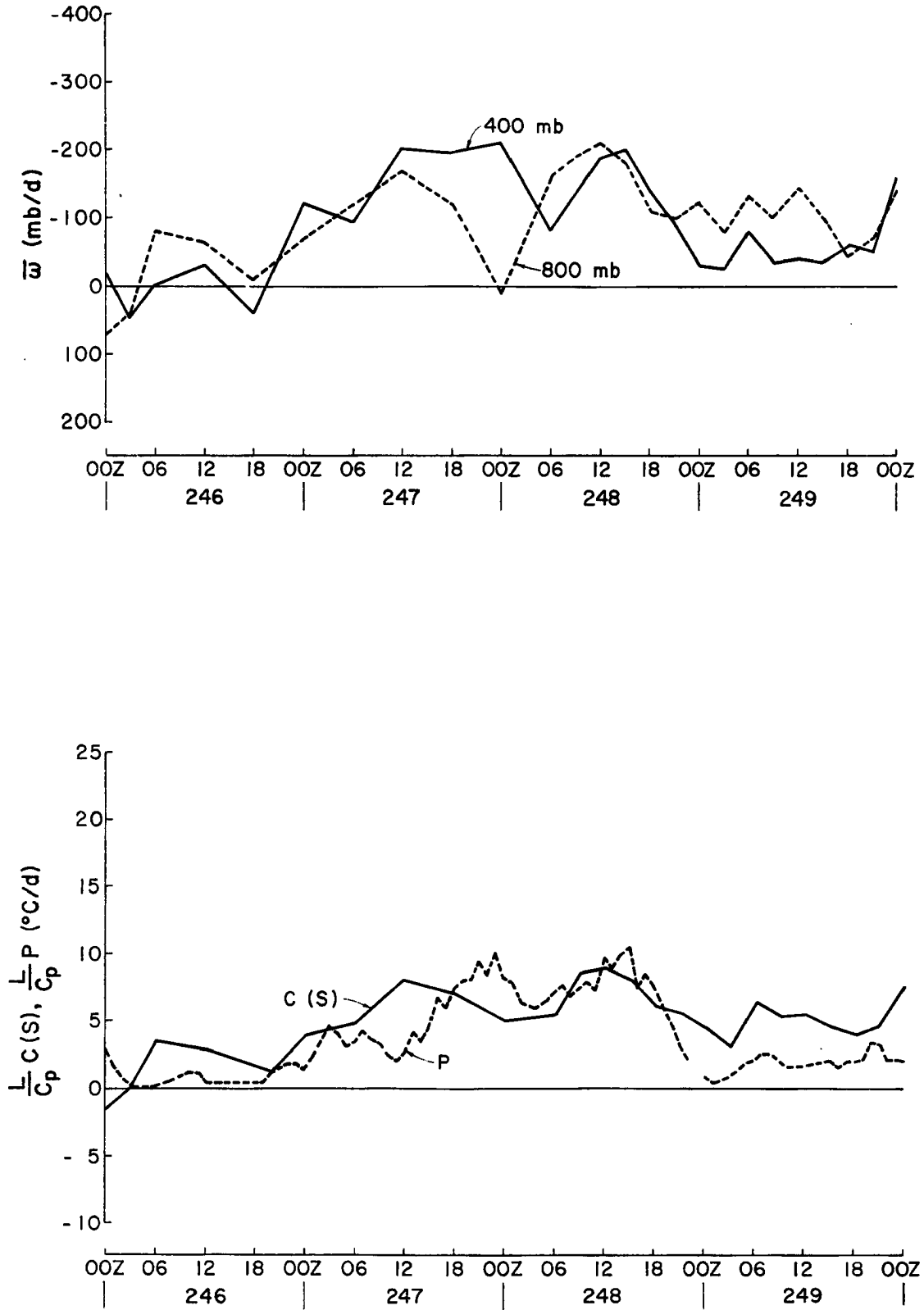


Fig. 13. Continued.

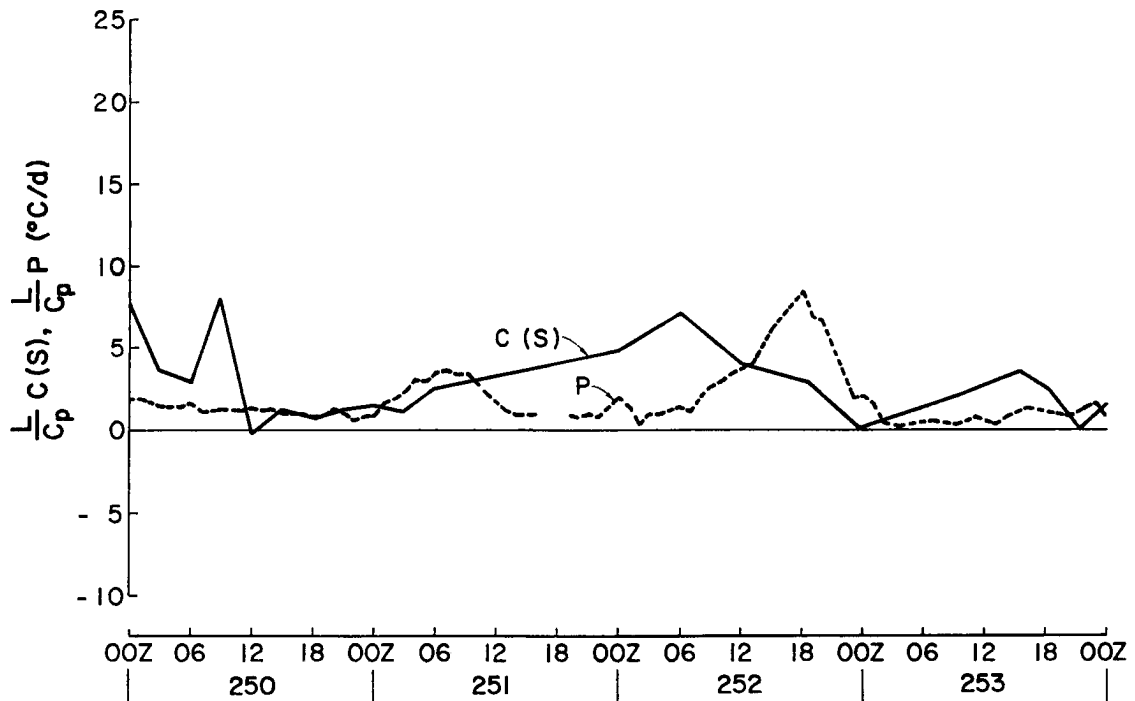
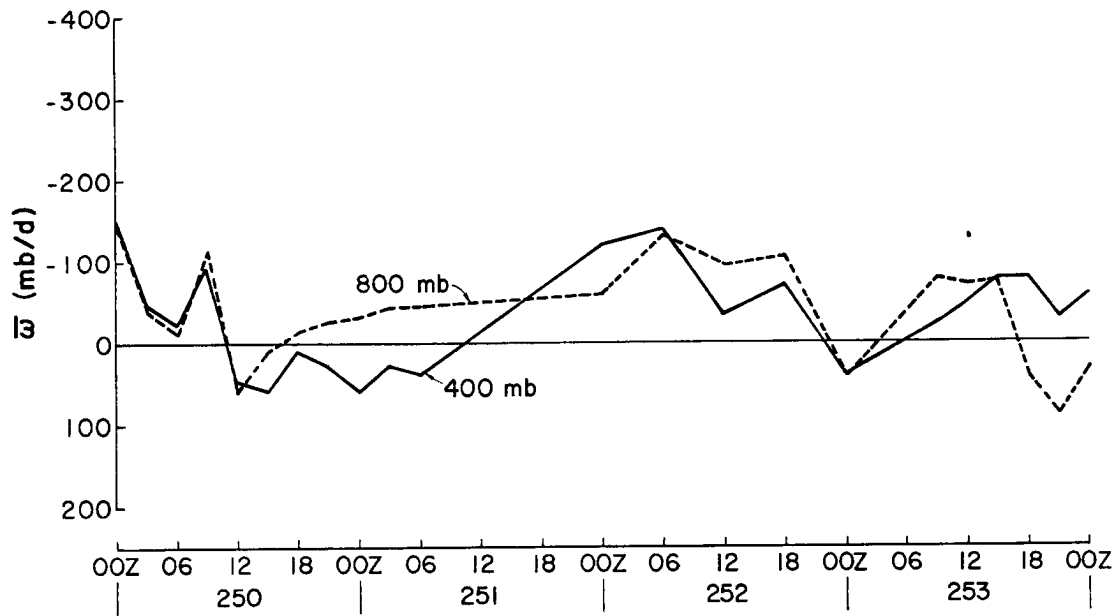


Fig. 13. Continued.

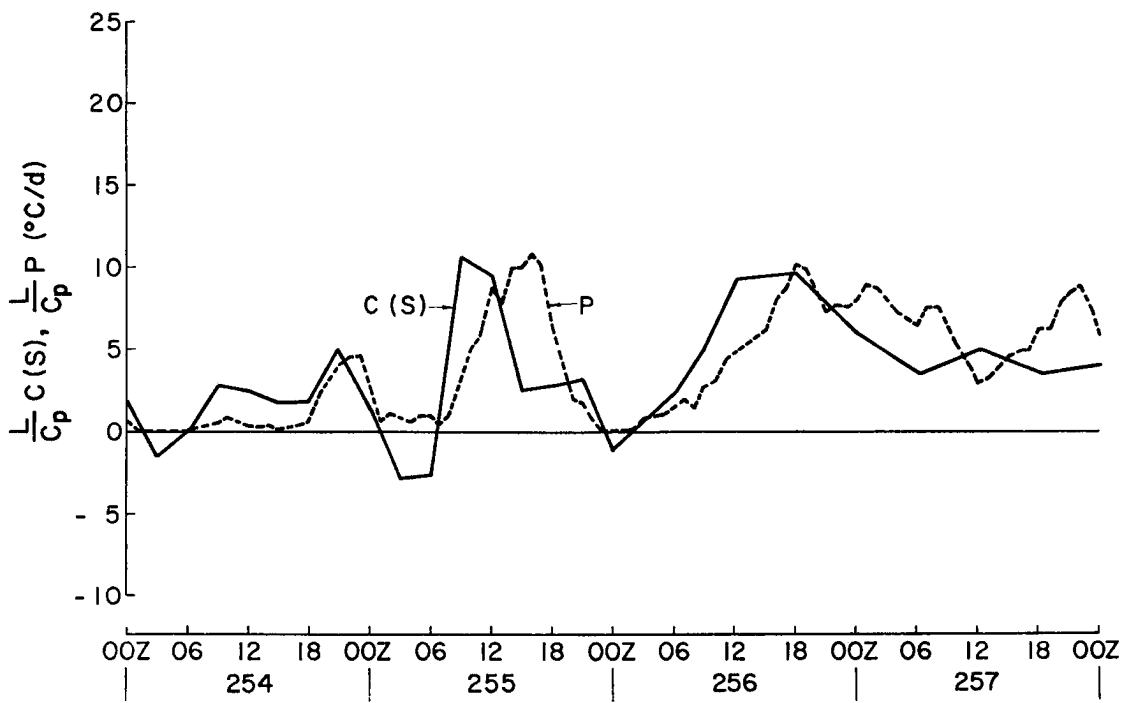
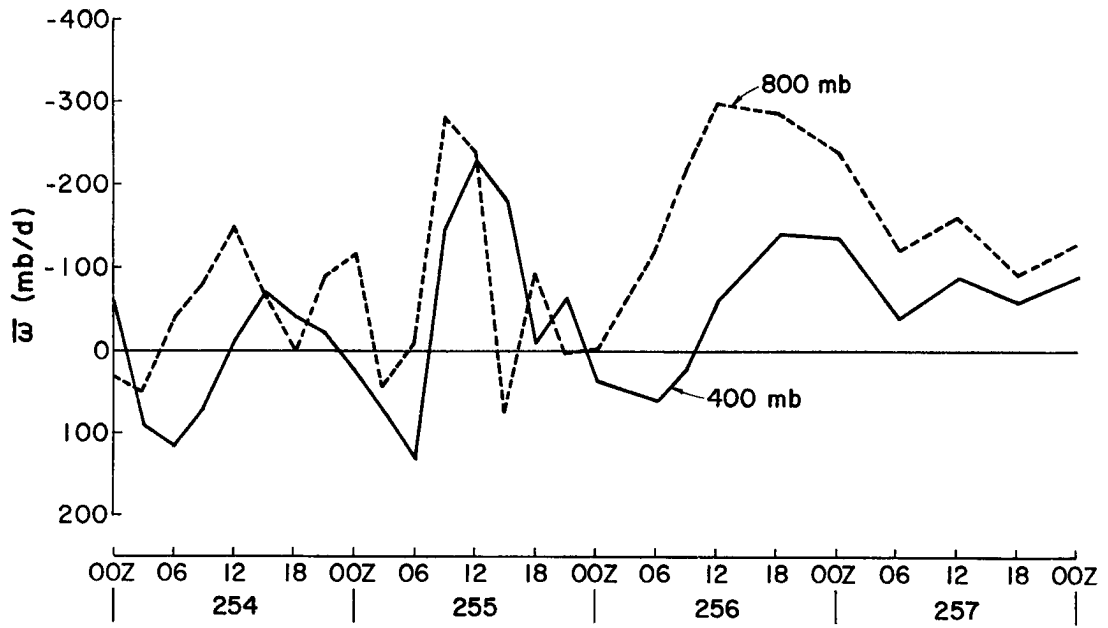


Fig. 13. Continued.

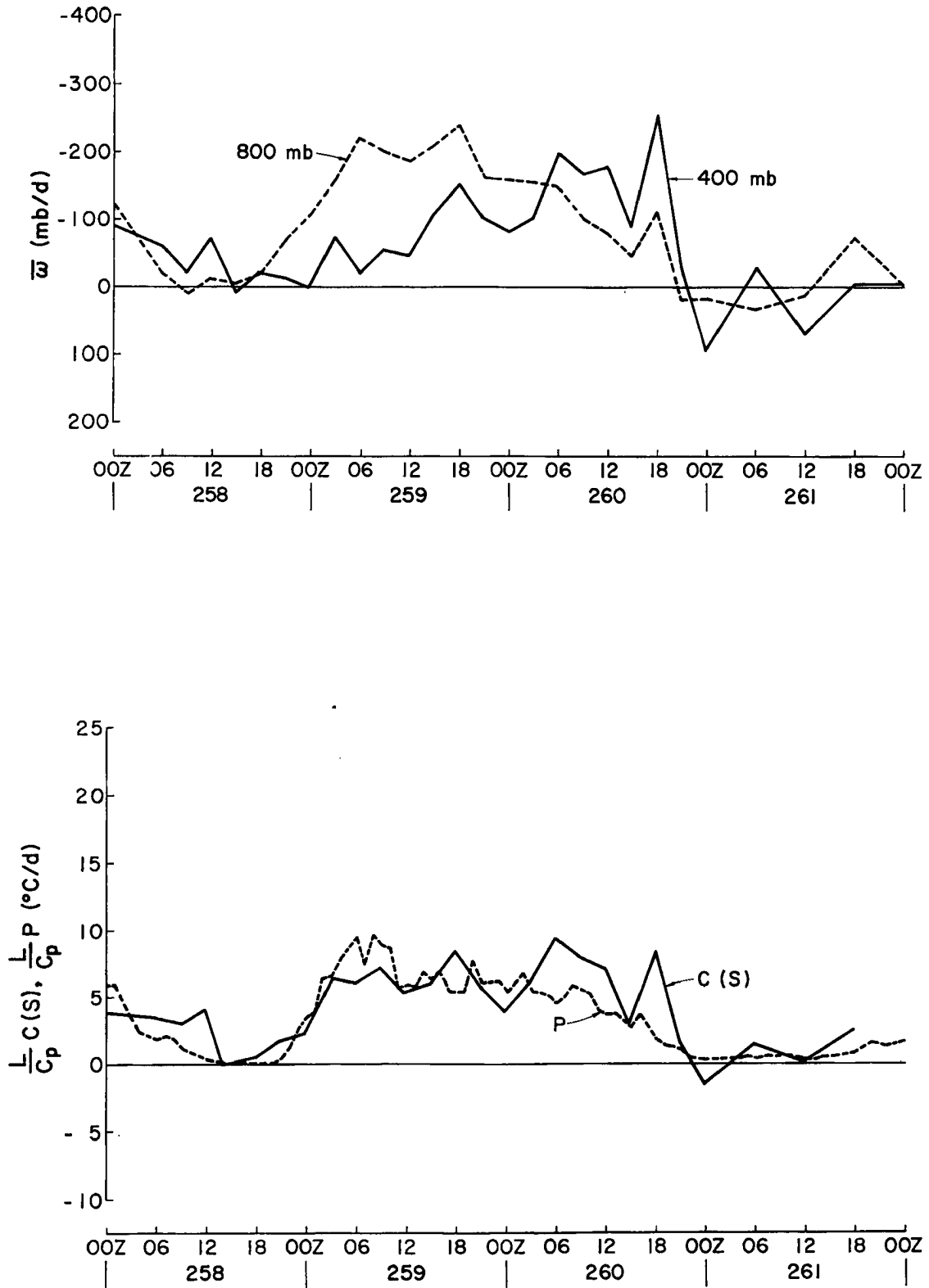


Fig. 13. Continued.

Figures 11-13 also show $\bar{\omega}$ at 400 mb. Both composite (Frank, 1978) and case studies (Ogura et al., 1977) have shown that GATE convective systems tend to be preceded by upper tropospheric subsidence. It is interesting to note that at least some subsidence occurs at 400 mb on the day prior to each of the convective episodes of Table 5. It is not yet clear whether this subsidence plays any role in the formation of the system which follows.

The vertical motion curves at 400 mb tend to confirm the previous reports of the upper level peaks in upward $\bar{\omega}$ lagging the lower level peaks (Reed et al., 1977; Frank, 1978) although this is not true in all cases. At some time periods there are substantial upward motions at 400 mb with mean subsidence at 800 mb, invariably occurring during the decaying stages of convective systems when downdrafts are strong.

4. TROPOSPHERIC WARMING BY CLOUDS AND RADIATION

It has long been known that the release of latent heat in convective clouds is a major component of the global tropospheric energy balance. It would be extremely convenient if one could merely observe or predict a cloud population, determine the vertical distribution of latent heat release from a simple cloud model, and apply that heating directly to the atmosphere at the proper levels. This works on a global scale. More recently, however, it has become clear that most of the net latent heat release in a convective cloud is transformed into potential energy within the cloud. The temperature increase of the bulk of the air between the clouds depends upon complex and scale dependent interactions between the clouds and their environments (Gray, 1973; Lopez, 1973; Yanai *et al.*, 1973; Grube, 1978).

A major objective of GATE was to determine the modes and scales of cloud and larger scale interactions. This section examines certain mean responses of the GATE A/B-scale area to latent heat release in cumulus clouds and to radiational heating.

Figures 14-16 compare the following parameters for Phases I-III: vertically integrated temperature and moisture deviations ($\overline{\Delta T}$, $\overline{\Delta q}$) deviation temperatures at the 700 mb and 300 mb levels, s-budget condensation and master array radar precipitation. Looking at the vertically integrated temperature deviations, it is immediately apparent that the temperature of the troposphere (surface to 100 mb) has a strong diurnally varying component. No obvious relationship exists between the rate of latent heat release and atmospheric temperature. Table 8 shows correlation coefficients relating $\partial \overline{\Delta T} / \partial t$ with Q_R , $P(R)$ and $C(S)$. Changes in the mean tropospheric temperature were significantly

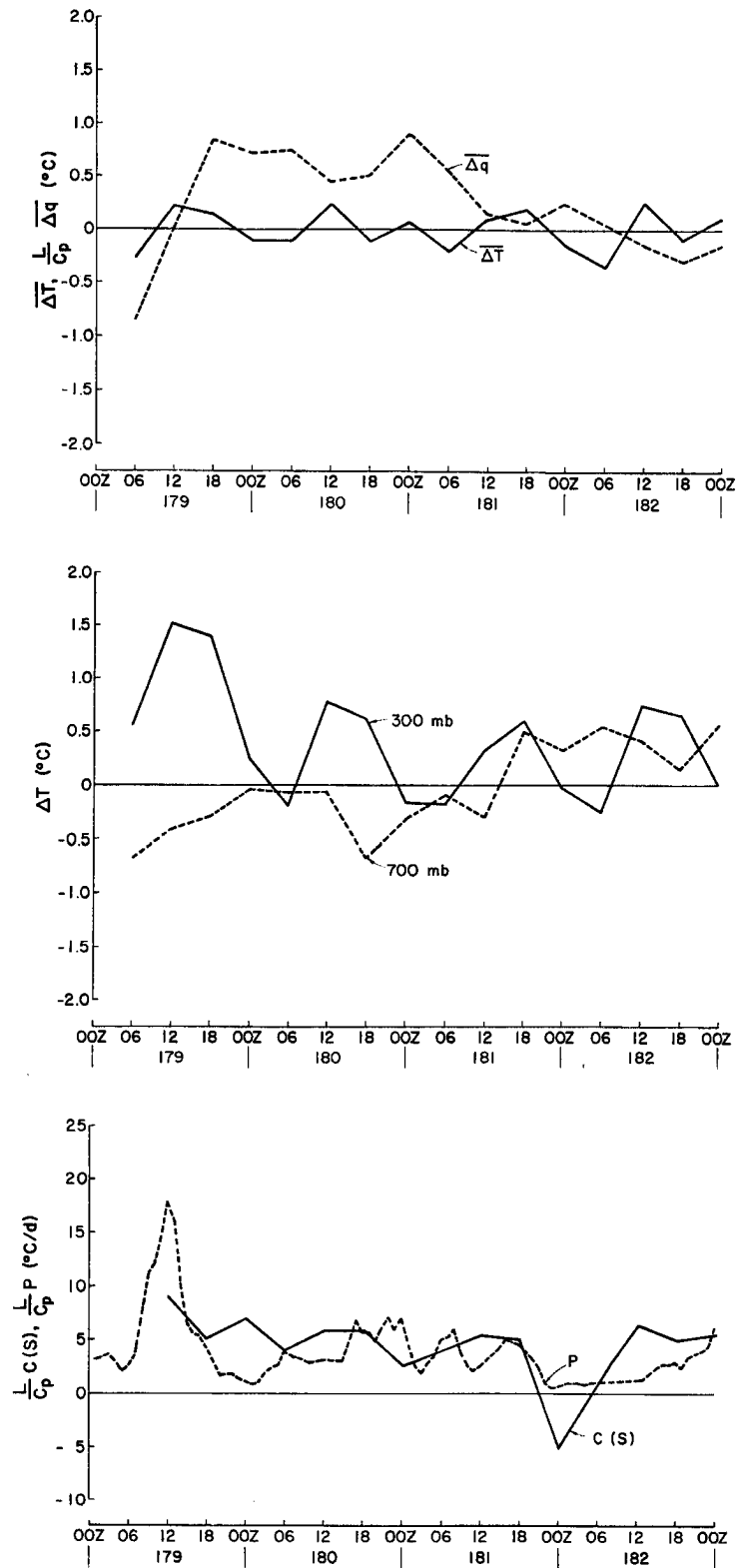


Fig. 14. Vertically integrated deviation temperature ($\overline{\Delta T}$) and moisture ($\overline{\Delta q}$) for the A/B-scale (upper curves); deviation temperature at 700 and 300 mb (middle curves); C(s) and P (lower curves as in Fig. 6). Phase I.

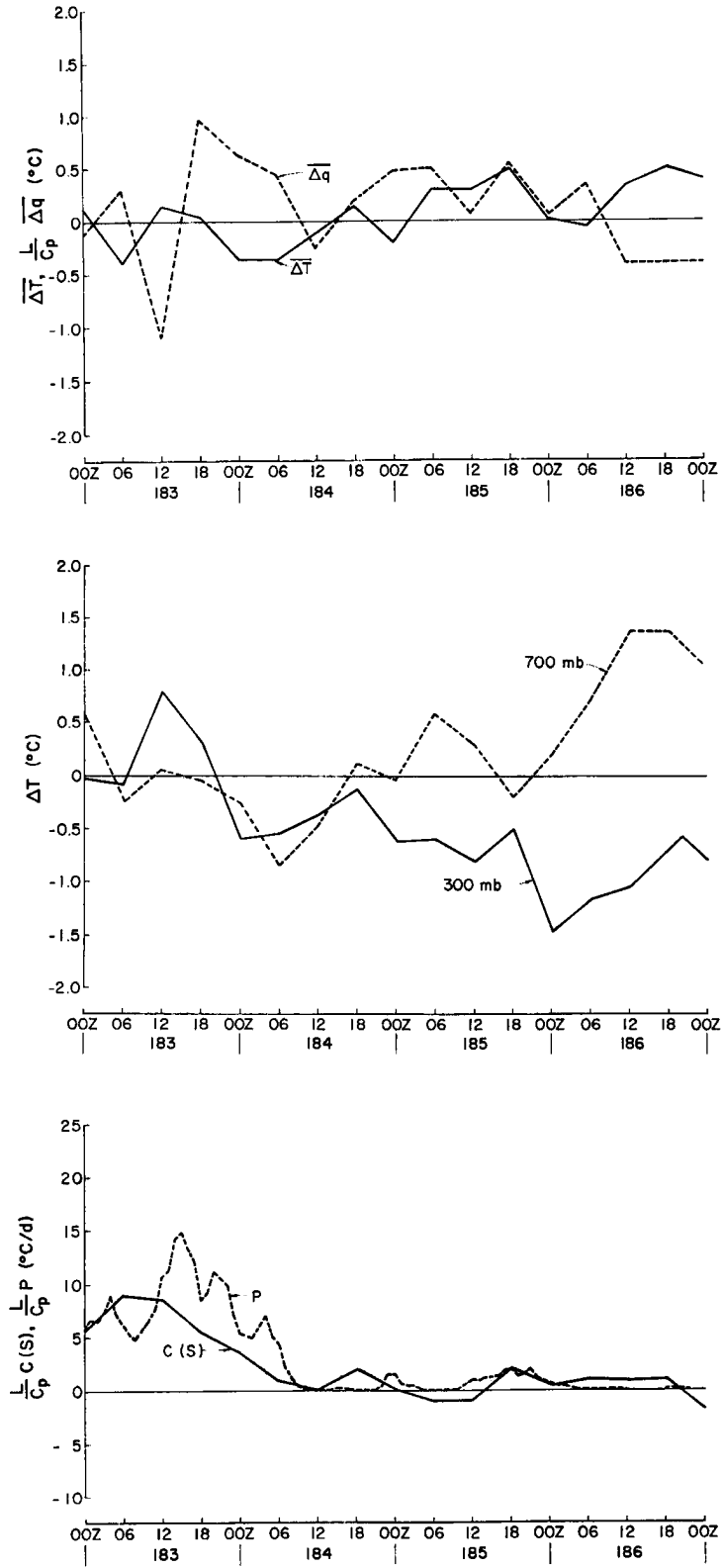


Fig. 14. Continued.

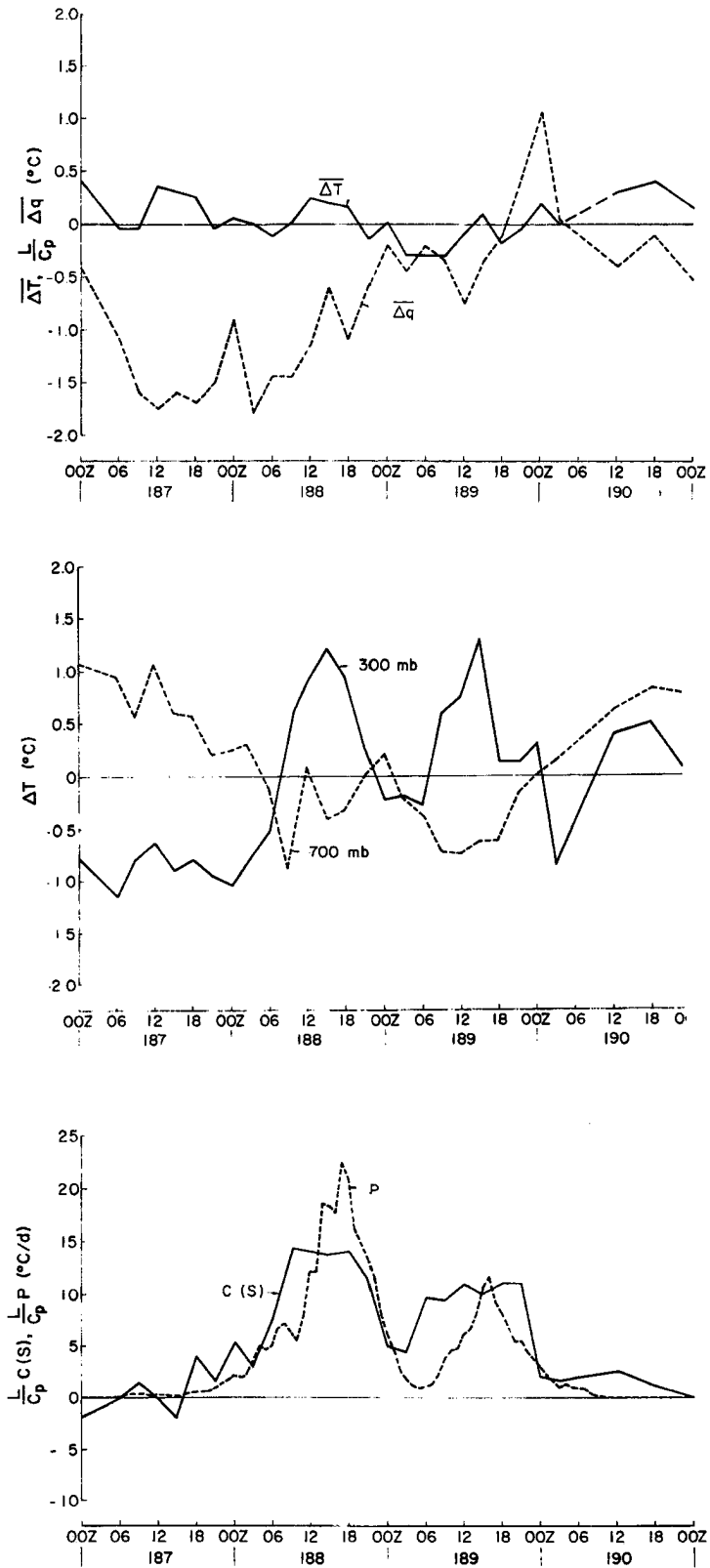


Fig. 14. Continued.

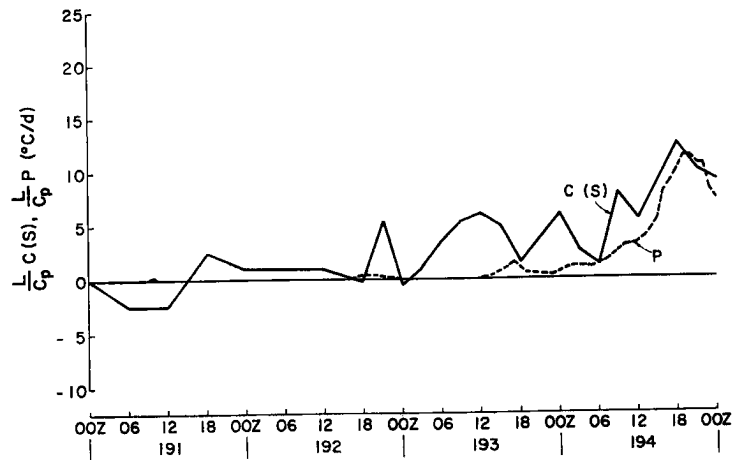
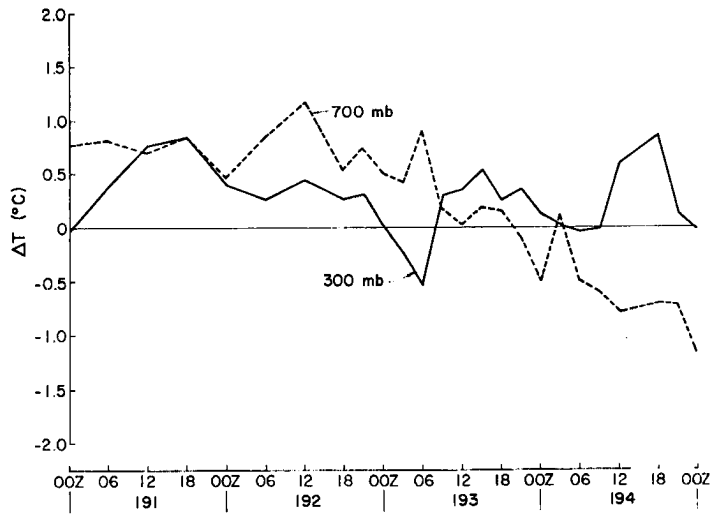
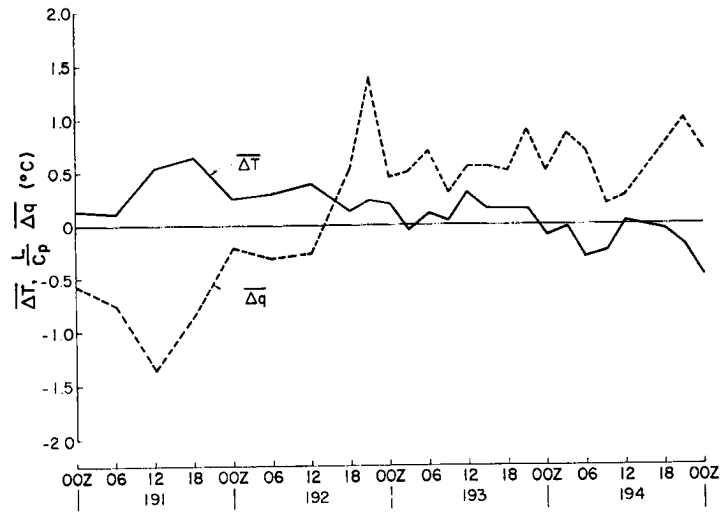


Fig. 14. Continued.

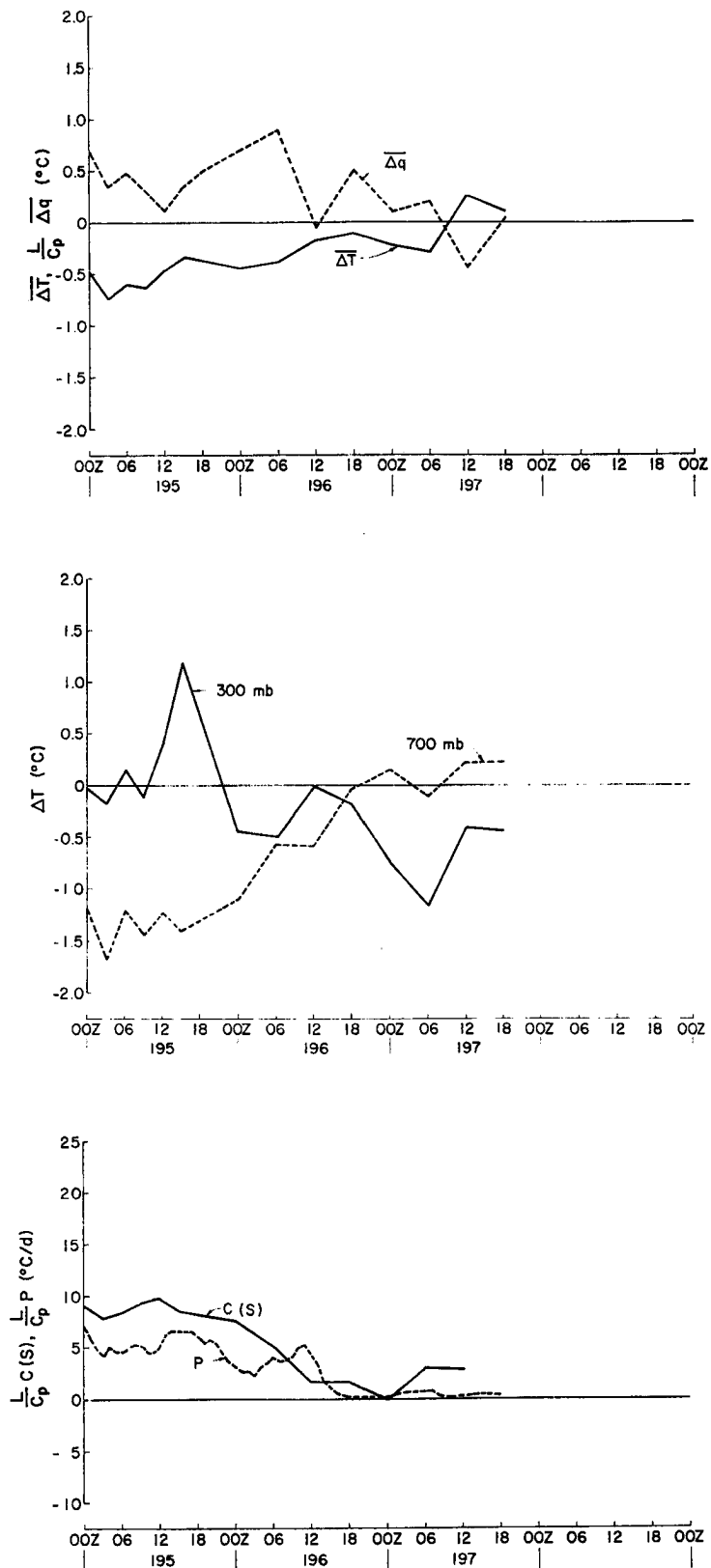


Fig. 14. Continued.

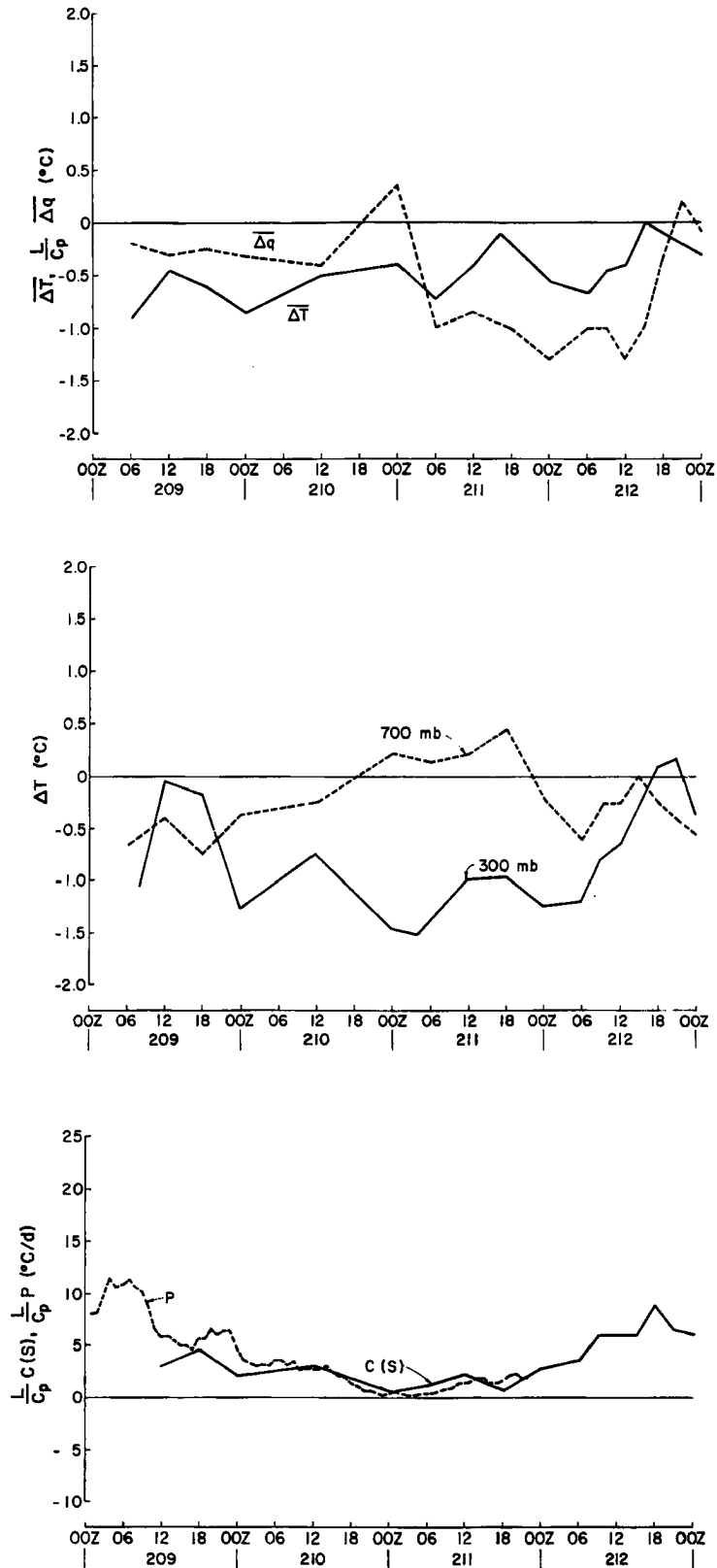


Fig. 15. Same as Fig. 14 except for Phase II.

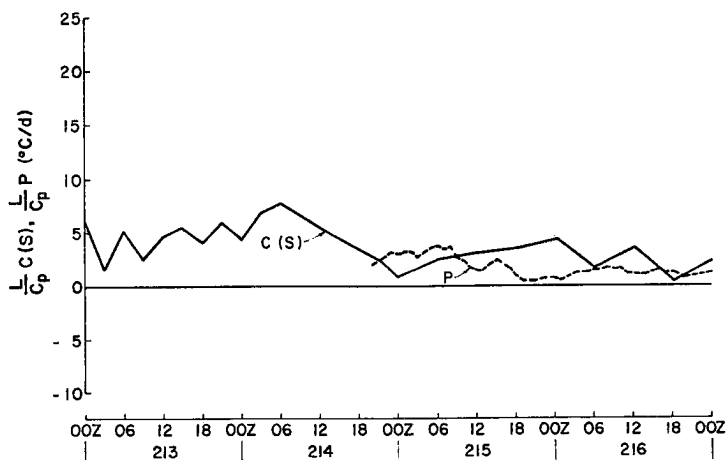
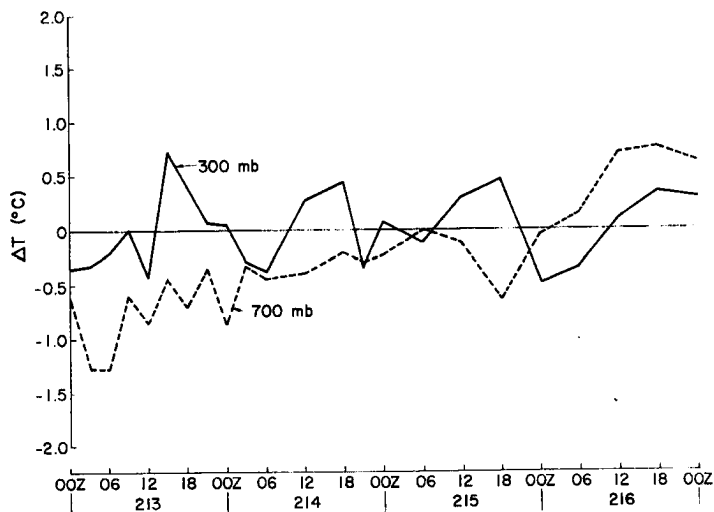
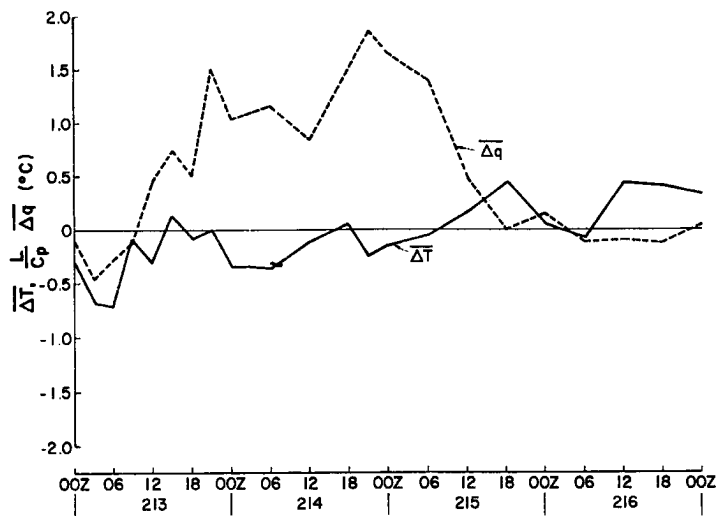


Fig. 15. Continued.

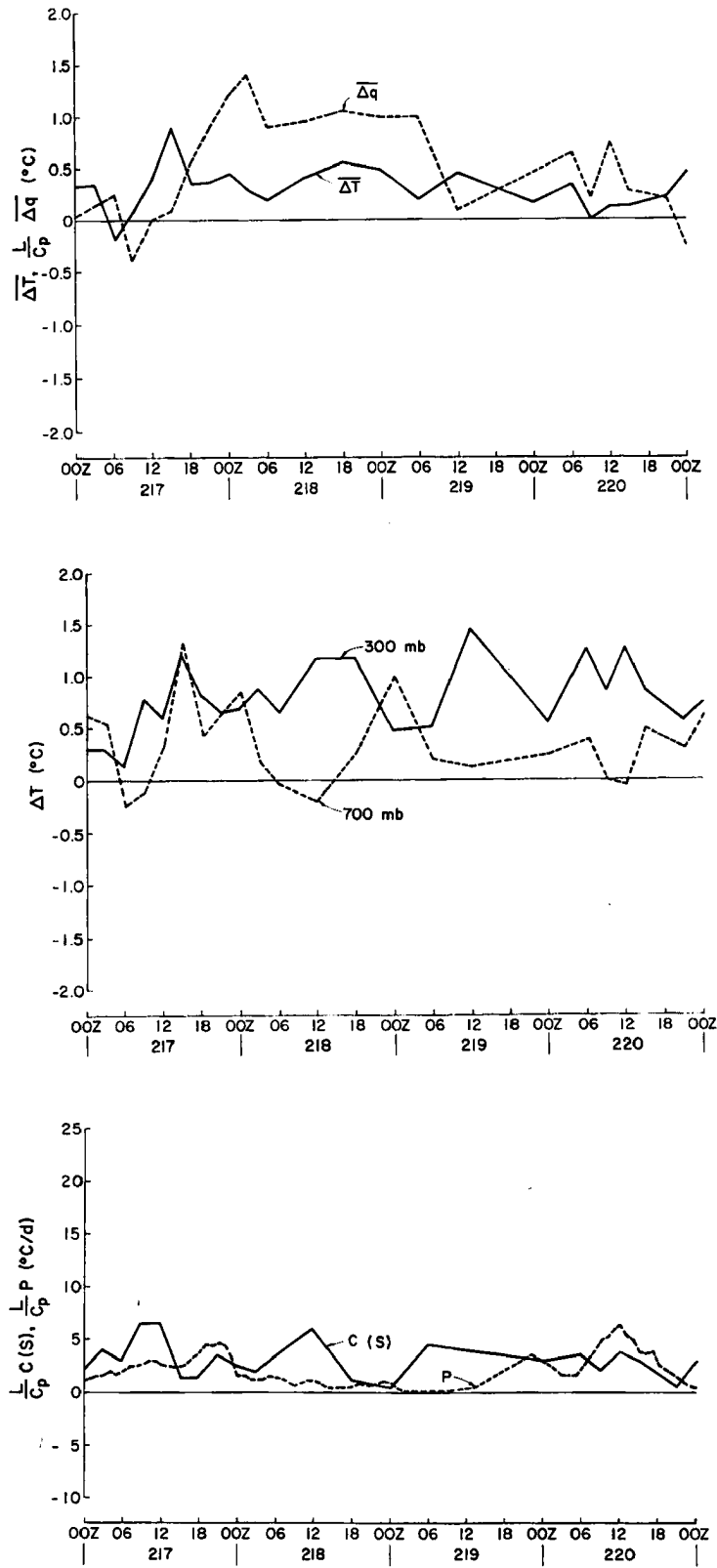


Fig. 15. Continued.

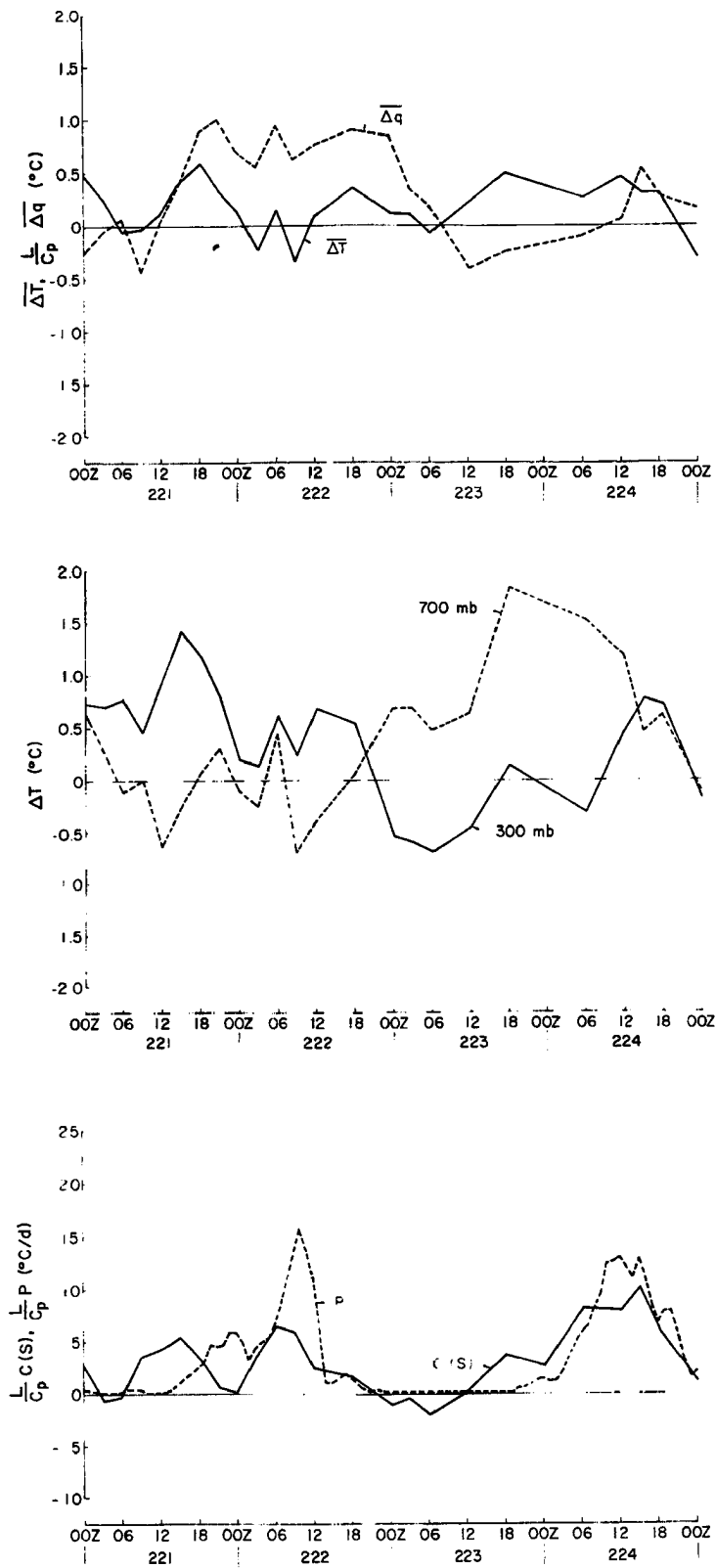


Fig. 15. Continued.

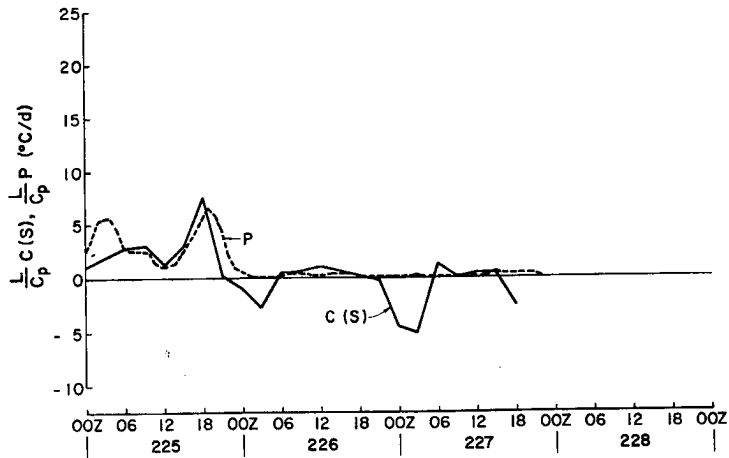
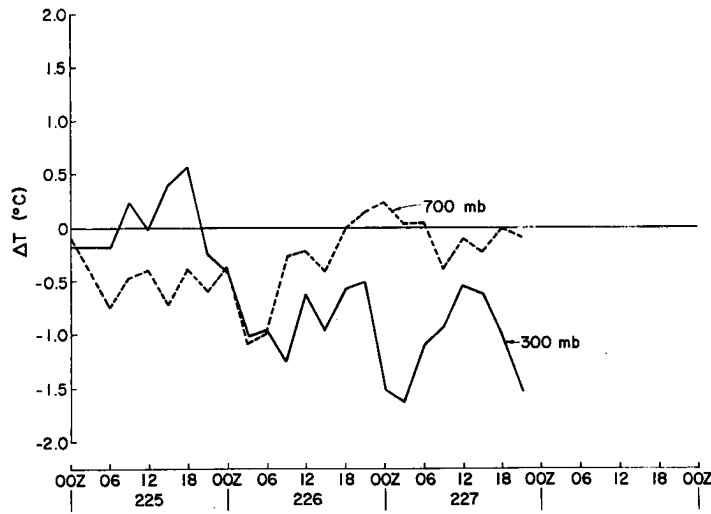
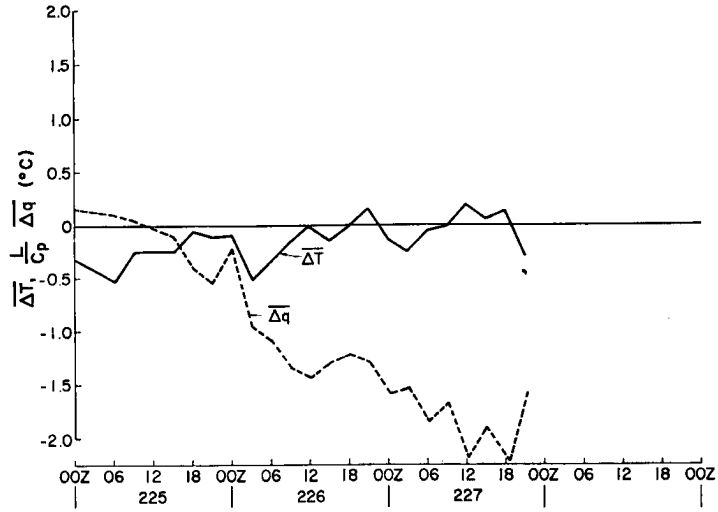


Fig. 15. Continued.

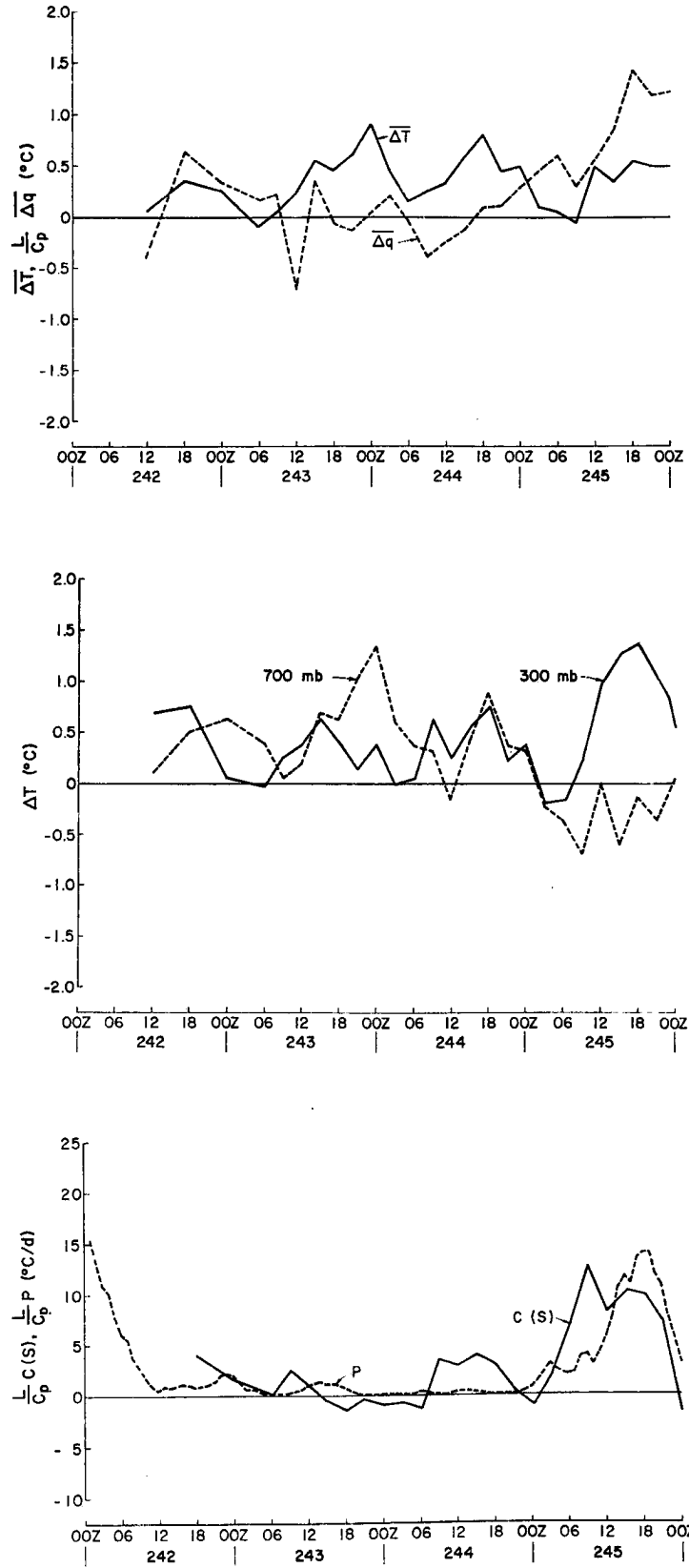


Fig. 16. Same as Fig. 14 except for Phase III.

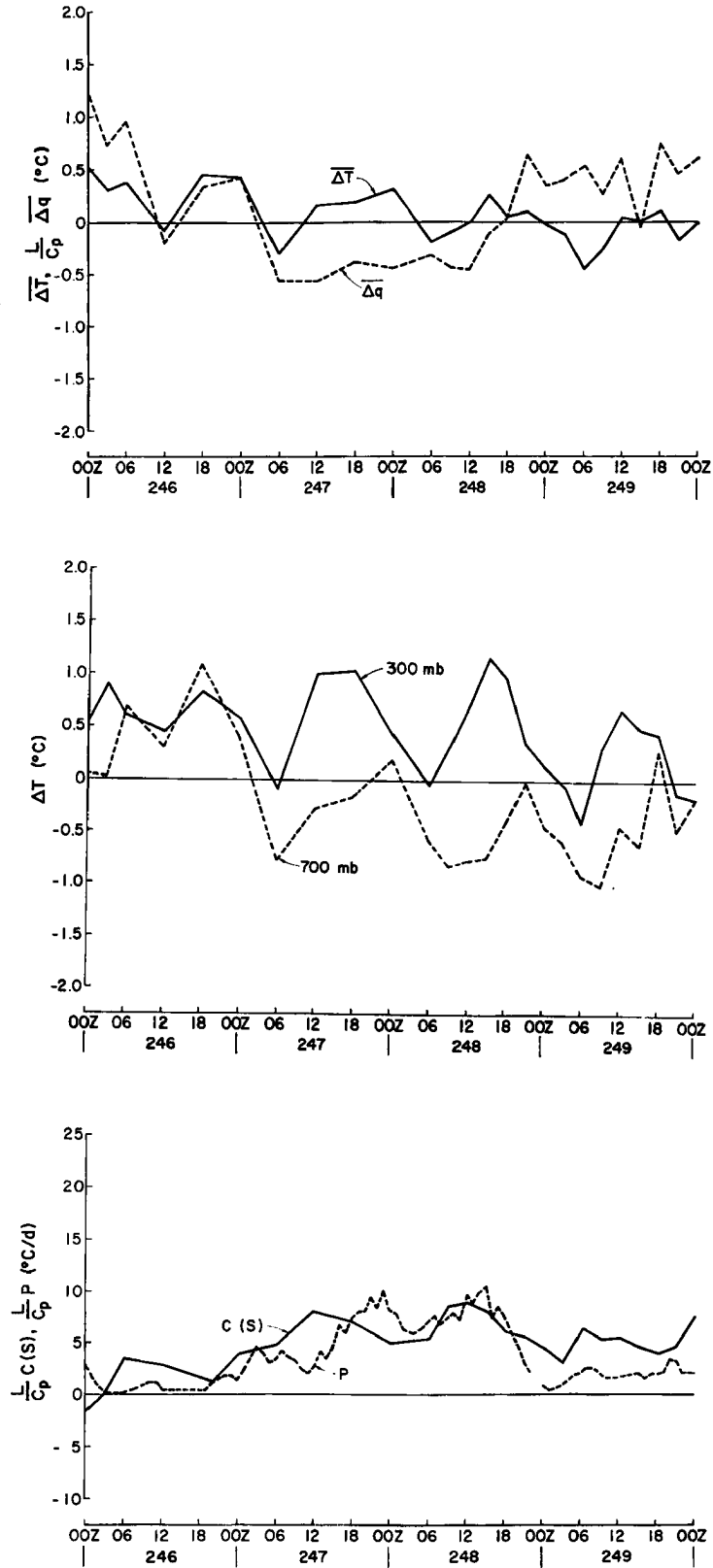


Fig. 16. Continued.

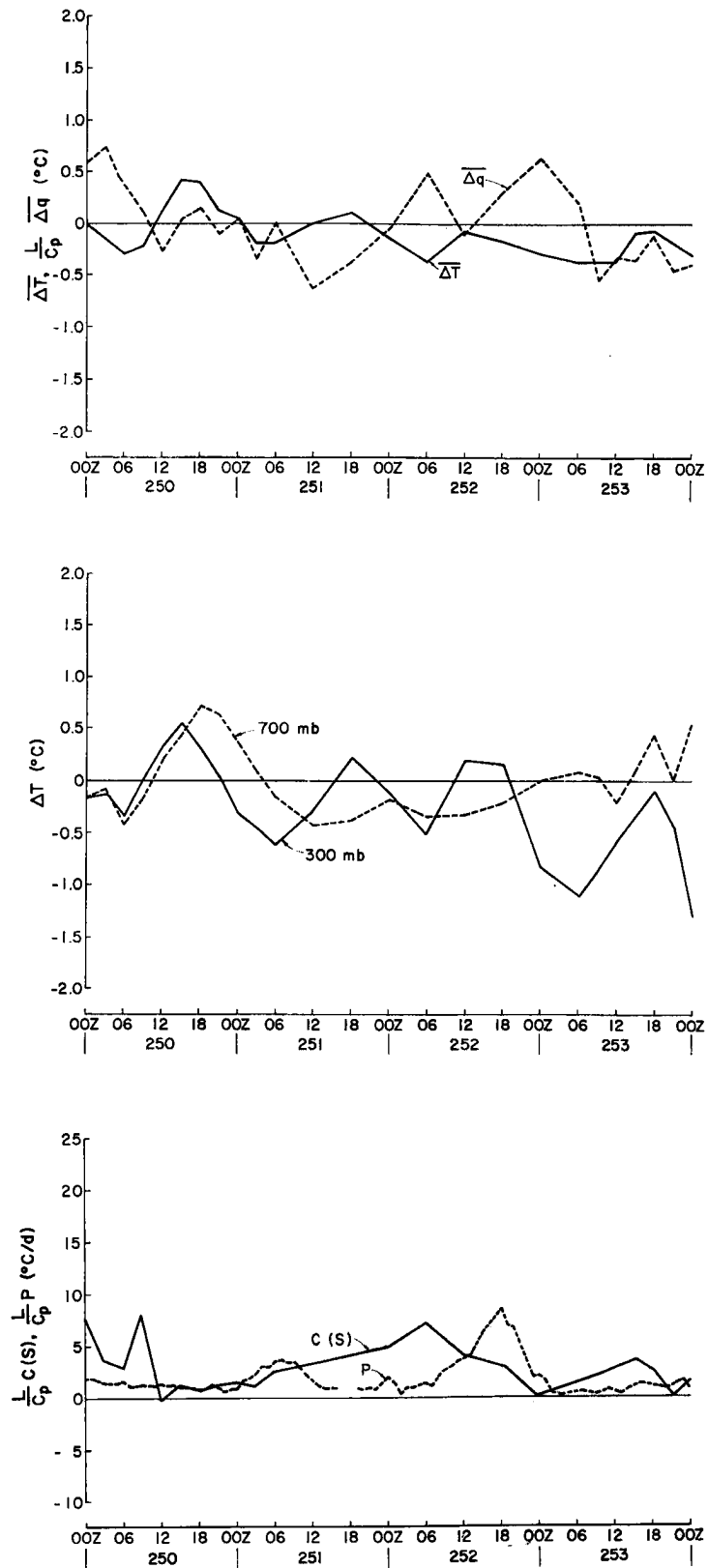


Fig. 16. Continued.

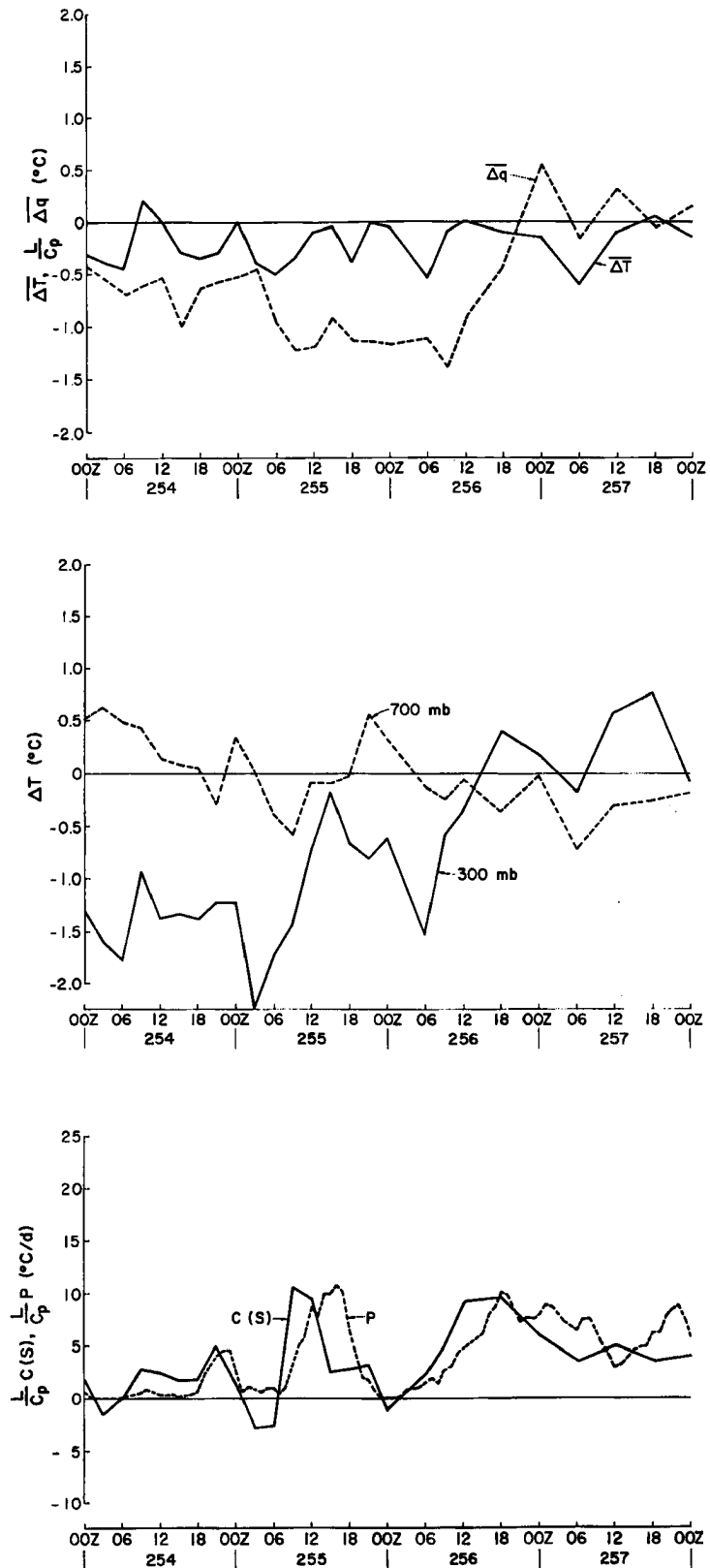


Fig. 16. Continued.

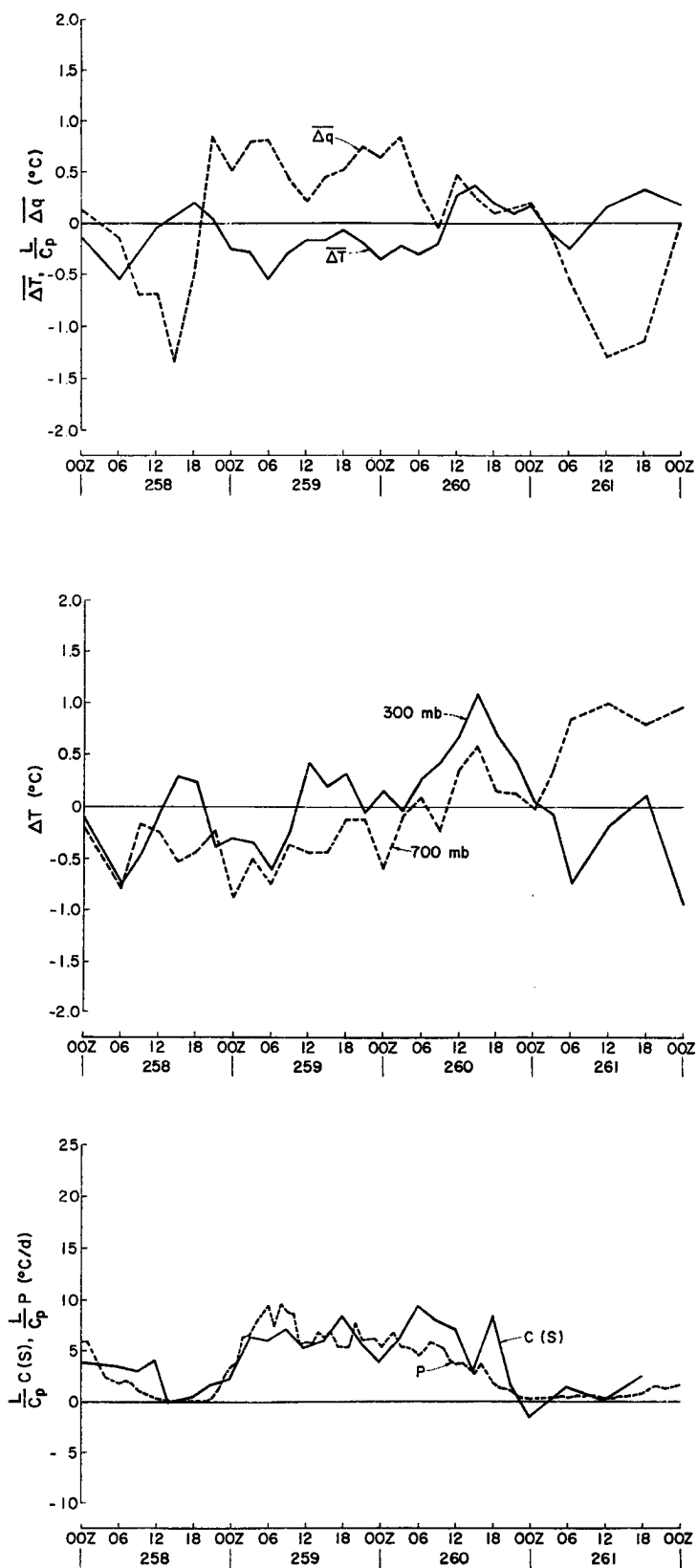


Fig. 16. Continued.

TABLE 8

Correlation coefficients (r) relating net tropospheric temperature change ($\partial\overline{\Delta T}/\partial t$) with radiational heating (Q_R), s-budget condensation ($C(s)$), and radar precipitation ($P(R)$).

Standard Deviation for an Uncorrelated Sample (σ_r)=.07

$$r [\partial\overline{\Delta T}/\partial t, Q_R] = .37$$

$$r [\partial\overline{\Delta T}/\partial t, C(S)] = .17$$

$$r [\partial\overline{\Delta T}/\partial t, P(R)] = -.12$$

correlated with radiational heating but were only weakly related to s-budget condensation. Radar precipitation was negatively correlated with $\partial\overline{\Delta T}/\partial t$.

Tropospheric temperature changes were dominated by variations in radiational heating. The variations in net tropospheric A/B-scale Q_R were dominated by the diurnal solar cycle rather than by variations in atmospheric structure or cloud population. This is shown in Fig. 17 which shows daytime (06-12 and 12-18 local time - LT averages) and nighttime (00-06 and 18-00 LT averages) radiational heating for 6-hour intervals vs. radar rainfall for the B-array. During the day there was no discernable variation in net Q_R with rainfall while at night the net cooling decreased only slightly with rainfall rate. Accepting the Cox and Griffith (1978) radiation data as correct, there are two reasons for this:

- 1) The moisture content of the GATE A/B-area atmosphere was very steady despite large variations in convective activity (see Table 7).
- 2) Upper level layer clouds, which are the primary modulators of radiational heating (the sun excepted) tend to redistribute Q_R in the vertical without greatly affecting the vertically integrated value. This is seen in Figs. 18 and 19 which show day and night A/B area Q_R profiles for the most convectively enhanced and suppressed intervals in Phase III. It is important to realize that the diurnal temperature cycle, while ultimately forced by radiation, is very complex and involves processes occurring on much larger scales than those studied here (Foltz, 1976; Gray and Jacobson, 1977).

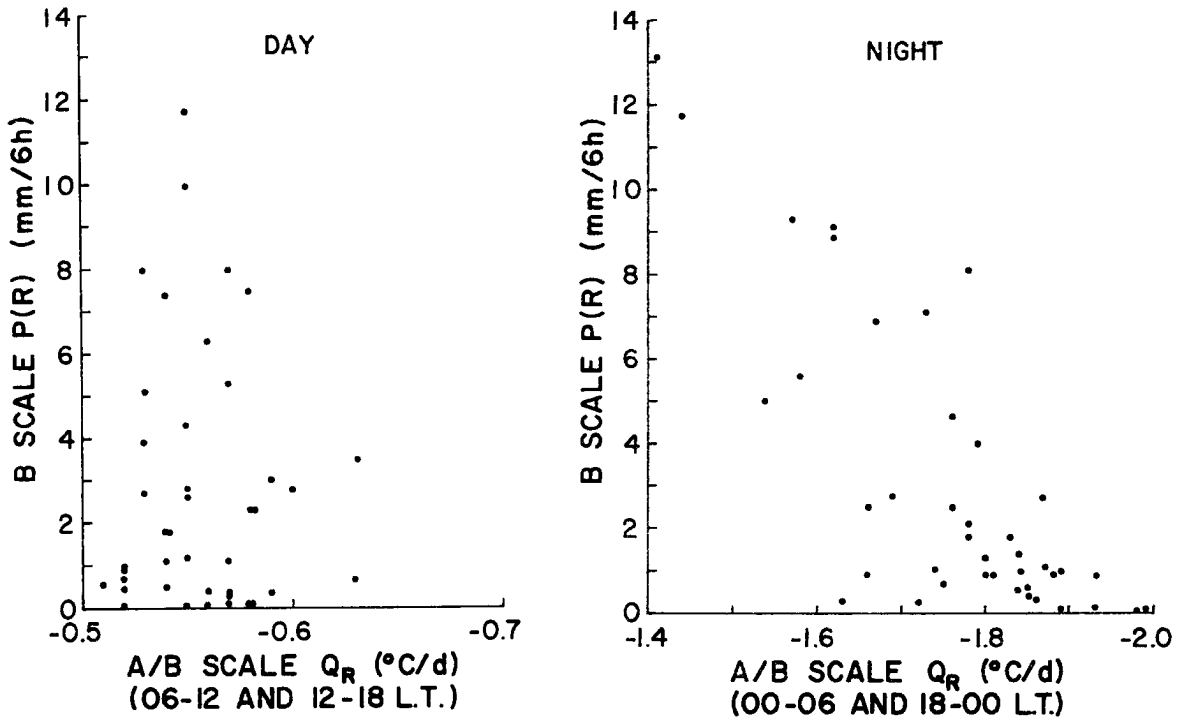


Fig. 17. A/B-scale mean radiation at individual time periods vs. B-scale radar rainfall. Left graph is for daytime (06-12, 12-18 Local Time - LT). Right graph is for night (18-00, 00-06 LT). Data are averaged for 6-h time periods (from Cox and Griffith, 1978).

The diurnal cycle of Q_R is further illustrated by the regularity with which the daily minima in $\overline{\Delta T}$ occurred near 0600 GMT (about 0430 local time - LT) as shown in Table 9. For the 53 days with temperatures recorded at all four even time periods, 43 days (or 81%) experienced the lowest temperatures at 06 GMT and another 6 days (11%) showed nighttime minima at 00 GMT (2230 LT).

If precipitation was randomly distributed throughout the day, the weak correlation between $\partial\overline{\Delta T}/\partial t$ and $c(s)$ (Table 8) would suggest that convective latent heat release slightly warms the troposphere on the A/B-scale. However, both budget and radar condensation/rainfall estimates show diurnal variations with daytime maxima (Fig. 20). $C(s)$ was maximum from 9-12Z (~ 9 LT) when the atmospheric temperature was rapidly increasing during both

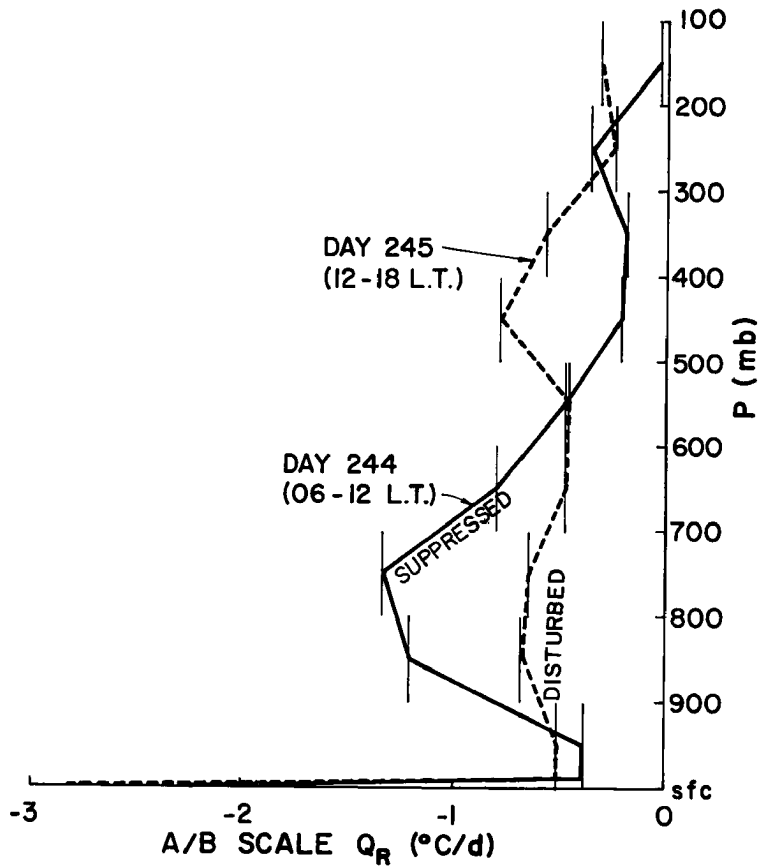


Fig. 18. Daytime radiational cooling during a highly disturbed (day 245, 12-18 LT) period and a very suppressed (day 244, 06-12 LT) period.

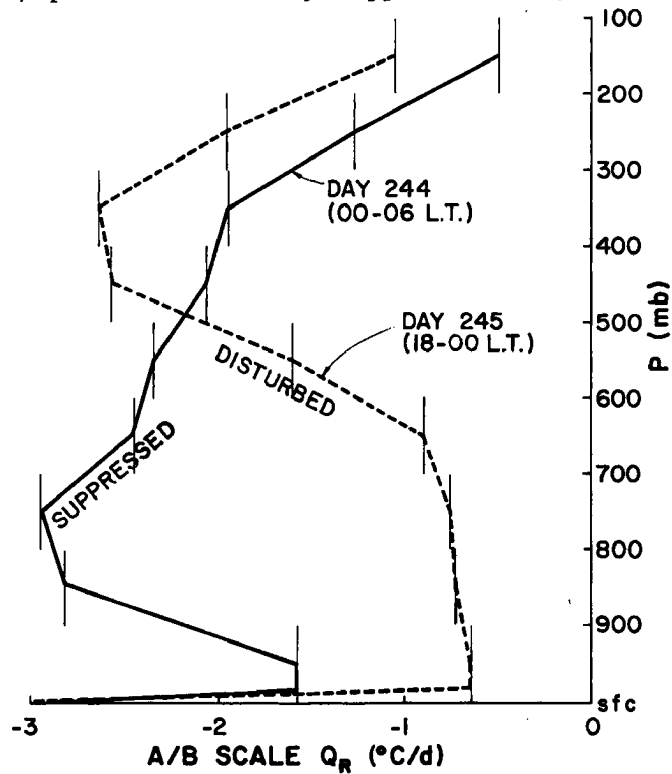


Fig. 19. Nighttime radiational cooling during a highly disturbed (day 245, 18-00 LT) period and a very suppressed (day 244, 00-06 LT) period.

TABLE 9

Distribution of times of daily minimum mean tropospheric temperatures (day is 00-23 GMT) using data at 6-hour intervals.

<u>Time:</u>	<u>00 GMT</u>	<u>06 GMT</u>	<u>12 GMT</u>	<u>18 GMT</u>	<u>TOTAL</u>
No. Days:	6	43	3	2	53

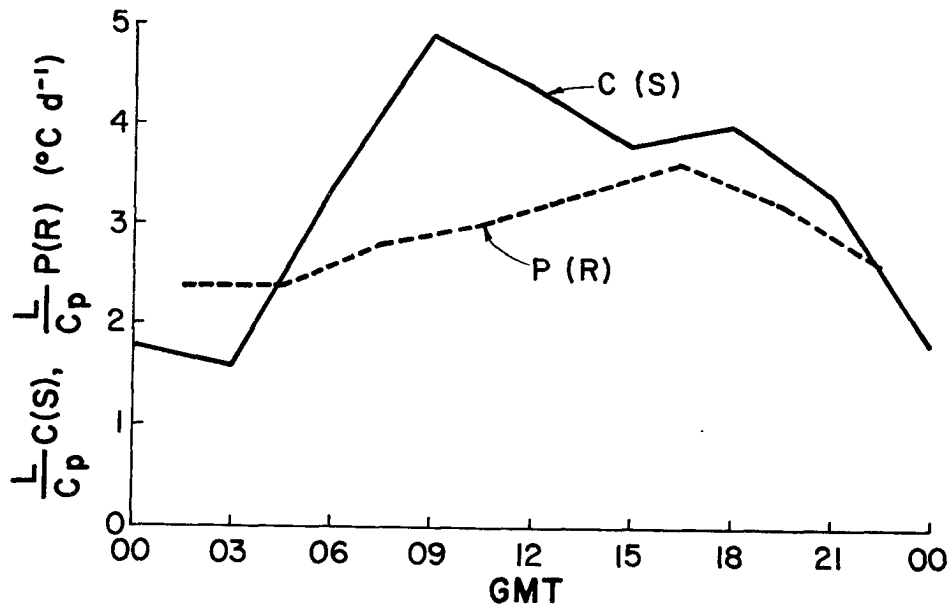


Fig. 20. Diurnal variations in C(s) (s-budget condensation) and P (master array radar rainfall) averaged for all phases.

convectively enhanced and suppressed periods. P(R) peaked during the afternoon hours near the time of daily maximum temperature. Both quantities are positively correlated with Q_R . The small correlations between $\overline{\partial\Delta T/\partial t}$ and C(s), P(R) are not meaningful by themselves since latent heating effects were obscured by the larger diurnal temperature variation induced by radiational heating.

While net condensation warming of the tropical troposphere on the A/B-scale was apparently smaller than the warming which occurred due to the mean diurnal variations, latent heating may have enhanced the divergence/vertical motion patterns on that scale by heating at upper levels and cooling the lower troposphere. Riehl (1948, 1954, 1969), Williams and Gray (1973) and Ruprecht and Gray (1976) have noted that tropical cloud clusters are warm core at upper levels and very weakly cold core in the lower troposphere. Reed and Recker (1971) and Reed *et al.* (1977) have noted a similar thermal structure in easterly wave troughs, and Frank (1978) showed upper level warming and lower level cooling during the development of GATE convective systems. Observational studies of cloud cluster to tropical cyclone transformation show that the temperature increase is strongest from about 200-400 mb (Yanai, 1961; Zehr, 1976). However, the profiles of Figs. 18-19 indicate that the upper levels of convective regions radiatively cool relative to surrounding suppressed areas while the lower layers of a cluster relatively warm. Hence, radiation alone would tend to induce a system with a cold core aloft and a warm core in the lower to middle troposphere.

Numerous cumulus parameterization schemes which have been devised lead to tropospheric warming in the presence of net condensation with a maximum effect in the upper troposphere. In general, these schemes have neglected or oversimplified radiational heating as a second order term due to the larger magnitude of total latent heat release. Alternatively, one may assume that latent heating is confined to relatively small and insulated "hot towers" (after Riehl and Malkus, 1958) which relegates this energy source to providing lift to low level air. The heating of the 95% of the air outside the updrafts could be

dominated by radiational effects. Gray and Jacobson (1977) have suggested that cloud/cloud free radiational differences are important for cloud cluster maintenance. They hypothesize that the horizontal pressure gradients which drive the circulation are dominated by differential radiational heating effects between cirrus covered and relatively clear areas. Recent modelling results by Fingerhut (1978) and observational studies by Dewart (1978) and McBride and Gray (1978) support this argument.

Temporal variations of ΔT at 300 and 700 mb are shown in Figs. 14-16. Both levels showed strong diurnal variations with minimum temperature occurring near 06 GMT and maxima generally in the afternoon. There also is strong tendency for the temperatures at the two levels to be out of phase with each other over periods of a few days, but this time scale is much too long to be associated with individual convective systems. It is not visually obvious whether or not temperatures at these levels were related to the latent heat release.

Correlation coefficients relating temperature changes at 300 and 700 mb to s-budget condensation, radar rainfall and net tropospheric radiational heating were determined for Phase III and are shown in Table 10. At both levels the temperature changes were significantly correlated with $\overline{Q_R}$. There was also a significant correlation between s-budget condensation and $\partial\Delta T/\partial t(300)\text{mb}$ although it was not as strong as the $\partial\Delta T/\partial t(300\text{mb})$ vs. $\overline{Q_R}$ correlation. On the other hand, P(R) showed no significant correlation with $\partial\Delta T/\partial t$ at either level, and $\partial\Delta T/\partial t(700\text{mb})$ was only weakly related to C(s).

Table 10 seems to indicate that the tropospheric temperature is much more directly related to radiation than to condensation. If it is hypothesized that convective heat release tends to warm the upper levels and cool the

5. CONVERGENCE VS. VORTICITY IN THE BOUNDARY LAYER

After the famous CISK (Conditional Instability of the Second Kind), papers of Charney and Eliassen (1964), Ooyama (1964) and Ogura (1964), it became fashionable to ascribe mass inflow into tropical convective systems to the influences of low level friction. Documentation of substantial middle tropospheric inflow into cloud clusters (Williams, 1970; Williams and Gray, 1973), easterly wave troughs (Reed and Recker, 1971), and even tropical cyclones (Frank, 1977a) indicated that the radial mass fluxes found in these systems greatly exceed those which could be driven by surface friction alone. While upward extension of friction through cumulus momentum transports undoubtedly contributes to middle level inflow in some systems (Frank, 1977b; Stevens et al., 1977), it is becoming increasingly apparent that the role of frictionally induced convergence into tropical weather systems has been greatly exaggerated. Gray (1978) estimated that surface friction accounted for only a small part of the surface to 900 mb convergence in West Pacific cloud clusters.

It can be shown that the area averaged frictionally induced convergence in the planetary boundary layer is related to the mean vorticity at the top of the boundary layer averaged over the area (Gray, 1972; Zehr, 1976). That is:

$$[\vec{\nabla} \cdot \vec{v}] \approx -(K)\bar{\zeta} \quad \text{or} \tag{16}$$

$$[V_r] \approx -(K) V_T$$

where the brackets denote averages from the surface to the top of the frictional boundary layer (usually about 900 mb) and $\bar{\zeta}$ (vorticity) and

V_T (tangential wind) are at the top of the boundary layer. K is a constant.

Based on a statistical treatment of winds over the tropical oceans, Gray (1972) has shown that $K \sim 0.1$ for winds in the 0-10 m/s regime. Therefore, frictional convergence occurs only when $V_T > 0$, and one would expect the frictional convergence in a relatively weak tropical system to be substantially smaller than the vorticity.

Figures 21-23 compare the A/B-scale vertical motion (ω) with the tangential winds at 900 mb. The vertical motion reflects the vertically integrated divergence from the surface to 900 mb and is plotted so that upward vertical motion and positive cyclonic vorticity have the same sign. An upward motion of 45 mb d^{-1} corresponds to about 1 m s^{-1} of mean radial inflow ($\overline{V_r}$).

The most striking feature of Figs. 21-23 is the independence of the two parameters. Upward vertical motion at 900 mb occurred most of the time during GATE, yet the low level vorticity was often weak or negative. There was no correlation between the magnitudes of $V_T(900)$ and $\omega(900)$. During periods of strong upward motion, the air went up without any obvious support from the vorticity field, and occasionally weak subsidence coincided with positive vorticity.

The relative unimportance of frictional convergence during GATE is further illustrated by Figs. 24-26. Comparison of the radial and tangential wind components at 950 mb shows that the mean A/B-scale divergence and vorticity fields were of similar magnitudes and were poorly related at individual time periods (there was typically very little change in V_T between 900 and 950 mb). It is obvious that frictional processes must have played an insignificant role even within the

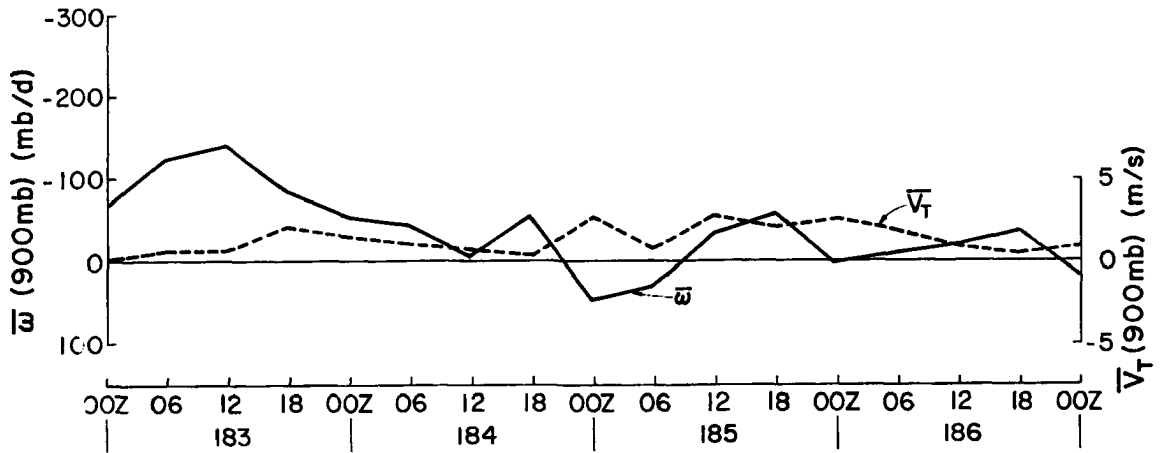
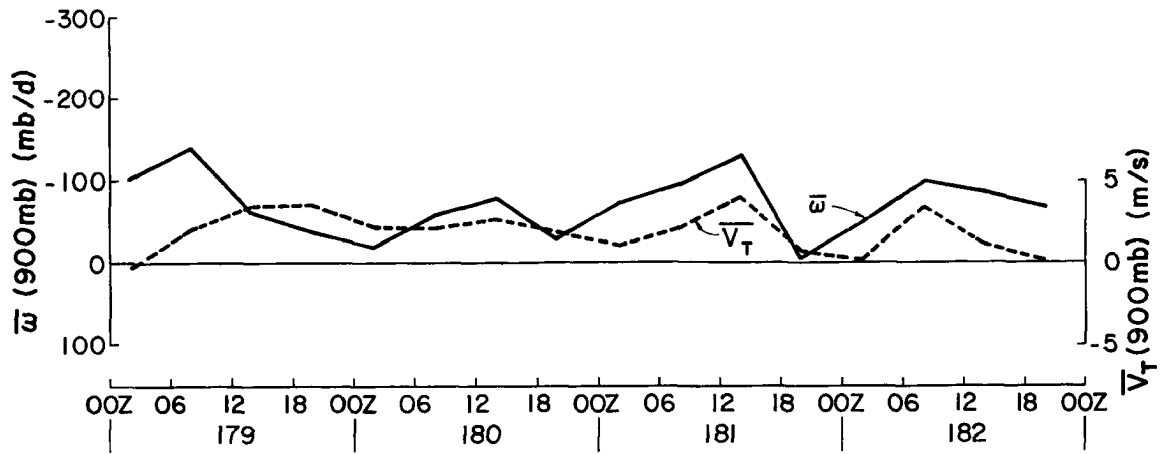


Fig. 21. Mean A/B-scale vertical motion ($\bar{\omega}$) at 900 mb and A/B-array mean tangential wind (V_T - proportional to mean A/B-area vorticity). Phase I.

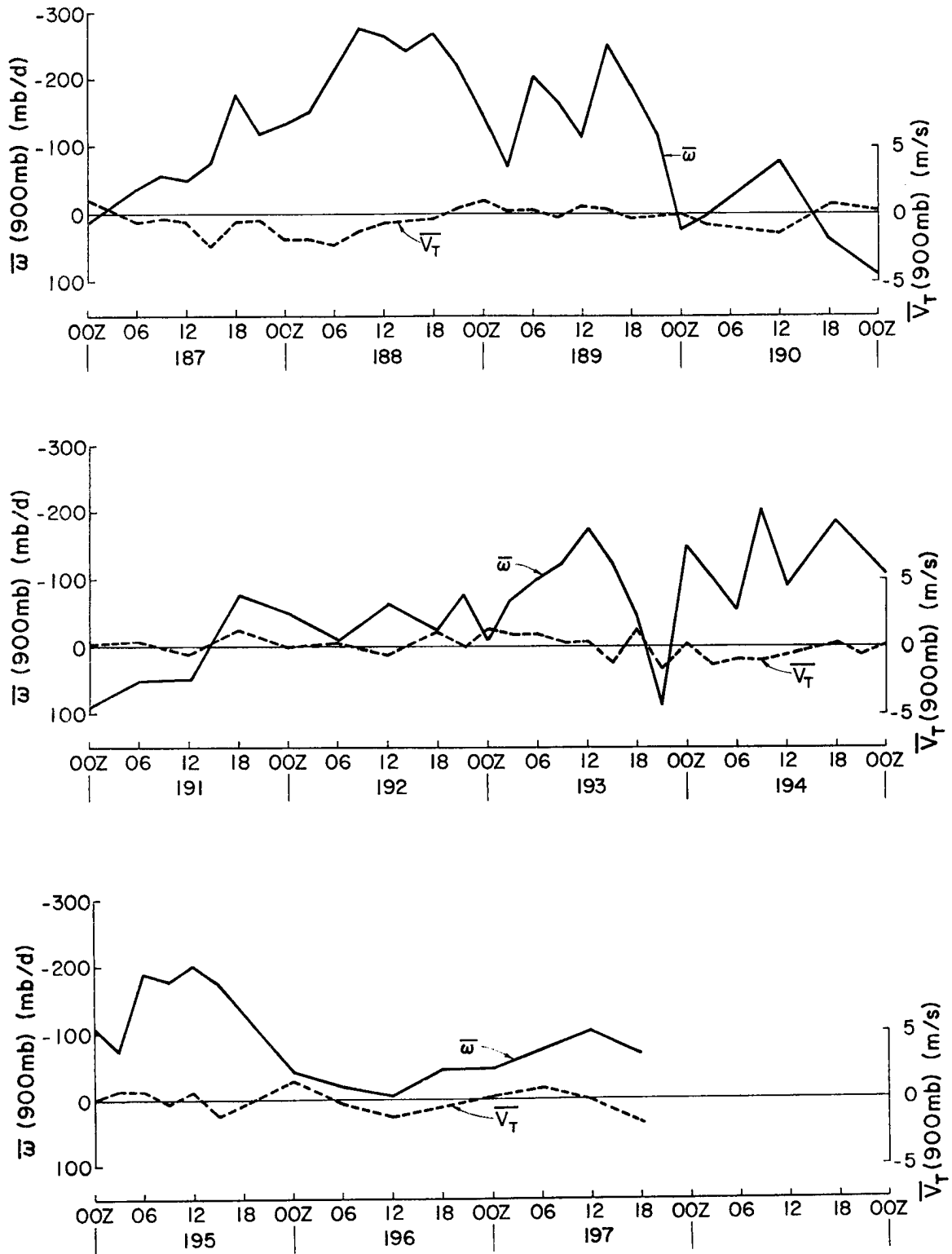


Fig. 21. Continued.

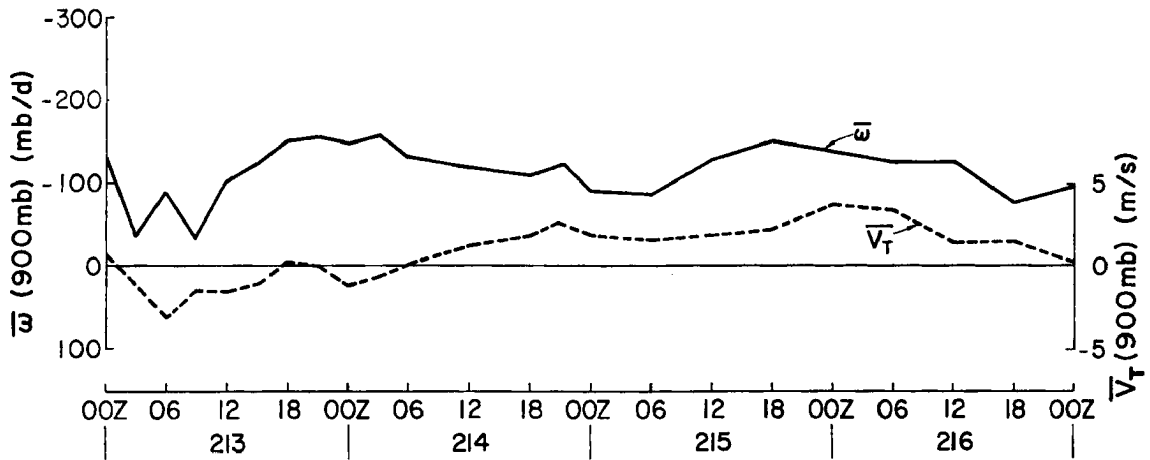
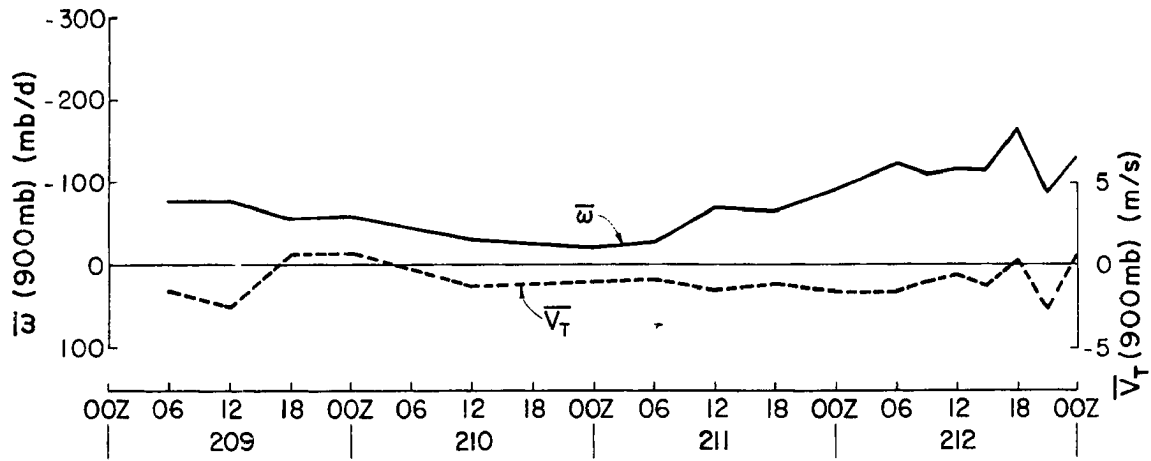


Fig. 22. Same as Fig. 21 except for Phase II.

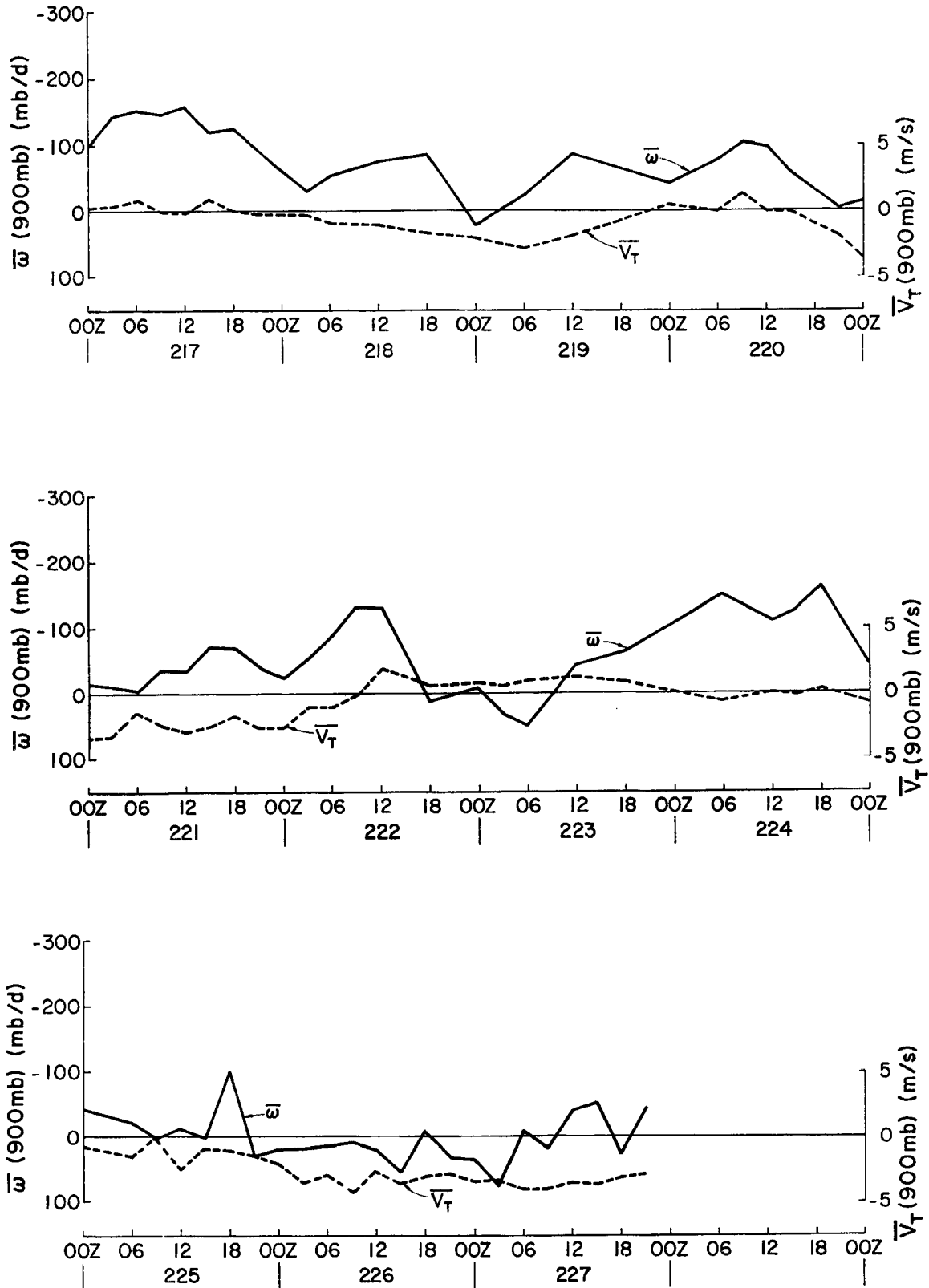


Fig. 22. Continued.

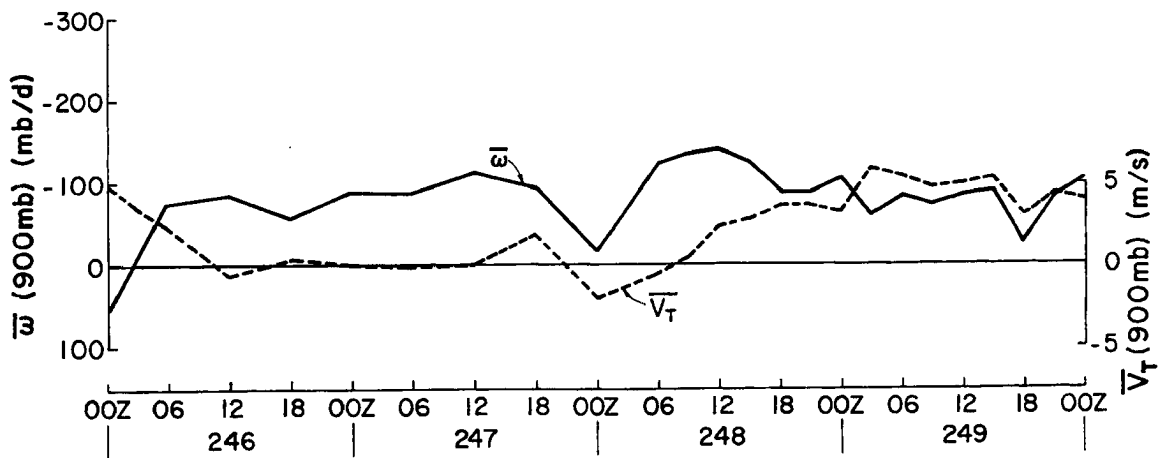
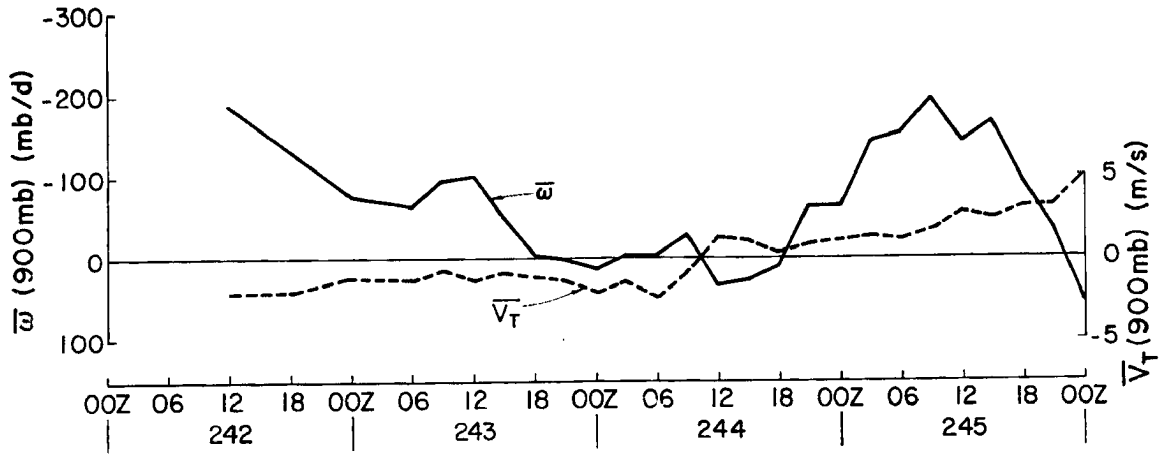


Fig. 23. Same as Fig. 21 except for Phase III.

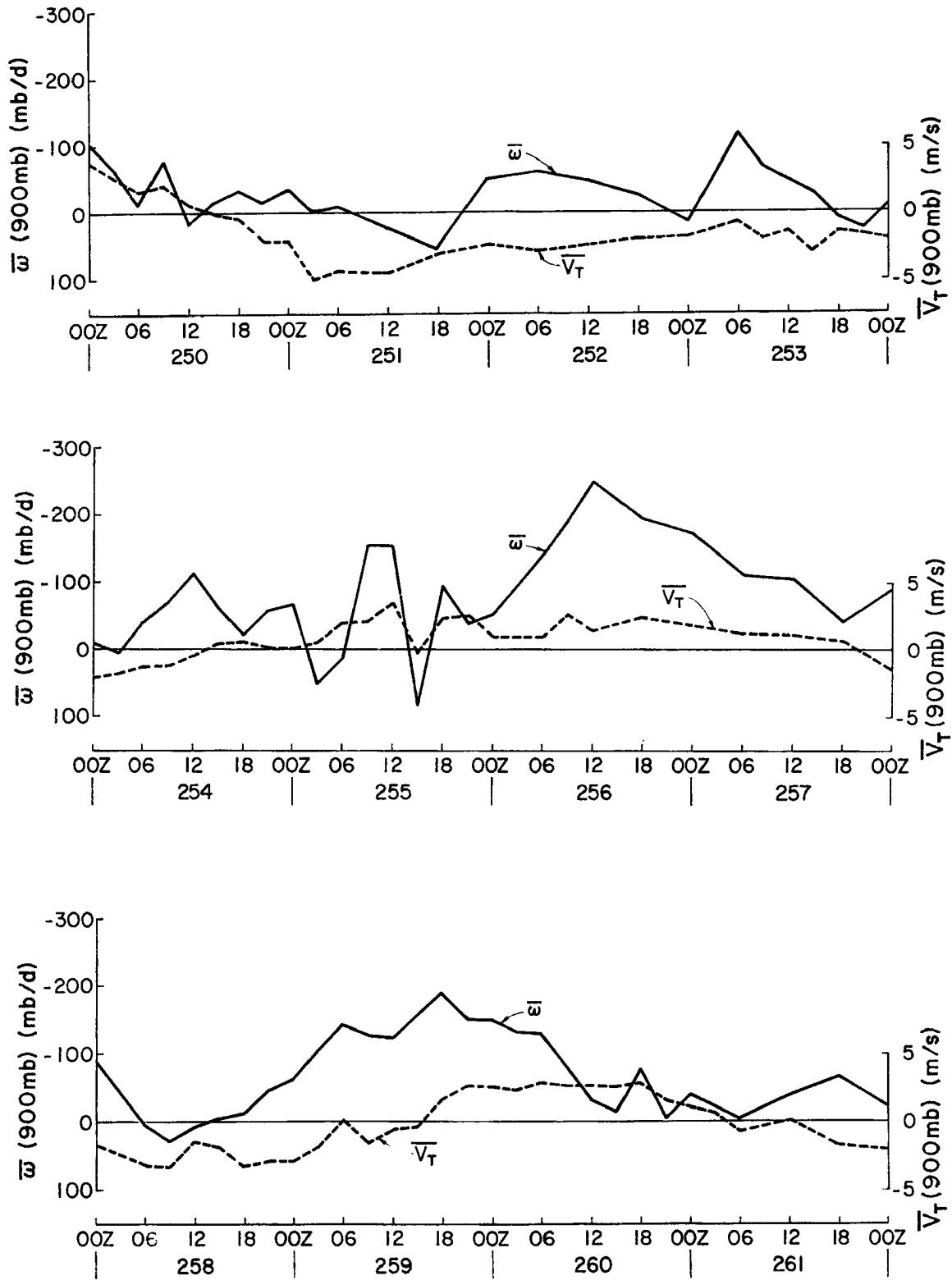


Fig. 23. Continued.

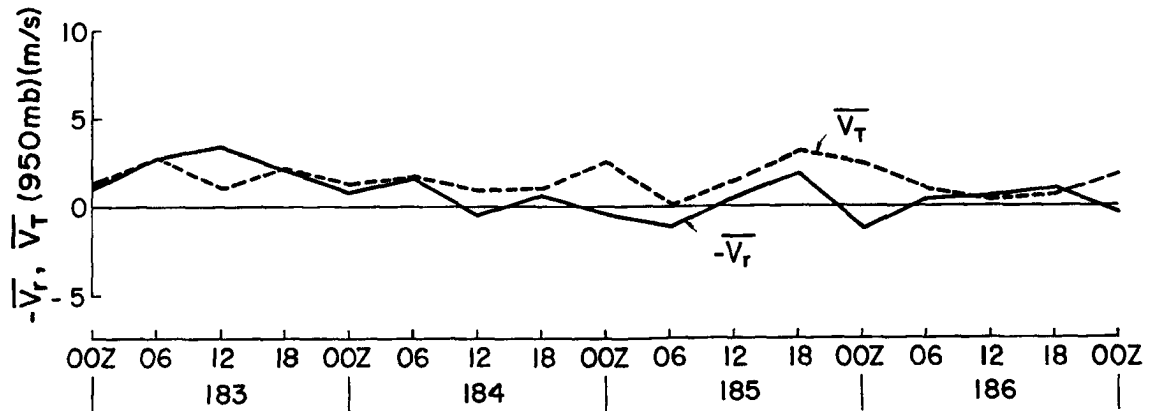
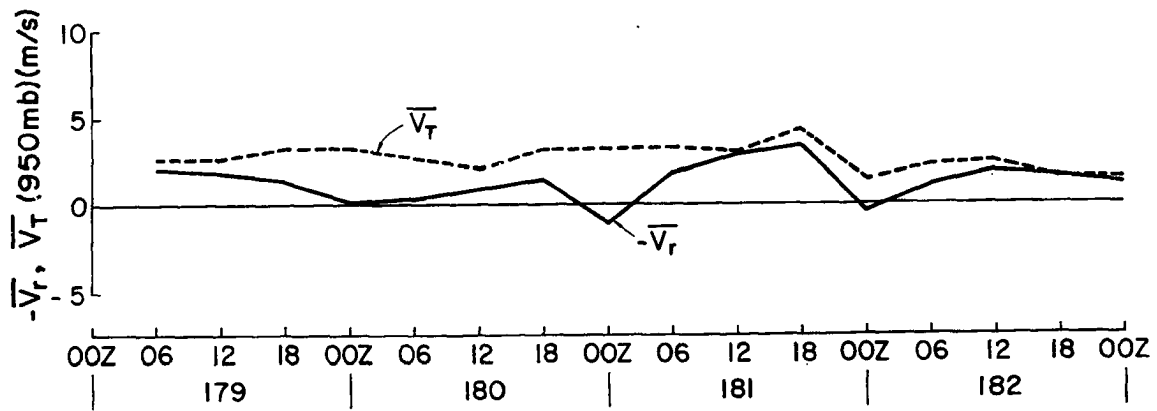


Fig. 24. Minus the mean A/B-array radial wind at 950 mb; mean A/B-array tangential wind at 950 mb. Radial wind is defined as positive outward. Phase I.

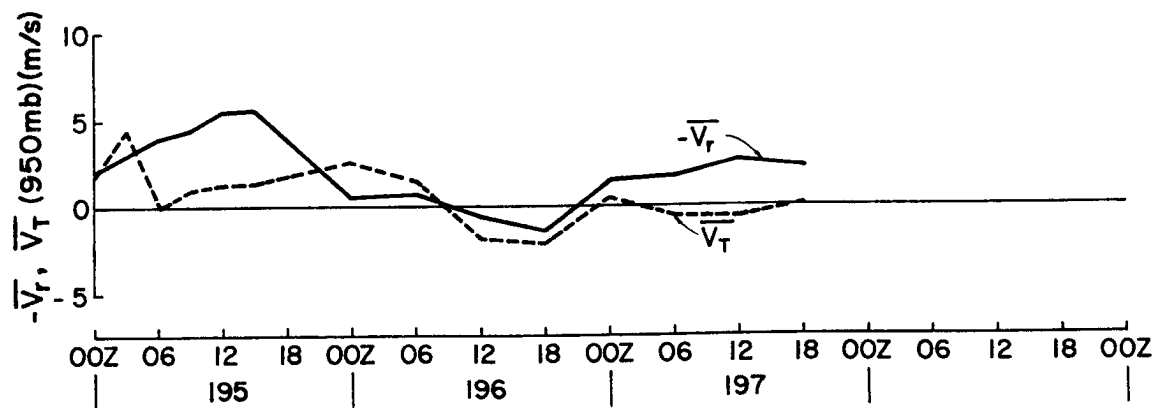
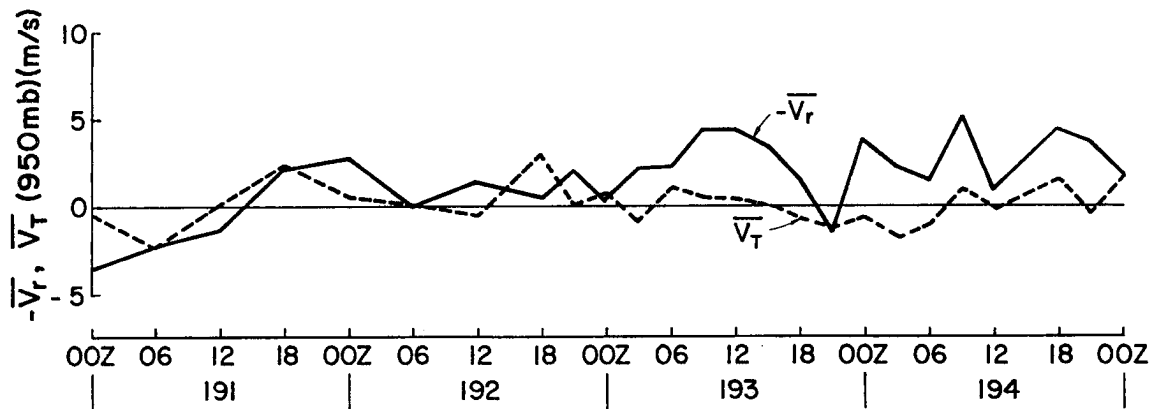
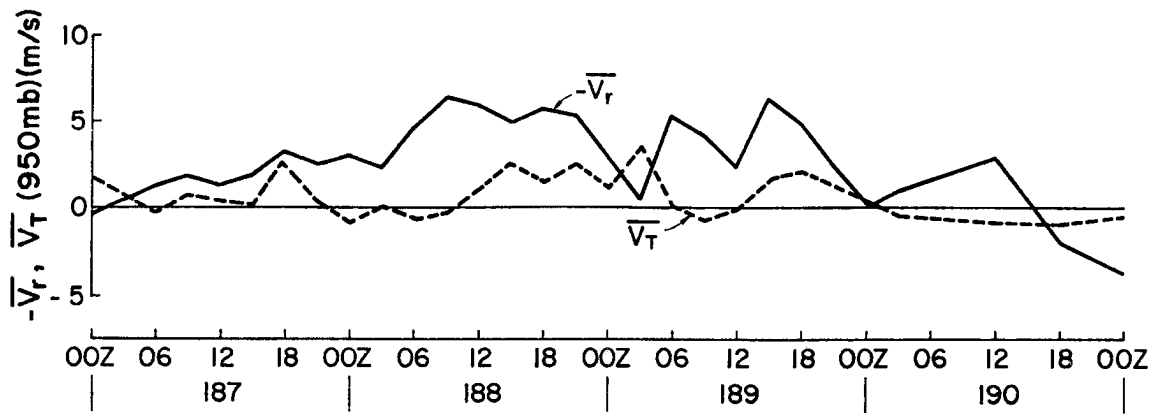


Fig. 24. Continued.

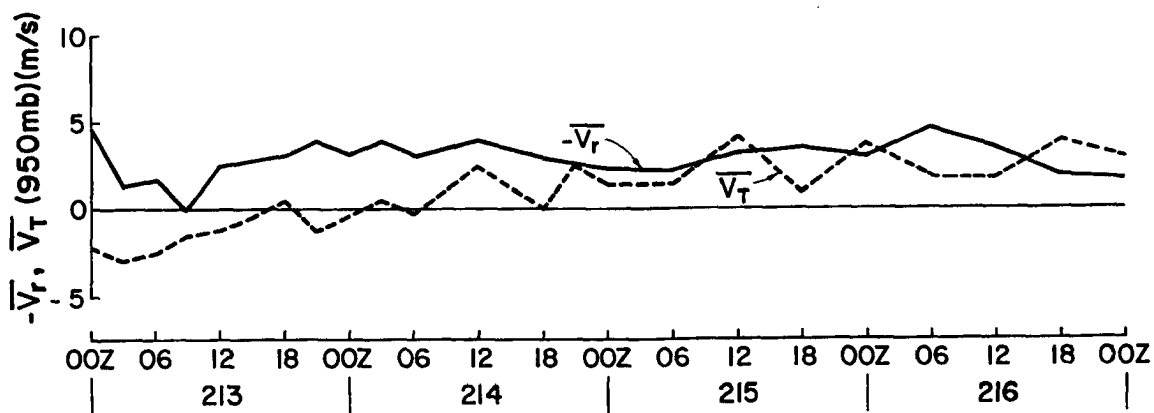
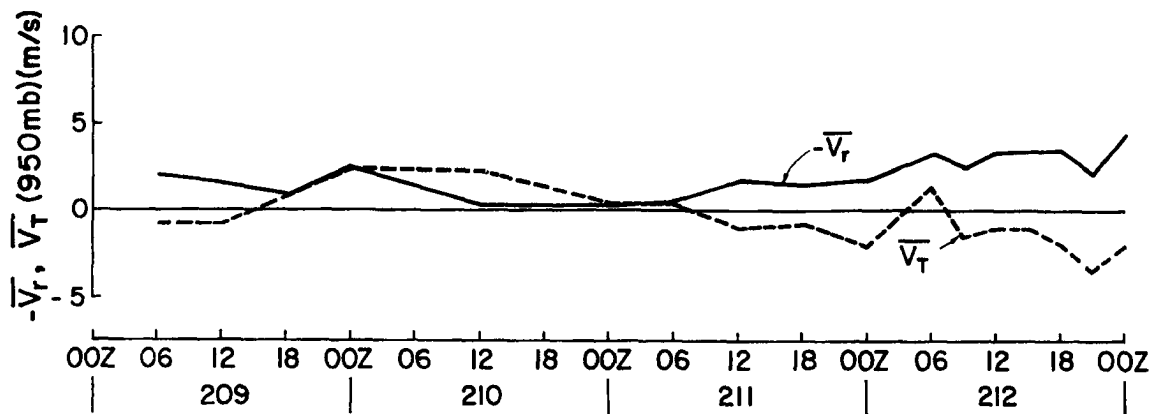


Fig. 25. Same as Fig. 24 except for Phase II.

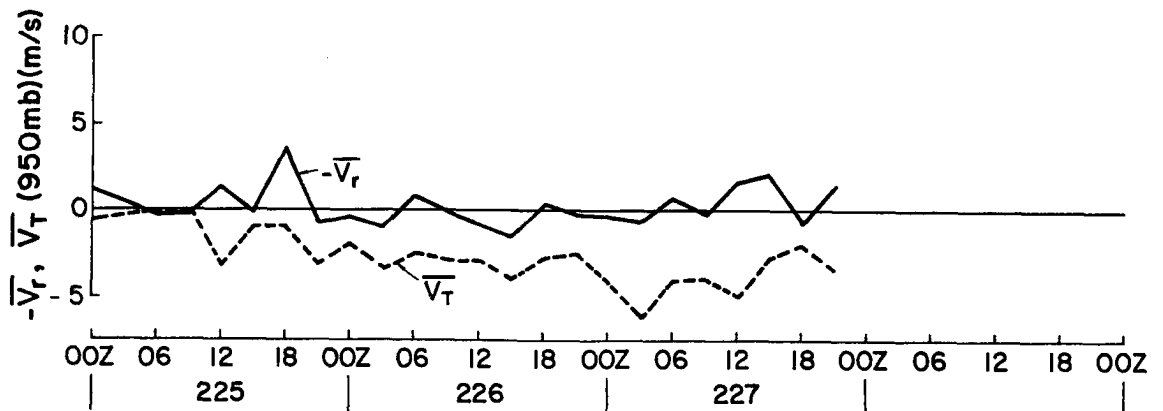
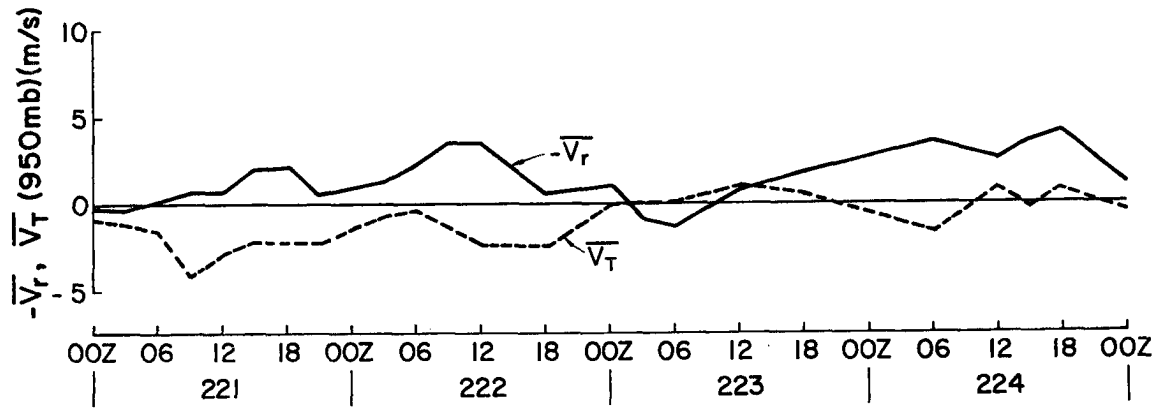
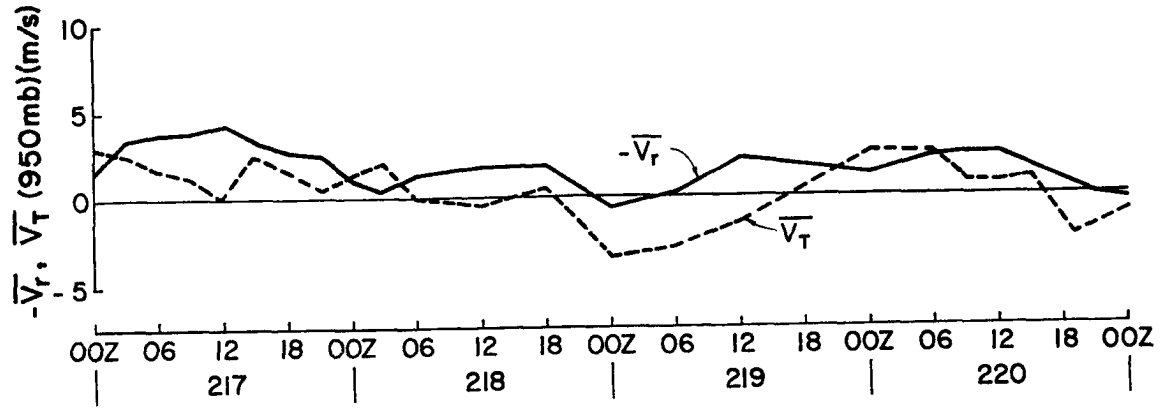


Fig. 25. Continued.

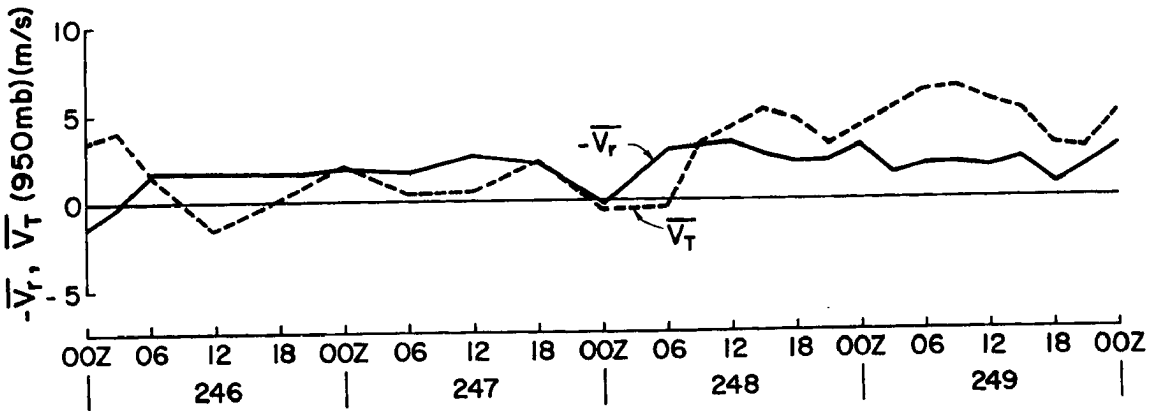
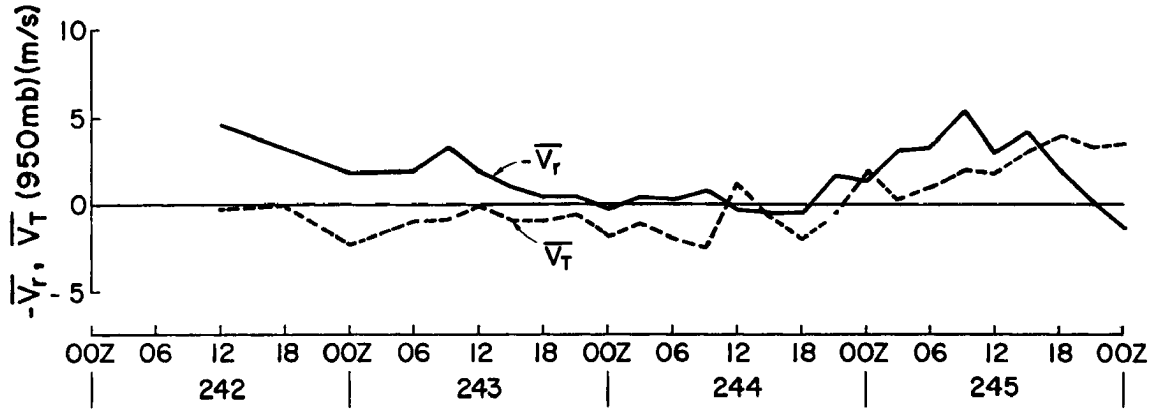
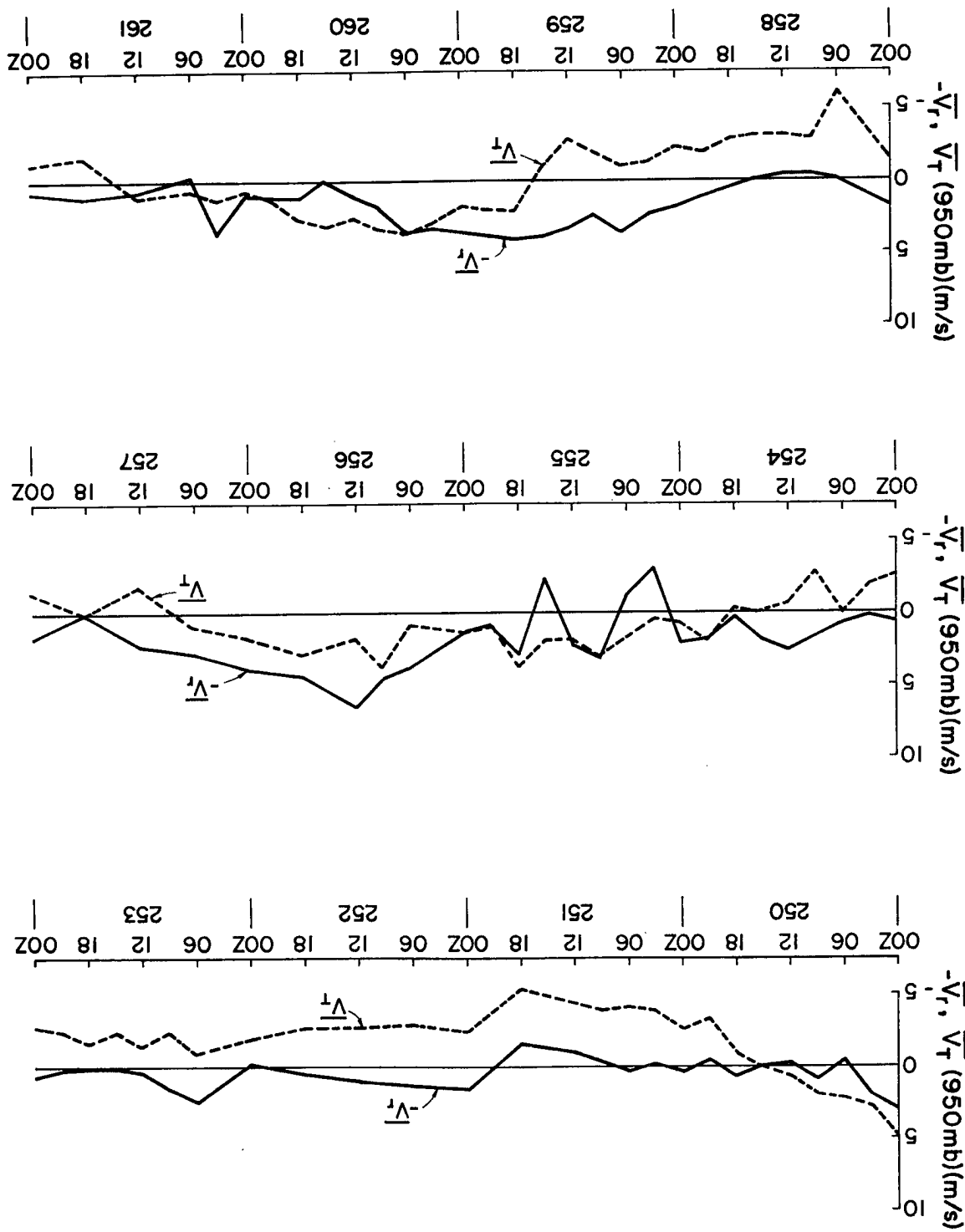


Fig. 26. Same as Fig. 24 except for Phase III.

Fig. 26. Continued.



boundary layer. The A/B-area divergence profile must respond to other (non-frictional) imbalances in the radial pressure/wind fields. The most probable source would seem to be the slow geostrophic adjustment times of the deep tropics. When the radial height gradients change due to diabatic heating or advective processes, convergence/divergence rapidly occurs. Due to low values of f , the tangential winds may never spin up/down enough to achieve balance. McBride and Gray (1978) present additional discussion of frictional convergence in tropical weather systems and the role of radiational forcing in system maintenance. This is a topic deserving substantial future research.

6. CONCLUSIONS

GATE rawinsonde data were analyzed to perform diagnostic budget analyses of moisture and dry static energy for the A/B-scale area. The results were compared with radar rainfall data for the master array to examine several aspects of temporal variations of the tropical atmosphere and of convective/larger scale interactions. Major findings were as follows.

GATE A/B-array rawinsonde data are sufficiently accurate to compute meaningful budgets at individual time periods. The resulting time resolution data will be valuable in many future studies. However, B-array winds are not accurate enough for quantitative analysis of divergence on the B-scale, and biases in the temperature data (particularly on the Russian Ships) limit one to the use of deviation analysis of the temperature fields.

Mean radar rainfall in all phases is less than net condensation estimates from the q and s budgets. It is concluded that radar estimates are too low during periods of light to moderate rainfall.

Radar precipitation lags condensation (and low level vertical motion) by about 4-6 hours. An incorrect Z-R relationship is the most likely cause. The current study suggests that rainfall should be increased for low reflectivities and decreased for higher values.

Mean q budget condensation slightly exceeds s-budget condensation. Since deviation dry advection is significant in all 3 phases, it is hypothesized that there is mean long-term advection of dry air into the A/B-area, maximum near the level of the 650 mb jet.

Precipitable water vapor is remarkably constant throughout all 3

phases. The A/B-scale atmosphere does not store significant quantities of water vapor during the early stages of convective system development.

Low level vertical motion is in phase with the S and q budget condensation rates within the resolution of the data. This means that low level mass convergence rapidly results in clouds and condensation. Since liquid water storage is relatively small, precipitation only slightly lags low level convergence and condensation. The 3-6 hour lag between convergence and echo development observed by Frank (1978) and Ogura et al. (1977) seems to be associated with the time required to concentrate convection into large echo-producing ensembles.

The temperature of the tropical troposphere responds more strongly to diurnal radiational forcing than to latent heat release. This is true at both 300 and 700 mb as well as for the surface to 100 mb layer. There is evidence that clouds act to warm the upper troposphere and cool lower levels, but the effects of convection are not large enough to overcome radiationally induced diurnal temperature changes. Level by level radiational differences between different regimes on the A/B-scale are of the same order as warming due to latent heat release despite the greater total energy involved in convective processes. Both effects must be included in modelling and analysis of tropical weather systems.

Frictionally forced convergence in the boundary layer is insignificant during GATE and can be neglected to a reasonable approximation. Research should focus on relationships between temporal height gradient changes and their resulting effects upon divergence.

ACKNOWLEDGEMENTS

The author is deeply grateful to Professor William M. Gray for his support and consultation. Thanks are also extended to Mr. Edwin Buzzell, Mr. Grant Burton and Ms. Elizabeth Keim for their programming and data processing assistance; and to Mrs. Barbara Brumit and Mrs. Dianne Schmitz who prepared the manuscript.

This research has been supported by the National Science Foundation Grant No. ATM-75-01424 A02.

BIBLIOGRAPHY

- Austin, P. M., S. G. Geotis, J. B. Cunning, J. L. Thomas, R. I. Sax and J. R. Gillespie, 1976: Raindrop size distributions and Z-R relationships for GATE. Paper presented by J. Cunning at the 10th Technical Conference on Hurricanes and Tropical Meteorology, AMS, Charlottesville, VA.
- Businger, J. and W. Seguin, 1977: Transport across the air-sea interface: Sea-air surface fluxes of latent and sensible heat and momentum. Paper appearing in the U.S. GATE Central Program Workshop, 25 July-12 August, NCAR, Boulder, CO, 441-453. [Available from the GATE Project Office, NOAA, Rockville, MD]
- Charney, J. C. and A. Eliassen, 1964: On the growth of the hurricane depression. J. Atmos. Sci., 21, 68-75.
- Cox, S. K. and K. Griffith, 1978: Tropospheric radiative divergence during Phase III of the GARP Atlantic Tropical Experiment (GATE). Atmos. Sci. Paper No. 291, Colo. State Univ., Ft. Collins, CO, 166 pp.
- Cunning, J. B. and R. I. Sax, 1977: A Z-R relationship for the GATE B-scale array. Mon. Wea. Rev., 105, 10, 1330-1336.
- Dewart, J. M., 1978: Diurnal variability in the GATE region. Atmos. Sci. Paper No. 298, Colo. State Univ., Ft. Collins, CO, 80 pp. 76 pp.
- Fingerhut, W. A., 1978: A numerical model of a diurnally varying tropical cloud cluster disturbance. Mon. Wea. Rev., 106, 2, 255-264.
- Foltz, G. S., 1976: Diurnal variation of the tropospheric energy budget. Atmos. Sci. Paper No. 262, Colo. State Univ., Ft. Collins, CO, 141 pp.
- Frank, W. M., 1977a: The structure and energetics of the tropical cyclone, Part I: Storm structure. Mon. Wea. Rev., 105, 9, 1119-1135.
- Frank, W. M., 1977b: The structure and energetics of the tropical cyclone, Part II: Dynamics and energetics. Mon. Wea. Rev., 105, 9, 1136-1150.
- Frank, W. M., 1978: The life cycles of GATE convective systems. J. Atmos. Sci., 35, 1256-1264.
- Gray, W. M., 1972: A diagnostic study of the planetary boundary layer over the oceans. Atmos. Sci. Paper No. 179, Colo. State Univ., Ft. Collins, CO, 95 pp.

BIBLIOGRAPHY (cont'd)

- Gray, W. M., 1973: Cumulus convection and large-scale circulations, Part I: Broad-scale and meso-scale interactions. Mon. Wea. Rev., 101, 839-855.
- Gray, W. M., 1978: Hurricanes/their formation, structure, and likely role in the tropical circulation. Paper submitted to the Quart. J. Roy. Meteor. Soc. (Accepted for publication).
- Gray, W. M. and R. Jacobson, Jr., 1977: Diurnal variation of deep cumulus convection. Mon. Wea. Rev., 105, 9, 1171-1188.
- Grody, N. C., 1976: Remote sensing of atmospheric water content from satellites using microwave radiometry. IEEE Transactions on Antennas and Propagation, Vol. AP-24, 2, 155-162.
- Grube, P. G., 1978: Influence of deep cumulus convection on upper tropospheric temperature changes in GATE. Forthcoming Dept. of Atmos. Sci. Paper, Colo. State Univ., Ft. Collins, CO.
- Hudlow, M., 1978: Personal communication.
- Hudlow, M. and F. Marks, 1977: Echo statistics and rainfall. Paper appearing in the U.S. GATE Central Program Workshop, 25 July-12 August, NCAR, Boulder, CO, 215-236. [Available from the GATE Project Office, NOAA, Rockville, MD]
- Lopez, R. E., 1973: Cumulus convection and larger scale circulations, Part II: Cumulus and mesoscale interactions. Mon. Wea. Rev., 101, 856-870.
- McBride, J. and W. M. Gray, 1978: Mass divergence and vertical velocity in tropical weather systems, Part I: Diurnal variation; Part II: Large scale controls on convection. Dept. of Atmos. Sci. Paper No. 299, Colo. State Univ., Ft. Collins, CO, 109 pp.
- McGarry, M. M. and R. J. Reed, 1978: Diurnal variations in convective activity and precipitation during phases II and III of GATE. Mon. Wea. Rev., 106, 1, 101-113.
- Miller, B. I., 1958: Rainfall rates in Florida hurricanes. Mon. Wea. Rev., 86, 258-264.
- Ogura, Y., 1964: Frictionally controlled, thermally driven circulation in a circular vortex with application to tropical cyclones. J. Atmos. Sci., 21, 610-621.
- Ogura, Y., 1975: On the interaction between cumulus clouds and the large-scale environment. Pure Appl. Geophys., 113, 869-890.

BIBLIOGRAPHY (cont'd)

- Ogura, Y., Y. L. Chen, J. Russell and S. T. Soong, 1977: On the formation of organized convective systems observed over the GATE A/B-array. Convection Series 77-5, Laboratory for Atmospheric Research, Univ. of Illinois, Urbana, IL, 41 pp.
- Ooyama, K., 1964: A dynamical model for the study of tropical cyclone development. Geofisica Internacional, 4, 187-198.
- Ooyama, Y. and S. Esbensen, 1977: Rawinsonde data quality. Report of the U.S. GATE Central Program Workshop, 25 July-12 August, NCAR, Boulder, CO, 131-164. [Available from the GATE Project Office, NOAA, Rockville, MD]
- Panofsky, H. A. and G. W. Brier, 1968: Some applications of statistics to meteorology. Earth and Mineral Sciences of Continuing Education, College of Earth and Mineral Sciences, The Pennsylvania State Univ., University Park, PA, 109-111.
- Reed, R. J., D. C. Norquist and E. E. Recker, 1977: The structure and properties of African wave disturbances as observed during phase III of GATE. Mon. Wea. Rev., 105, 3, 317-333.
- Reed, R. J. and E. E. Recker, 1971: Structure and properties of synoptic-scale wave disturbances in the equatorial western Pacific. J. Atmos. Sci., 28, 1117-1133.
- Riehl, H., 1948: On the formation of typhoons. J. Meteor., 5, 247-264.
- Riehl, H., 1954: Tropical Meteorology. McGraw-Hill, New York, 213-219.
- Riehl, H., 1969: Some aspects of cumulonimbus convection in relation to tropical weather disturbances. Bull. Amer. Meteor. Soc., 50, 587-595.
- Riehl, H. and J. S. Malkus, 1958: On the heat balance in the equatorial trough zone. Geophysica, Helsinki, 503-537.
- Ruprecht, E. and W. M. Gray, 1976: Analysis of satellite-observed tropical cloud clusters, Part I: Wind and dynamic fields; Part II: Thermal, moisture and precipitation. Tellus, 28, 391-426.
- Stevens, D. E., R. S. Lindzen and L. J. Shapiro, 1977: A new model of tropical waves incorporating momentum mixing by cumulus convection. Dyn. Atmos. Oceans, 1, 365-425.
- Thompson, R. M., S. W. Payne, E. E. Recker and R. J. Reed, 1978: Structure and properties of synoptic-scale wave disturbances in the intertropical convergence zone of the eastern Atlantic. (Submitted for publication in J. Atmos. Sci.)

BIBLIOGRAPHY (cont'd)

- Williams, K. T., 1970: A statistical analysis of satellite-observed trade wind cloud clusters in the western North Pacific. Atmos. Sci. Paper No. 161, Colo. State Univ., Ft. Collins, CO, 80 pp.
- Williams, K. T. and W. M. Gray, 1973: Statistical analysis of satellite-observed cloud clusters in the western Pacific. Tellus, 21, 313-336.
- Yanai, M., 1961: A detailed analysis of typhoon formation. J. Meteor. Soc. Japan, 39, 187-214.
- Yanai, M., S. Esbensen and J. H. Chu, 1973: Determination of bulk properties of tropical cloud clusters from large-scale heat and moisture budgets. J. Atmos. Sci., 30, 611-627.
- Zehr, R., 1976: Tropical disturbance intensification. Atmos. Sci. Paper No. 259, Colo. State Univ., Ft. Collins, CO, 91 pp.

APPENDIX

Three-Dimensional Regression. The horizontal gradients of u , v , ΔT and Δq used in the divergence and advection calculations were determined by fitting the data to a plane of regression (Panofsky and Brier, 1968). This plane has a minimum of least squares scatter. For the divergence computation, wind data from the six A/B-array ships plus the Vize and the Vanguard (center of array and northernmost B-array position) were used. These ships all used compatible wind measurement systems. For the advections of ΔT and Δq , data from all 12 A/B and B-array ships were employed.

Example:

An equation for a plane regression is:

$$\bar{u} = a_1 x + a_2 y + a_3$$

$$\frac{\partial \bar{u}}{\partial x} = a_1, \quad \frac{\partial \bar{u}}{\partial y} = a_2$$

$$a_1 = \frac{s_u}{s_x} \left(\frac{\Gamma_{ux} - \Gamma_{uy} \Gamma_{xy}}{1 - \Gamma_{xy}^2} \right)$$

$$a_2 = \frac{s_u}{s_y} \left(\frac{\Gamma_{uy} - \Gamma_{ux} \Gamma_{xy}}{1 - \Gamma_{xy}^2} \right)$$

where: s_x, s_y, s_u = standard deviations

$$(s_u = \sqrt{\frac{\sum u^2}{N} - (\bar{u})^2})$$

and: $\Gamma_{ux}, \Gamma_{uy}, \Gamma_{xy}$ = correlation coefficients

$$(\Gamma_{xy} = \frac{\overline{xy} - \bar{x} \bar{y}}{s_x s_y}) .$$

W. M. GRAY'S FEDERALLY SUPPORTED RESEARCH PROJECT REPORTS SINCE 1967

CSU Dept. of
Atmos. Sci.
Report No.

Report Title, Author, Date, Agency Support

104	The Mutual Variation of Wind, Shear, and Baroclinicity in the Cumulus Convective Atmosphere of the Hurricane (69pp). W. M. Gray. February 1967. NSF Support.
114	Global View of the Origin of Tropical Disturbances and Storms (105pp). W. M. Gray. October 1967. NSF Support.
116	A Statistical Study of the Frictional Wind Veering in the Planetary Boundary Layer (57pp). B. Mendenhall. December 1967. NSF and ESSA Support.
124	Investigation of the Importance of Cumulus Convection and Ventilation in Early Tropical Storm Development (88pp). R. Lopez. June 1968. ESSA Satellite Lab. Support.
Unnumbered	Role of Angular Momentum Transports in Tropical Storm Dissipation over Tropical Oceans (46pp). R. F. Wachtmann. December 1968. NSF and ESSA Support.
Unnumbered	Monthly Climatological Wind Fields Associated with Tropical Storm Genesis in the West Indies (34pp). J. W. Sartor. December 1968. NSF Support.
140	Characteristics of the Tornado Environment as Deduced from Proximity Soundings (55pp). T. G. Wills. June 1969. NOAA and NSF Support.
161	Statistical Analysis of Trade Wind Cloud Clusters of the Western North Pacific (80pp). K. Williams. June 1970. ESSA Satellite Lab. Support.
---	A Climatology of Tropical Cyclones and Disturbances of the Western Pacific with a Suggested Theory for Their Genesis/Maintenance. W. M. Gray. NAVWEARSCHFAC Technical Paper No. 19-70 (225pp). November 1970. (Available from U.S. Navy, Monterey, CA). U.S. Navy Support.
179	A Diagnostic Study of the Planetary Boundary Layer over the Oceans (95pp). W. M. Gray. February 1972. Navy and NSF Support.
182	The Structure and Dynamics of the Hurricane's Inner Core Area (105pp). D. J. Shea. April 1972. NOAA and NSF Support.
188	Cumulus Convection and Larger-Scale Circulation, Part I: A Parametric Model of Cumulus Convection (100pp). R. E. Lopez. June 1972. NSF Support.

CSU Dept. of
Atmos. Sci.
Report No.

Report Title, Author, Date, Agency Support

- 189 Cumulus Convection and Larger-Scale Circulations, Part II: Cumulus and Meso-Scale Interactions (63pp). R. E. Lopez. June 1972. NSF Support.
- 190 Cumulus Convection and Larger-Scale Circulations, Part III: Broadscale and Meso-Scale Considerations (80pp). W. M. Gray. July 1972. NOAA-NESS.
- 195 Characteristics of Carbon Black Dust as a Tropospheric Heat Source for Weather Modification (55pp). W. M. Frank. January 1973. NSF Support.
- 196 Feasibility of Beneficial Hurricane Modification by Carbon Black Seeding (130pp). W. M. Gray. April 1973. NOAA Support.
- 199 Variability of Planetary Boundary Layer Winds (157pp). L. R. Hoxit. May 1973. NSF Support.
- 200 Hurricane Spawned Tornadoes (57pp). D. J. Novlan. May 1973. NOAA and NSF Support.
- 212 A Study of Tornado Proximity Data and an Observationally Derived Model of Tornado Genesis (101pp). R. Maddox. November 1973. NOAA Support.
- 219 Analysis of Satellite Observed Tropical Cloud Clusters (91 pp). E. Ruprecht and W. M. Gray. May 1974. NOAA-NESS Support.
- 224 Precipitation Characteristics in the Northeast Brazil Dry Region (56pp). R. P. L. Ramos. May 1974. NSF Support.
- 225 Weather Modification through Carbon Dust Absorption of Solar Energy (190pp). W. M. Gray, W. M. Frank, M. L. Corrin, and C. A. Stokes. July 1974.
- 234 Tropical Cyclone Genesis (121pp). W. M. Gray. March 1975. NSF Support.
- Tropical Cyclone Genesis in the Western North Pacific (66pp). W. M. Gray. March 1975. U.S. Navy Environmental Prediction Research Facility Report. Technical Paper No. 16-75. (Available from the U.S. Navy, Monterey, CA). Navy Support.
- 241 Tropical cyclone Motion and Surrounding Parameter Relationships (105pp). J. E. George. December 1975. NOAA Support.

CSU Dept. of
Atmos. Sci.
Report No.

Report Title, Author, Date, Agency Support

- 243 Diurnal Variation of Oceanic Deep Cumulus Convection. Paper I: Observational Evidence, Paper II: Physical Hypothesis (106pp). R. W. Jacobson, Jr. and W. M. Gray. February, 1976. NOAA NESS Support.
- 257 Data Summary of NOAA's Hurricane Inner-Core Radial Leg Flight Penetrations 1957-1967, and 1969 (245pp). W. M. Gray and D. J. Shea. October, 1976. NSF and NOAA Support.
- 258 The Structure and Energetics of the Tropical Cyclone (180 pp). W. M. Frank. October, 1976. NOAA (NHEML), NOAA (NESS) and NSF Support.
- 259 Typhoon Genesis and Pre-typhoon Cloud Clusters (79pp). R. M. Zehr. November, 1976.
- Unnumbered Severe Thunderstorm Wind Gusts (81pp). G. W. Walters. December, 1976. NSF Support.
- 262 Diurnal Variation of the Tropospheric Energy Budget (141 pp). G. S. Foltz. November, 1976. NSF Support.
- 274 Comparison of Developing vs Non-Developing Tropical Disturbances (81 pp). Steven L. Erickson. July, 1977. U.S. Army Support.
- 277 Tropical Cyclone Cloud and Intensity Relationships (154 pp). Charles P. Arnold. November, 1977. U.S. Army and NHEML Support.
- 297 Diagnostic Analyses of the GATE A/B-scale Area at Individual Time Periods (102 pp). W. M. Frank. November, 1978. NSF Support.
- 298 Diurnal Variability in the GATE Region (80 pp). Jean M. Dewart. November, 1978. NSF Support.
- 299 Mass Divergence in Tropical Weather Systems, Paper I: Diurnal Variation; Paper II: Large-scale Controls on Convection (109 pp). John. L. McBride and W. M. Gray. November, 1978. NOAA-NHEML Support.

BIOGRAPHIC DATA SHEET	1. Report No. CSU-ATSP- 297	2.	3. Recipient's Accession No.
4. Title and Subtitle DIAGNOSTIC ANALYSES OF THE GATE A/B SCALE AREA AT INDIVIDUAL TIME PERIODS		5. Report Date November 1978	6.
		7. Author(s) William M. Frank	
9. Performing Organization Name and Address Atmospheric Science Department Colorado State University Fort Collins, Colorado 80523		10. Project/Task/Work Unit No.	
		11. Contract/Grant No. ATM75-01424 A02	
12. Sponsoring Organization Name and Address National Science Foundation Washington, DC 20550		13. Type of Report & Period Covered Project Report	
		14.	
15. Supplementary Notes			
<p>16. Abstracts</p> <p>GATE rawinsonde data are analyzed at all individual time periods. Moisture and static energy budgets are performed over the A/B area.</p> <p>Budget derived rainfall exceeds radar estimates, particularly during periods of light rainfall. The radar rainfall lags budget condensation by 4-6 hours.</p> <p>Temperature changes of the tropical troposphere are found to be more dependent upon radiational heating than latent heat release although condensation does act to warm the upper troposphere and cool lower levels.</p> <p>Frictional convergence is shown to be a relatively minor component of GATE A/B scale divergence.</p>			
<p>17. Key Words and Document Analysis. 17a. Descriptors</p> <p>Cumulus Convection Tropical Weather Disturbances GATE Experiment</p> <p>17b. Identifiers/Open-Ended Terms</p> <p>17c. COSATI Field/Group</p>			
18. Availability Statement		19. Security Class (This Report) UNCLASSIFIED	21. No. of Pages 102 pp.
		20. Security Class (This Page) UNCLASSIFIED	22. Price